DEPARTMENT OF MECHANICAL AND MANUFACTURING ENGINEERING

ELUCIDATION OF THE EFFECTS OF SOLID STRESS ON FIBROBLASTS AND CANCER CELLS BEHAVIOR IN SOLID TUMORS

DOCTOR OF PHILOSOPHY DISSERTATION

MARIA KALLI

2019

DEPARTMENT OF MECHANICAL AND MANUFACTURING ENGINEERING

ELUCIDATION OF THE EFFECTS OF SOLID STRESS ON FIBROBLASTS AND CANCER CELLS BEHAVIOR IN SOLID TUMORS

DOCTOR OF PHILOSOPHY DISSERTATION

MARIA KALLI

A Dissertation Submitted to the University of Cyprus in Partial Fulfillment of the Requirements for the Degree of Doctor of Philosophy

April 2019

VALIDATION PAGE

Doctoral Candidate: MARIA KALLI

Doctoral Thesis Title: Elucidation of the effects of solid stress on fibroblasts and cancer cells behavior in solid tumors

This Doctoral Dissertation was submitted in partial fulfillment of the requirements for the degree of Doctor of Philosophy at the ***Department of Mechanical and Manufacturing Engineering*** *and approved on the …….. by the* ***Examination Committee****.*

Examination Committee:

Research Advisor:

Dr.Triantafyllos Stylianopoulos ……..……..……

Other Members:

Dr.Anna Fahlgren ……...……...

Dr. Theodora Krasia ……..

Dr. Panagiotis Papageorgis……..……..……

Dr. Vasileios Vavourakis……..…….....

DECLARATION OF DOCTORAL CANDIDATE

The present doctoral dissertation was submitted in partial fulfilment of the requirements for the degree of Doctor of Philosophy of the University of Cyprus. It is a product of original work of my own, unless otherwise mentioned through references, notes, or any other statements.

Name and Signature of the Doctoral Candidate:

…… [Full Name of Doctoral Candidate]

……[Signature]

Περίληψη

Οι συμπαγείς καρκινικοί όγκοι αποτελούνται από καρκινικά και μη καρκινικά κύτταρα, όπως είναι οι ινοβλάστες και τα κύτταρα του ανοσοποιητικού συστήματος, από την εξωκυττάρια μήτρα η οποία είναι ένα πλέγμα από πρωτεΐνες και μακρομοριακές αλυσίδες (κολλαγόνο, υαλουρονικό οξύ, ινωνεκτίνη) καθώς και από το αγγειακό του σύστημα. Η υπερβολική παραγωγή των πρωτεϊνών αυτών στην εξωκυττάρια μήτρα, μια κατάσταση γνωστή ως *δεσμοπλασία*, μαζί με τον ανεξέλεγκτο πολλαπλασιασμό των καρκινικών κυττάρων στον περιορισμένο χώρο του οργάνου στο οποίο αναπτύσσονται, οδηγούν στην ανάπτυξη μηχανικών δυνάμεων συμπίεσης εντός του όγκου, για το οποίο χρησιμοποιείται ο αγγλικός όρος *solid stress*. Το solid stress είναι βασικό χαρακτηριστικό της βιομηχανικής αρκετών συμπαγών όγκων, συμπεριλαμβανομένου του καρκίνου του μαστού, του παχέος εντέρου, του παγκρέατος και του εγκεφάλου, και έχει αποδειχθεί ότι μπορεί να επηρεάσει τον πολλαπλασιασμό και τη μετανάστευση των καρκινικών κυττάρων. Ωστόσο, οι μοριακοί μηχανισμοί για το πώς εμπλέκεται στην εξέλιξη του όγκου και ιδιαίτερα στην μετάσταση δεν είναι ακόμη πλήρως κατανοητοί. Επιπλέον, ενώ η επίδραση των μηχανικών τάσεων στα καρκινικά κύτταρα ήδη διερευνάται, δεν υπάρχει ακόμα κάποια σχετική μελέτη που να εξετάζει την επίδρασή τους στους ινοβλάστες, οι οποίοι αποτελούν σημαντικό συστατικό στο μικροπεριβάλλον ενός όγκου. Αυτό γιατί όταν οι ινοβλάστες βρίσκονται σε καρκινικό περιβάλλον αποκτούν ένα συνεχώς ενεργοποιημένο φαινότυπο παράγοντας υπερβολικές ποσότητες πρωτεϊνών της εξωκυττάριας μήτρας οδηγώντας σε δεσμοπλασία, ενώ ταυτόχρονα αλληλεπιδρούν με τα καρκινικά κύτταρα προωθώντας την εξέλιξη του όγκου. Προκειμένου να διερευνηθεί η επίπτωση των μηχανικών τάσεων στα καρκινικά κύτταρα και στους ινοβλάστες που συναντώνται σε ένα καρκινικό μικροπεριβάλλον, χρησιμοποιήσαμε μια αυτοσχέδια διάταξη για την εφαρμογή προκαθορισμένης μηχανικής τάσης σε καρκινικά κύτταρα και ινοβλάστες παγκρέατος, καθώς επίσης και σε καρκινικά κύτταρα εγκεφάλου. Το μέγεθος των τάσεων που χρησιμοποιήθηκαν ήταν παρόμοιο με αυτό που δέχονται τα

κύτταρα σε πραγματικούς όγκους. Τα αποτελέσματά μας δείχνουν ότι η μηχανική τάση διεγείρει την ενεργοποίηση των ινοβλαστών και αυξάνει έντονα την έκφραση του παράγοντα διαφοροποίησης ανάπτυξης-15 (Growth Differentiation Factor-15, GDF15). Επιπλέον, η συν-καλλιέργεια των συμπιεσμένων αυτών ινοβλαστών με καρκινικά κύτταρα παγκρέατος φάνηκε να προάγει σημαντικά τη μετανάστευση των καρκινικών κυττάρων, η οποία αναστέλλεται μετά από τεχνική μείωση των επιπέδων του GDF15 στους ινοβλάστες. Στη συνέχεια, με εφαρμογή μηχανικής συμπίεσης απευθείας πάνω σε καρκινικά κύτταρα παγκρέατος, παρατηρήθηκε αύξηση της μεταναστευτικής τους ικανότητας συνοδευόμενη από έντονη αύξηση του παράγοντα GDF15. Πραγματοποιώντας μια ανάλυση των επιπέδων φωσφο-πρωτεϊνών στα καρκινικά κύτταρα, ανακαλύψαμε ότι ο μηχανισμός με τον οποίο μεταφέρεται το σήμα της μηχανικής συμπίεσης βασίζεται στο σηματοδοτικό μονοπάτι Akt / CREB1 το οποίο μπορεί να ρυθμίζει μεταγραφικά την έκφραση του GDF15 στα καρκινικά κύτταρα, έτσι ώστε να προωθήσει στην συνέχεια την μετανάστευσή τους. Τέλος, διαπιστώσαμε ότι η μηχανική τάση μπορεί να εμποδίσει την ανάπτυξη καρκινικών σφαιροειδών του εγκεφάλου, και ταυτόχρονα να ρυθμίσει διαφορικά την μεταναστευτική ικανότητα και γονιδιακή έκφρασή τους. Συγκεκριμένα, εντοπίσαμε μία έντονη αύξηση στην έκφραση του παράγοντα GDF15 σε δύο διαφορετικές κυτταρικές σειρές καρκίνου του εγκεφάλου ανεξάρτητα από το μεταναστευτικό τους δυναμικό, ενώ παρατηρήθηκε μια αύξηση και μείωση της έκφρασης του παράγοντα RhoB GTPase στα λιγότερο μεταναστευτικά κύτταρα γλοιώματος και στα επιθετικά κύτταρα γλοιοβλαστώματος, αντίστοιχα. Παρόλο που απαιτούνται περαιτέρω πειράματα για να προτείνουμε έναν ολοκληρωμένο μηχανισμό με τον οποίο η μηχανική τάση μπορεί να προωθήσει τη μετανάστευση των καρκινικών κυττάρων του εγκεφάλου, τα μέχρι τώρα αποτελέσματά μας υποδηλώνουν έναν καθοριστικό ρόλο της μηχανικής τάσης στην εξέλιξη του όγκου, καθιστώντας το GDF15 και άλλα μόρια όπως το RhoB ως δυνητικούς βιοδείκτες για την παρουσία μηχανικών τάσεων σε πραγματικούς όγκους και προτείνοντας αυτά τα γονίδια

σαν νέους μοριακούς στόχους για μελλοντικές καινοτόμες θεραπείες ενάντια στην ρυθμιζόμενη από μηχανικές τάσεις μετάσταση.

Abstract

Apart from cancer cells, solid tumors consist of non-cancerous cells, such as fibroblasts and immune cells, an extracellular matrix (ECM) that forms a network of fibrillar proteins and macromolecular chains, including collagen, hyaluronan and fibronectin, and a vascular system. The excessive production of ECM proteins, a condition known as *desmoplasia,* along with the uncontrolled proliferation of cancer cells in the confined space of the host tissue, leads to the development of compressive forces within the tumor, generating the so-called *solid stress*. Elevated solid stress is a characteristic biomechanical abnormality of several solid tumors, including breast, colon, pancreatic and brain cancer, and it has been previously shown to affect cancer cell proliferation and migration. However, the underlying mechanisms of how it is implicated in tumor progression, and especially in metastatic dissemination of cancer cells, is not yet fully understood. Moreover, while the effect of solid stress on cancer cells is currently being investigated, there is no pertinent study considering its effect on fibroblasts and whether these effects contribute to tumor progression. In fact, fibroblasts are continuously gaining ground as an important component of tumor microenvironment. They might acquire a constantly activated phenotype producing excessive amounts of extracellular matrix leading to desmoplasia, while they dynamically interact with cancer cells to promote tumor progression. The objective of this research was to investigate the implication of solid stress in cancer cells and fibroblasts. For this purpose, we employed a custom-made device to apply a predefined compressive stress on pancreatic cancer cells and fibroblasts, as well as on brain cancer cells, similar in magnitude to that experienced by cells in native tumors. Our results suggest that solid stress stimulates fibroblasts activation and strongly upregulates Growth Differentiation Factor-15 (*GDF15*) expression. Moreover, co-culture of compression-induced activated fibroblasts with pancreatic cancer cells significantly promotes cancer cell migration, which is inhibited by shRNA-mediated silencing of *GDF15* in fibroblasts. By applying mechanical compression

directly on pancreatic cancer cells, we found an increase in their metastatic potential accompanied by a strong upregulation of GDF15 expression. Subsequently, with the use of a phosphoprotein screening, we identified a solid stress-induced mechanism relied on the Akt/CREB1 pathway that can transcriptionally regulate *GDF15* expression in order to promote cancer cell migration. Finally, we found that solid stress can impair the growth of brain cancer multicellular spheroids and it can differentially regulate their migration and gene expression profile. Specifically, we identified a strong increase in GDF15 expression of two distinct brain cancer cell lines regardless of their metastatic potential, while an upregulation and downregulation of RhoB GTPase was observed in the less metastatic glioma cells and highly aggressive glioblastoma cells, respectively. Even though future studies are needed to reveal a comprehensive mechanism of how solid stress induces the migration of brain cancer cells, our results suggest a novel regulatory role of solid stress in tumor progression, rendering GDF15 and other molecules such as RhoB, as potential biomarkers for the presence of solid stress *in vivo* and molecular targets for future anti-metastatic therapeutic innovations.

Acknowledgments

I would like to offer my special thanks to Dr. Triantafyllos Stylianopoulos for his valuable assistance, motivation and guidance as well as for encouraging my research and for allowing me to grow as an independent research scientist. It has been an honor to be one of his Ph.D. students.

Of course, the completion of this project could not have been accomplished without the helpful advices, discussions and ideas of Dr. Vassiliki Gkretsi, Dr. Christiana Polydorou, Dr. Stylianou Andreas.

I am also grateful to all the members of the Cancer Biophysics lab, Dr. Chrysovalantis Voutouri, Maria Louca, Myrophora Panagi, Fotios Mpekris and our technician Kypros Stylianou. Their friendliness, support and encouragement through all these years were also important for my dissertation.

Contents

1 Introduction

1.1 Unravelling the tumor microenvironment

Cancer is a common disease that affects one in two people during their lifetime [1]. The mechanism of how cancer is developed is a multistep process of an accumulation of DNA alterations (mutations) over time. Mutations are either single changes in the DNA sequence or large chromosomal aberrations, such as chromosomal translocations [1]. These changes give a growth advantage to a cell over its neighbours, resulting in the selection and survival of the fittest. A cell with growth advantage continues to change in order to survive and proliferate, and finally creates a mass of clone cells, the tumor. Tumor cells differ from normal cells because they can auto-regulate their growth, escape programmed cell death, avoid immune system and proliferate uncontrollably. Tumors in situations of low concentration of oxygen and nutrients may also promote the construction of a new vascular system, a process called angiogenesis. This process provides further the ability of cancer cells to migrate from their site of origin through the vascular system. This ability distinguishes tumors into benign and malignant, where benign tumors do not spread throughout the body, in contrast with malignant tumors that can metastasize [1].

Moreover, many tumors, especially breast and pancreatic cancers and sarcomas, contain an extremely dense extracellular matrix (ECM), consisting of collagen, hyaluronan, fibronectin and other extracellular fibers. The tumor microenvironment is also composed of non-cancerous, stromal cells such as immune cells and fibroblasts and capillaries [2] (**Figure 1-1**). Fibroblasts are key regulators of ECM composition and organization, and physiologically remain in quiescent state with negligible metabolic and transcriptomic

activities[3, 4]. In response to tissue damage, fibroblasts become activated and are characterized by the expression of alpha-smooth muscle actin (a-SMA). In this activated state, fibroblasts over-produce ECM proteins, mainly collagen type I and fibronectin, secrete cytokines and growth factors, and exert contractile forces modifying tissue architecture[3, 4]. In tumors, in particular, fibroblasts tend to acquire a constantly activated phenotype as a response to several growth factors secreted from the highly proliferative cancer cells, including Transforming Growth Factor-β (TGFβ), Epidermal Growth Factors (EGFs) and Bone Morphogenic Proteins (BMPs)[3, 4]. Activated tumor-infiltrated fibroblasts, which are commonly known as Cancer Associated Fibroblasts (CAFs), initiate a chronic wound healing-like response toward cancer cells, which leads to an excessive accumulation of fibrillar ECM proteins, a condition known as **desmoplasia**[4]. Under this desmoplastic reaction, CAFs continuously produce and remodel the tumor ECM increasing tumor stiffness[4, 5]. Desmoplasia and ECM stiffening characterize many tumor types, especially breast, brain and pancreatic cancers, and it usually promotes tumor progression[5-7].

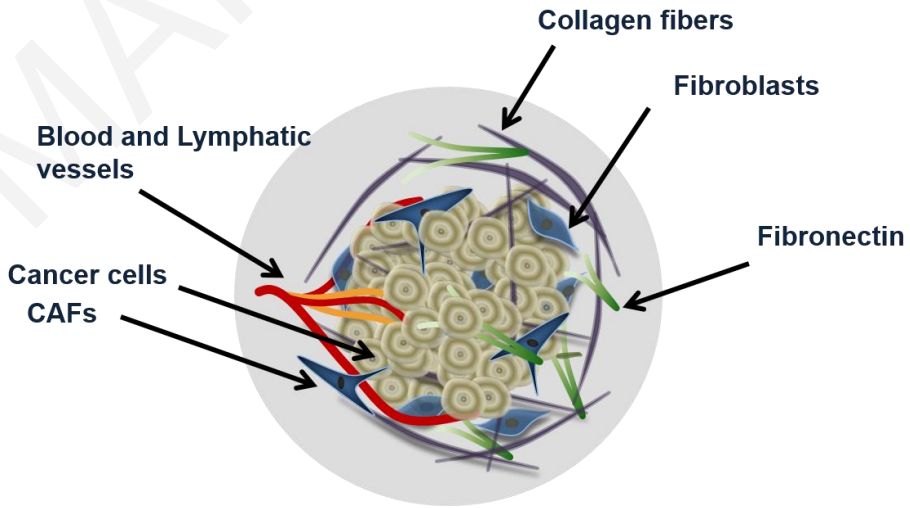

Figure 1-1. **Schematic of the tumor microenvironment.** The tumor microenvironment is constituted by cancer cells, blood and lymphatic vessels and by an extracellular matrix. Fibroblasts

are cells of the connective tissue and are placed in the extracellular regions. These cells, upon activation, produce proteins such as collagen type I and fibronectin and all together constitute a 3D network, referred to as extracellular matrix or ECM. In this activated state, fibroblasts are also known as Cancer Associated Fibroblasts (CAFs).

1.2 Solid stress and matrix stiffness are two distinct biomechanical abnormalities of the tumor microenvironment

As the density of cancer cells, stromal cells and ECM constituents increases within the restricted environment of the host tissue, it leads to the development of mechanical stress (i.e., force per unit area) within the tumor[5, 8-11]. This stress, derived from the structural components of a tumor, is known as solid stress and can be divided into two parts. A part of it, known as growth-induced stress, is accumulated during tumor growth due to microscopic interactions among the components of the tumor microenvironment, and it remains in the tissue even if the tumor is removed[5, 10]. These interactions might include collagen stretching by contractile CAFs and hyaluronan and cancer cell swelling to resist compression[12-15]. Moreover, as tumors grow and exert forces on the adjacent host tissue, a reciprocal compressive stress is applied from the host tissue to the tumor, in order to resist tumor expansion[5]. This stress is known as externally-applied stress, and it diminishes when the tumor is excised[5]. The total solid stress in a tumor interior is compressive (i.e., tends to reduce the size of an object), while near the interface between the tumor and normal tissue, the stress can become tensile (i.e., tends to increase the size of an object)[16, 17] (**Figure 1-2**).

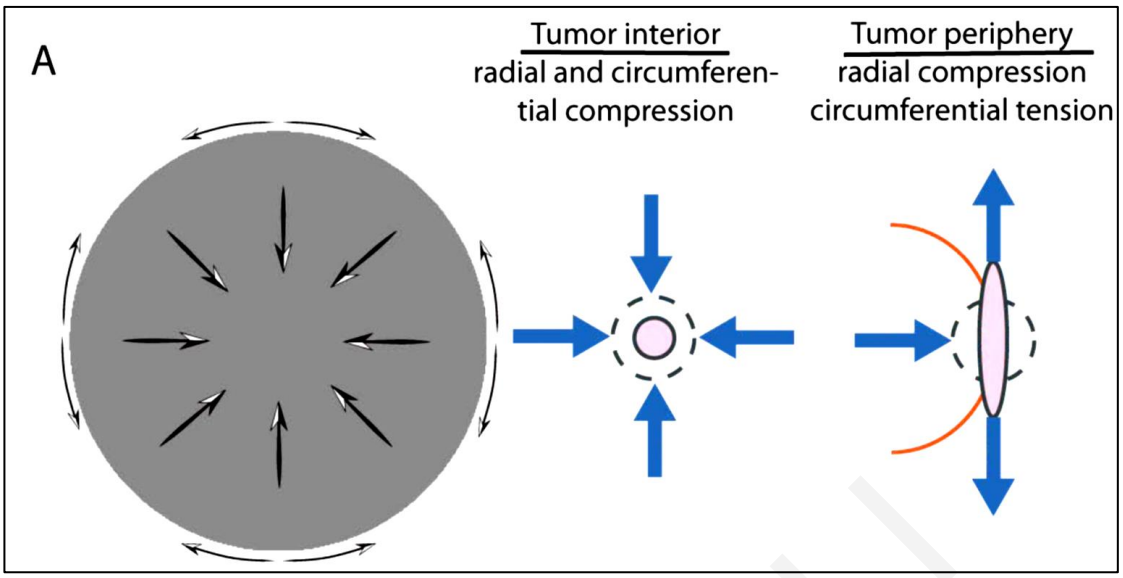

Figure 1-2. **Development of solid stress in the tumor microenvironment.** As tumors grow and exert forces on the adjacent host tissue, a reciprocal compressive stress is applied from the host tissue to the tumor, in order to resist tumor expansion. The total solid stress in a tumor interior is compressive in all directions (i.e., tends to reduce the size of an object), while near the interface between the tumor and normal tissue, the stress can become tensile (i.e., tends to increase the size of an object) [5].

It is not clearly defined in the pertinent literature whether matrix stiffness and solid stress refer to the same term or they are two distinct biomechanical abnormalities of a tumor that are related to each other. By definition, stiffness is a material property, which describes the extent to which a material resists deformation, while solid stress is a force per unit area which can cause either compaction (compression) or expansion (tension) of a material [18]. In solid tumors, stiffness is mainly determined by ECM composition and organization and also by cellular density, while solid stress arises by the sum of the physical forces exerted during tumor growth. These forces can be generated in the subcellular level by cytoskeletal filaments that control cellular processes such as filopodia formation and extension. At the cellular level, forces are exerted due to cell contractions (such as in CAFs) and cell-ECM interactions during migration of cancer and stromal cells, while at the tissue level forces are exerted between the tumor and the host tissue[19-22].

The relationship between tumor stiffness and solid stress can be described using the analogy of a mechanical spring of a specific elastic modulus (E) that obeys Hooke's law[18] (**Figure 1-3**). According to the equation of Hooke's law for linear elastic materials, $\sigma = E \cdot \varepsilon$, when a tumor of an elastic modulus E grows and pushes the surrounding host tissue of elastic modulus E*'*, causes the development of a stress σ_1 and deformation ε_1. As a consequence, the host tissue returns an equal and opposite stress σ_1*'*, the so called externally-applied solid stress. At the same time, growth-induced solid stress is accumulated in the tumor interior owing to interactions among tumor components (**Figure 1-3 (A**)). Thus, the total solid stress accumulated intratumorally is the sum of the externally-applied and the growth-induced solid stress. In the case that the stiffness of the tumor E_2 is greater than E_1, then the tumor can displace the host tissue with a greater deformation and the externally-applied solid stress σ_2 can be greater than σ_1 (**Figure 1-3 (B)**). Therefore, in this case a solid tumor creates a stiffer matrix in order to push against the normal tissue and grow in size. Indeed, it has been demonstrated using mathematical modeling that the stiffness of a solid tumor should be at least 1.5 times greater than that of the host tissue, in order for the tumor to be able to displace the tissue and grow in size[15].

As for the growth-induced solid stress, however, it increases during tumor growth[23], while the matrix stiffness might stop changing[17]. In this case the further increase in total solid stress accumulated in the tumor interior can become less depended on matrix stiffness (**Figure 1-3 (C)**). This hypothesis has been confirmed by the experimental data of Nia et al.[17], suggesting that the total solid stress transmitted into the cells can depend only in part on tumor stiffness and thus, the two terms should not be used without a distinction. In particular, the effects of matrix stiffness and solid stress on tumorigenesis and metastasis

should be studied separately[24], thus our study was mainly focused on the elucidation of the effect of solid stress on cancer cells and fibroblasts in the absence of ECM stiffness.

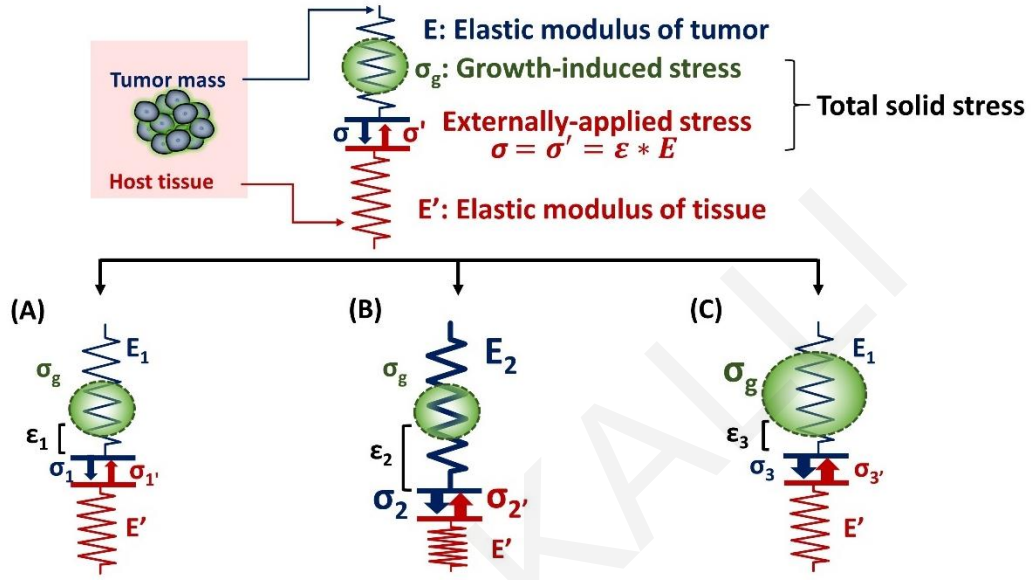

Figure 1-3. **Solid stress and stiffness are two distinct biomechanical abnormalities present in the tumor microenvironment**. **(A)** According to the simple analogy of a spring that obeys Hooke's law ($\sigma = E \cdot \varepsilon$), when a tumor grows and pushes the surrounding host tissue of elastic modulus E*'*, results in a deformation ε_1 and a stress σ_1. As a consequence, the host tissue returns an equal and opposite stress σ_1*'*, which is defined as externally-applied solid stress. This stress, in combination with the growth-induced stress (σ_g) constitute the total solid stress transmitted in the tumor interior. **(B)** In the case that the tumor stiffens so that E_2 is greater than E_1 ($E_2 > E_1$), the tumor can increase in size and the deformation ε_2 is greater than ε_1 ($\varepsilon_2 > \varepsilon_1$). The externally-applied stress (σ_2*'*) and finally the total solid stress accumulated in the tumor interior is greater than that in case (A) without any change in the growth-induced stress. **(C)** The growth-induced solid stress, however, increases during growth, while tumor stiffening might remain the same [17]. In this case the externally-applied solid stress σ_3*'* can be equal to σ_1' but total solid stress increases. Therefore, the resultant stress transmitted in the tumor interior is greater than that in case (A) without any change in tumor stiffness.

1.2.1 Effects of matrix stiffness on cancer and stromal cells

The effect of ECM stiffness on cancer and stromal cells has been studied using *in vitro* two-dimensional substrates (2D) and three-dimensional tumor analogs (3D). In 2D models cells are seeded on coating substrates such as collagen type I or fibronectin[25-28]

(**Figure 1-4A (i)**), while the 3D models include single cells or tumor spheroids embedded in gels mainly composed of collagen type I or matrigel[29-38] (**Figure 1-4A (ii,iii)**). In both cases, stiffness is increased by changing the protein density or the degree of crosslinking of the matrix, in order to study the effects of ECM-originating mechanical cues on cancer and stromal cells.

Matrix stiffness is shown to activate intracellular signaling pathways to regulate cellular behavior. Cancer cells recognize the increase in ECM stiffness and respond by generating increased traction forces on their surroundings through actomyosin and cytoskeleton contractility[9, 39, 40]. Moreover, the changes in matrix rigidity are sensed and transmitted intracellularly through mechano-sensors such as p130 CRK-associated proteins, growth factor receptors, stretch-activated ion channels or integrin-ECM adhesion plaques[8, 9, 28, 40-45]. These mechano-sensors can subsequently recruit focal adhesion molecules such as FAK, SRC, paxillin, RAC, RHO GTPase/ Rho-associated kinase (ROCK) and RAS GTPases to trigger signaling cascades and cytoskeleton organization[8, 9, 39, 40, 44, 46-49]. These signaling cascades finally regulate gene expression and induce quantifiable changes in cell shape, motility, survival, migration and invasion[9, 40, 44, 48]. For example, it has been shown that tissue stiffness indirectly activates the nuclear translocation of the transcription factor TWIST1 in breast cancer cells, which inhibits the expression of E-Cadherin and promotes cell invasion[40, 50]. Furthermore, in a 3D model consisting of breast tumor spheroids growing in collagen type I matrix, the Ras-suppressor-1 (RSU-1), a cell-ECM adhesion protein, was shown to be upregulated as a response to increasing stiffness. Interestingly, tumor spheroids knockdown for RSU-1 or actin polymerization regulator (VASP) lost their invasiveness through the 3D matrix[36, 51]. Matrix stiffening is also shown to induce fibroblast activation and migration, which leads to a fibrotic response setting a positive feedback to matrix

stiffness[13, 14, 40, 52, 53]. However, in these studies it cannot be distinguished explicitly whether the observed effects are emerged by increased cell-ECM adhesion sites owing to increased ECM density, or by stiffness-induced solid stress generation.

1.2.2 Experimental setups studying the effect of solid stress in vitro

While the role of ECM stiffness in both cancer and stromal cells is actively studied, data regarding the effect of solid stress in tumor progression are elusive. There are several experimental setups that mimic the solid stress developed in the tumor microenvironment. These setups include models consisted of tumor spheroids growing in a confined environment that induce the development of solid stress[54-61], and models employing a transmembrane pressure device that applies a mechanical compression on a cell monolayer or on single cells embedded in a matrix[62 57, 63, 64] (**Figure 1-4 (B)).**

Regarding the first method, cancer cells are growing as spheroids in a polymer gel (e.g. agarose) and the surrounding matrix resists to its expansion by developing a solid stress acting to the spheroid (**Figure 1-4 (B),** ***(i)***). Helmlinger et al. (1997) using spheroids of colon adenocarcinoma cells, estimated that the accumulated solid stress was in the range of 45-120 mmHg (6-16 kPa), which depended on the concentration of the agarose gel and the size of the spheroid[54]. In an analogous study, Cheng et al. (2009) estimated the solid stress to be around 28 mmHg (3.73 kPa), when 67NR mammary carcinoma cell spheroids were growing in a 0.5% agarose matrix for 30 days[57]. In these studies was shown that increasing compressive stress inhibited tumor growth[54, 56-58], however this effect was resumed when loads were removed[54, 57]. It was also observed that solid stress can regulate tumor morphology, since mechanical loads can induce apoptotic cell death through the

mitochondrial pathway in regions with high compressive stress and allow proliferation in low-stress regions of the tumor spheroid[57].

More recent studies developed novel techniques to mimic solid stress developed during tumor growth in the absence of a matrix. Alessandri et al. (2013) employed a microfluidic method based on the encapsulation and growth of cells inside permeable, elastic and hollow microspheres[59] (**Figure 1-4 (B),** ***(ii)***). This approach offered the ability to produce size-controlled multicellular spheroids growing in confined conditions. Specifically, they found that the confined spheroids exhibited a necrotic core compared with the unconfined spheroids. In contrast, peripheral cells were more proliferative and highly migratory, suggesting that mechanical cues from the surrounding microenvironment may trigger cell invasion from a growing tumor[59]. Desmaison et al. (2013) designed polymer polydimethylsiloxane (PDMS) microdevices to restrict the growth of spheroids and subsequently to induce the development of mechanical stress[60] (**Figure 1-4 (B),** ***(iii)***). They showed that the mitosis of mechanically confined spheroids was suppressed in comparison to spheroids grown in suspension[60]. Furthermore, it was demonstrated that a population of cells within the confined tumor spheroids was arrested at mitosis, which was due to the inhibition of bipolar spindle assembly[60]. Later, Fernandez-Sanchez et al (2015) developed a method that allows the delivery of a defined mechanical pressure *in vivo*, by subcutaneously inserting a magnet close to the mouse colon[61]. The implanted magnet generates a magnetic force on ultra-magnetic liposomes, stabilized in the mesenchymal cells of the connective tissue surrounding colonic crypts after intravenous injection[61]. The magnetically induced pressure was similar in magnitude to the endogenous stress in the order of 9.0 mmHg (1.2 kPa), without affecting tissue stiffness, as monitored by ultrasound strain imaging and shear wave elastography[61]. The magnetic pressure stimulated Ret activation

and the subsequent phosphorylation of b-catenin, impairing its interaction with the E-cadherin in adherens junctions[61]. These data suggested that tumor progression could be driven by signaling pathways that are directly activated by mechanical pressure.

In order to study the effect of a predefined solid stress on cancer cells, the transmembrane pressure device has been introduced (**Figure 1-4 (B),** ***(iv)***). Setups employed consist of a transwell insert that fits in a well of a 6-well culture plate. The insert is separated in the lower chamber containing culture medium and the upper chamber containing the cell monolayer. A piston of a preferable weight is applied on the cell monolayer, while the water, nutrients and oxygen from the culture media are freely diffused through the pores of the transmembrane. This device provides a tool to mimic the solid stress in a preferable and predefined manner according to the stress magnitudes measured in native tumor tissues.

Munn's team (2009) used this device to study the effect of solid stress on murine mammary carcinoma cells. In this study, they applied a stress ranging from 0 mmHg-60 mmHg (0-8 kPa) and they observed increased apoptosis with increased stress levels[57]. In a following study, they used the same experimental setup to study the migration of cancer cells using a scratch wound assay[64]. They applied a maintained stress of 5.8 mmHg (0.77 kPa) and they concluded that in these levels of compression cancer cells stopped proliferating and started to create a leader cell formation, which allowed them to move toward the scratch having an invasive phenotype[64]. Mitsui et al. (2006) used a similar device for bone osteosarcoma cells, in order to identify the effect of compressive stress on the expression of matrix metalloproteinases (MMPs) and plasminogen activators (PARs). These proteins degrade the extracellular matrix and have a role in bone resorption and formation, as well in the migration of cancer cells. Scientists have observed enhanced protein and mRNA levels

of these molecules, under low mechanical compression of bone cells (0-2.20 mmHg or 0-0.29 kPa)[63].

Another device that was developed in order to study the effect of solid stress in a more realistic way involved the use of single cancer cells growing in an agarose matrix (**Figure 1-4 (B)-*(v)***). This device was composed of two custom-made parts, the well pressor and the optic pressor[62]. Both devices consisted of a chamber containing a 3D gel with single cells embedded, a screw and a nut for pressure application, and their housing support. Specifically, the well pressor applied a strain that compressed the cell-contained agarose gels to 50% of their original volume. This stress was maintained for 3 hours, and was estimated to be ~0.37 mmHg (~0.05 kPa), much smaller than normal loads measured by other studies[10, 54, 57, 62]. However, this stress was high enough to cause differential gene expression profiles of metastasis-associated genes in glioblastoma and breast cancer cells. In addition, the optic pressor provided a quantification of changes in cell circularity and orientation with respect to the direction of the applied force. In particular, cells were found to adopt an oval morphology and perpendicular orientation to the direction of the applied force, after the application of the compressive strain[62]. **Figure 1-4 (C)** summarizes all the *in vitro* and *in vivo* studies aimed to investigate the role of solid stress in tumor progression and their main biological outcome.

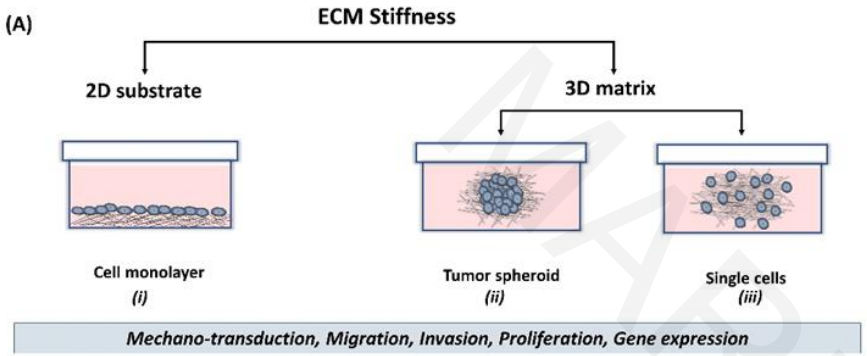

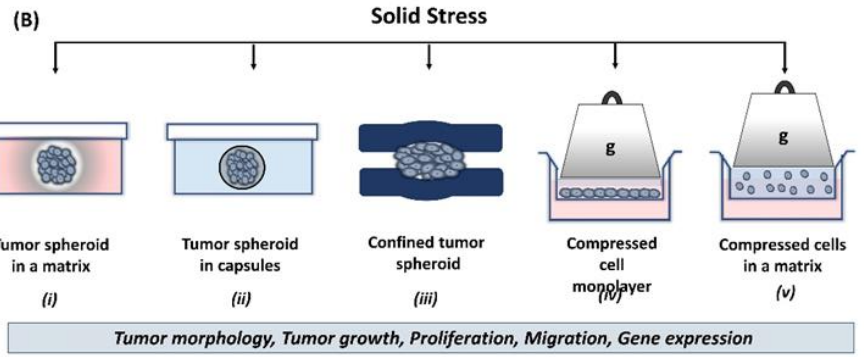

(C)

Summary of studies revealing the effect of solid stress in tumor progression

Study	Experimental Setup	Cancer Model	Level of solid stress		Biological Outcome
			Stress Applied	Stress Estimated	
Helmlinger G., et al., Nature Biotechnology (1997)	Figure 2B (ii)	Human colon adenocarcinoma, Murine mammary carcinoma, Rat rhabdomyosarcoma cancer cells	–	45-120 mmHg (6-16 kPa)	Estimation of growth-induced solid stress and how it affects tumor growth
Mitsui N., et al., Life Sciences (2006)	Figure 2B (iv)	Bone osteosarcoma cancer cells	0.4-2.2 mmHg (0.05-0.29 kPa)	–	Effect of solid stress on gene expression
Cheng G., et al., PloS one (2009)	Figure 2B (i), (iv)	Human breast cancer cells	0-60 mmHg (0-8 kPa)	~28 mmHg (3.7 kPa)	Estimation of growth-induced solid stress and how it affects tumor growth
Demou Z., Annals of Biomedical engineering (2010)	Figure 2B (v)	Human brain and breast cancer cells	0.37-1.87 mmHg (0.05-0.25 kPa)	–	Effect of solid stress on gene expression and cell shape
Tse J.M., et al., PNAS (2012)	Figure 2B (iv)	Human breast cancer cells	5.8 mmHg (0.77 kPa)	–	Effect of solid stress on cancer cell migration and invasion
Stylianopoulos T., et al., PNAS (2012)	*In vivo (In situ)*	Human melanoma, Human glioblastoma, Human fibrosarcoma, Human colon and pancreatic adenocarcinoma, Murine melanoma, pancreatic and mammary adenocarcinoma	–	2.8 to 60.1 mmHg (0.37–8.01 kPa)	Estimation of growth-induced solid stress and how solid stress affects drug delivery
Alessandri K., et al., PNAS (2013)	Figure 2B (ii)	Mouse colon carcinoma cells	15 mmHg (2 kPa)	15 mmHg (2 kPa)	Effect of solid stress on tumor growth and cancer cell migration
Desmaison A., et al., PloS one (2013)	Figure 2B (iii)	Human colorectal cancer cells	–	–	Effect of solid stress on tumor growth and cancer cell mitosis
Delarue M. et al., Biophysical journal (2014)	Figure 2B (i)	Human and mouse colon adenocarcinoma cells, Human breast cancer cells, Mouse sarcoma cells and Murine Schwann cells	37.5-75 mmHg (5-10 kPa)	–	Effect of solid stress on tumor growth and cell proliferation
Fernández-Sánchez M.E., et al., Nature (2015)	*In vivo*	Mouse colon adenocarcinoma	8.95 ± 4.95 mmHg (1.194 ± 0.660 kPa)	0-42 mmHg (0-5.6 kPa)	Effect of solid stress developed by tumor on the adjacent normal tissue
Nia H., et al., Nature Biomedical engineering (2016)	*In vivo (In situ)*	Breast, Pancreatic, Brain cancer models	–	1.56-52.5 mmHg (0.21-7 kPa)	Estimation of solid stress and its relationship with tumor and/or tissue stiffness

Figure 1-4. **Experimental methods employed to analyze the effects of stiffness and solid stress on cancer and stromal cells *in vitro*. (A**) Experimental setups studying the effect of ECM stiffness on cancer and stromal cells. There are two-dimensional models (2D), consisting of ***(i)*** a cell monolayer seeded on coating substrates (e.g. collagen type I or fibronectin) and three-dimensional models (3D) consisting of ***(ii)*** tumor spheroids or ***(iii)*** single cells embedded in a matrix (e.g. collagen type I, matrigel). Both models were aimed to investigate the effect of changes in extracellular rigidity on the transduction of mechanical signals into the cells as well as on the migration, invasion, proliferation and gene expression of cancer and stromal cells (**B**) Experimental setups studying the effect of solid stress on cancer and stromal cells. Setups include tumor spheroids that grow within ***(i)*** a polymer matrix, ***(ii)*** within elastic capsules or ***(iii)*** in a confined polymer device. In cases ***(iv)*** and ***(v)***, the set-ups are composed of cells seeded on the inner chamber of a transwell insert on the top of which an agarose cushion is placed, or are embedded in a polymer matrix. A piston with adjustable weight applies a predefined and measurable compressive solid stress on the cells. These models provided useful information about the direct effect of solid stress on tumor growth and morphology as well as on cancer cell proliferation, migration and gene expression. (**C**) A summary of the *in vitro* and *in vivo* studies revealing the effect of solid stress in tumor progression.

1.3 **Aim of this thesis**

Collectively, the above *in vitro* studies suggest that mechanical forces regulate tumor morphology, tumor growth as well as the metastatic potential of cancer cells in the absence of matrix stiffness. In light of recent studies showing that increased matrix stiffness and elevated solid stress are two distinct tumor abnormalities, and given the fact that most pertinent studies are focused on the effects of stiffness, it becomes clear that scientific efforts should turn to the implications of solid stress in tumor progression and metastasis in the absence of matrix stiffening[17, 24]. Regarding the solid stress-induced tumor progression, further studies are required to shed light upon the mechanisms by which solid stress is transmitted and guides cellular behaviour of cancer cells and CAFs, that are both experienced solid stress in the tumor microenvironment. CAFs exert contractile forces that contribute to the accumulation of solid stress in the tumor interior. Therefore, it is necessary to include both cell types when solid stress and ECM stiffness are being studied. It has been also shown that CAFs dynamically interact with cancer cells to promote tumor progression[65]. In fact, CAFs mediate the invasiveness of colon, pancreatic and breast cancer cells when co-injected into mice[23, 65-68], while breast and prostate tumors containing CAFs grew faster than tumors injected with normal fibroblasts[69, 70]. Nevertheless, there is no pertinent study considering the effect of solid stress on the interaction of cancer cells and CAFs, and vice versa the implication of tumor-stromal interactions in ECM stiffening and solid stress accumulation. For these reasons, the objectives of this thesis are related to (i) identify whether and how solid stress affects the activation, viability and gene expression of human normal fibroblasts, (ii) examine whether and how solid stress is implicated in the crosstalk between fibroblasts and cancer cells, ultimately affecting cancer cell behavior (i.e., migration) and (iii) investigate whether solid stress can directly affect the viability, migration

and gene expression of human pancreatic and brain cancer cells. We are mainly focused on pancreatic and brain tumor models, which along with breast and colon tumors are known to be exposed to high solid stress levels *in vivo*, however data regarding the effect of solid stress on these tumor types have not been elucidated yet.

2 Chapter 2: Solid stress facilitates fibroblasts activation to promote pancreatic cancer cell migration

This research has been published in Annals of Biomedical Engineering: **Maria Kalli**, Panagiotis Papageorgis, Vasiliki Gkretsi and Triantafyllos Stylianopoulos. Solid stress facilitates fibroblasts activation to promote pancreatic cancer cell migration. Ann Biomed Eng. 2018 May;46(5):657-669 [doi: 10.1007/s10439-018-1997-7].

2.1 **Introduction**

Pancreatic cancer is among the deadliest forms of cancer worldwide [71]. Most pancreatic tumors contain an extremely dense extracellular matrix (ECM) and have already been characterized for the presence of high solid stress levels [17].

As described in the previous section, several studies have dealt with the effect of compressive stress on breast and colon cancer cells [54, 57, 58, 62, 64] using different experimental setups. To date, results indicated that solid stress impairs cancer cell proliferation and promotes cancer cell migration [54, 55, 57, 58, 62, 64], however there are no studies taking into account the effect of solid stress on other cellular components of the tumor microenvironment, such as fibroblasts. In fact, tumor fibroblasts are increasingly gaining ground as an important component of tumor microenvironment [4]. This is based on the fact that fibroblasts continuously produce fibrillar proteins such as fibronectin and collagen type I providing cell-matrix interactions which in turn promote cancer cell invasion through the extracellular matrix [4, 72, 73]. At the same time, they remodel the ECM organization by altering fibers orientation and by producing matrix degrading proteins, such as matrix metalloproteinases (MMPs). These events enable cancer cells to migrate and invade into the matrix in order to escape the highly desmoplastic primary tumor site[4, 5, 65, 73, 74]. Moreover,

fibroblasts secrete cytokines and growth factors, such as Transforming Growth Factor-β (TGFβ), that directly promote the proliferation and migration of cancer cells[4, 72, 75]. Indeed, in an orthotopic model of pancreatic cancer, the size of the primary tumor as well as the number of distant metastasis were greater when cancer cells were co-injected with fibroblasts [68, 76]. Thus, it is well established that tumor-infiltrated activated fibroblasts dynamically interact with cancer cells to promote tumor progression and malignancy [68, 70, 77], nevertheless it is still unclear whether solid stress affects these tumor-stromal interactions.

A plausible hypothesis is that solid stress regulates the expression of specific factors in fibroblasts, which in turn mediates cancer cell behaviour. One such candidate could be the Growth Differentiation Factor 15 (*GDF15*), which is known to regulate responses to cellular stress as well as responses to morphological and cytoskeletal changes, but it has never been linked to solid stress [78, 79]. *GDF15*, also known as macrophage inhibitory cytokine 1 (*MIC-1*), belongs to the TGFβ superfamily of cytokines and has attracted much attention because of its role in several physiological or pathological processes [78]. More specifically, GDF15 has been reported to play a dual role in cancer, either by inducing apoptosis and inhibiting tumor growth [80] or by stimulating cancer cell proliferation, invasion and metastasis [81]. Moreover, GDF15 has been found to be upregulated in several aggressive tumor types including glioblastoma, pancreatic, prostate, breast and colorectal, while high levels of GDF15 in serum samples from cancer patients have been associated with poor prognosis and patient survival [82-86]. Interestingly, recent studies have indicated that fibroblast-derived GDF15 stimulates prostate cancer cell growth, migration and invasion *in vitro* and *in vivo* [87], however the underlying molecular mechanism that promotes GDF15 upregulation in the tumor microenvironment remains elusive.

Hence, in order to investigate the effect of solid stress on fibroblasts and its implication in tumor-stromal interactions, we used as a model the pancreatic cancer as this type of tumor contains an extremely dense extracellular matrix (ECM) consisting mainly of collagen and hyaluronan and has already been characterized for the high solid stress levels. In addition, we employed a previously described transmembrane pressure device [57, 63, 64] to simulate the compressive solid stress encountered in the tumor microenvironment [5, 10, 17]. Using this experimental setup, we were able to identify the molecular effect of a defined compressive stress on normal pancreatic fibroblasts, as well as on two distinct pancreatic cancer cell lines, CFPAC-1 and MIA PaCa-2, using a novel co-culture system.

2.2 **Methods**

Cell culture. Human normal pancreatic fibroblasts were obtained from Neuromics (Edina, MN) and were maintained in Vitro Plus III medium (Neuromics) supplemented with 1 % antibiotics. MIA PaCa-2 and CFPAC-1 pancreatic cancer cell lines were obtained by American Type Culture Collection (ATCC) and were cultured in Dulbecco's Modified Eagle's Medium (DMEM) supplemented with 10 % Fetal Bovine Serum (FBS) and 1 % antibiotics. For co-culture experiments, both cell lines were cultured in 2 % FBS-containing DMEM. All cells were incubated at 37ºC and 5 % CO_2 in a humidified incubator.

In vitro transmembrane pressure device. For the application of a defined and controlled compressive solid stress on fibroblasts, we employed a previously described transmembrane pressure device used in pertinent studies [57, 63, 64]. Briefly, 2-4x10^5 cells were cultured overnight in the inner chamber of a 24 mm diameter transwell insert (Greiner Bio-one,) with 0.4 μm pores, which permits nutrient and oxygen diffusion and prevents cell migration. A 2 % low melting agarose cushion was placed on top of the cells preventing any

direct contact between piston and cells and providing a uniform distribution of the applied force. A 24 mm diameter piston of adjustable weight was placed on the top of the agarose gel (**Figure 2-1A**) and the cells were subjected to 1.0, 2.0, 4.0 or 6.0 mmHg stress for 6 hours, or to 4.0 mmHg stress for 48 hours. These solid stress levels were lower but similar in magnitude to those estimated in pancreatic tumors [11, 17], as very high levels of solid stress were shown to cause significant cell death [57, 64]. Control cells were covered with an agarose cushion only (i.e., 0.0 mmHg).

Co-culture experiments. For the co-culture experiments, approximately $2x10^5$ fibroblasts or *GDF15*-knockdown fibroblasts and MIA PaCa-2 or CFPAC-1 cells, were separately seeded in transwell inserts and 6-well plates, respectively. After overnight incubation, cells were set in a co-culture system and fibroblasts were subjected to a compression of 4.0 mmHg (**Figure 2-1B**). Cells were allowed to grow for 48 hours in 2 % FBS-containing DMEM at 37 ^oC and 5 % CO_2 in a humidified incubator.

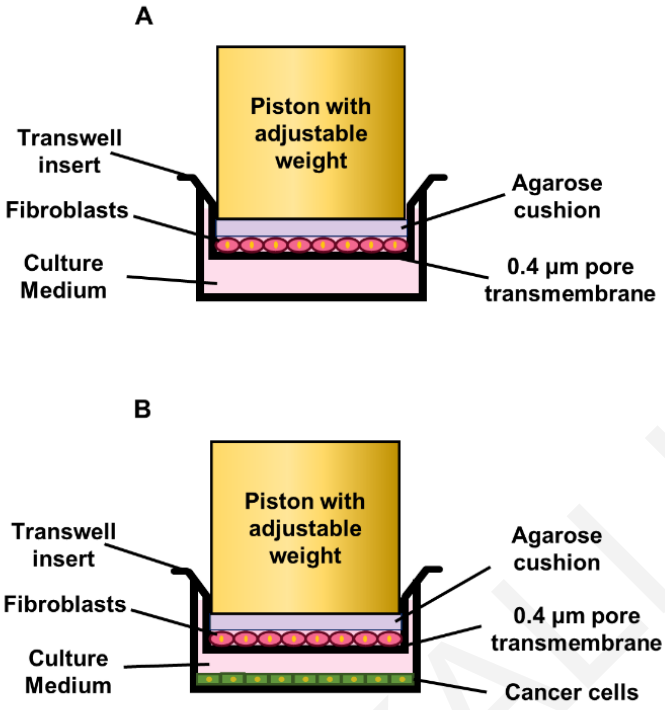

Figure 2-1. **A schematic of the *in vitro* transmembrane pressure device**. **(A)** Fibroblasts were grown as a monolayer on the transmembrane of a 0.4 µm transwell insert and a piston of adjustable weight was applying a compressive stress. Control cells were covered with an agarose cushion only. **(B)** The experimental set-up of the co-culture system consisted of fibroblasts and pancreatic cancer cells (MIA PaCa-2 or CFPAC-1) in the upper and lower chamber of a transwell insert, respectively. A piston with adjustable weight, applying 4.0 mmHg of compressive stress on fibroblasts for 48 hours is shown. A co-culture system consisting of fibroblasts and cancer cells without a compressive load was used as a control.

Alamar Blue Assay. Fibroblasts were subjected to a cell viability test following compression using Alamar Blue reagent (Thermo), according to the manufacturer's instructions.

Quantitative Real Time PCR. Total RNA was extracted from both fibroblasts and cancer cells using Trizol (Invitrogen) and reverse transcribed to cDNA using Superscript Reverse Transcriptase (Invitrogen). Quantification of gene expression was performed by real-time PCR using SYBR Green Supermix (KAPA Biosystems) in a real-time PCR

detection system (BioRad). The primers for the *β-actin* housekeeping gene were used as an internal control. Each sample was measured in triplicate for each gene. The relative quantification of gene expression was analyzed by the ΔΔCt quantification method, using a relevant calibrator as specified in each figure legend. Real-time PCR primers for target genes are listed in **Table 1, in Appendices.**

Western Blotting. For protein expression analysis, total cell lysates from fibroblasts compressed by 4.0 mmHg for 48 hours were obtained using radio immunoprecipitation assay (RIPA) buffer containing a protease inhibitor cocktail tablet (Sigma). Protein concentration was determined by the BCA protein assay kit (Pierce) and cell lysates were run on a 12 % acrylamide gel and transferred to a PVDF membrane using the BioRad Semi-dry transfer system. Membrane was blocked in 5 % non-fat milk or Bovine Serum Albumin (BSA) in TBS-T buffer and then incubated with anti-alpha-smooth muscle actin (a-SMA) (Abcam), anti- Collagen I (Abcam) or anti-GDF15 (Cell signalling) antibodies overnight. Following standard western blot procedure steps, the detection of antibodies was performed with enhanced chemiluminescent system (Pierce) using Kodak Biomax light films. Relative protein expression of GDF15, Collagen I and a-SMA was quantified with β-tubulin or β-actin as loading control using ImageJ software. The mean relative protein expression from different immunoblots from at least 2 independent experiments was used.

Immunofluorescence staining. To determine the effect of compression on a-SMA protein expression in fibroblasts, cells were fixed in 4% paraformaldehyde, permeabilized in PBS containing 0.25 % Triton X-100 and blocked with PBS containing 0.1 % Tween-20 and 1 % BSA. Cells were then stained with anti-a-SMA (Abcam) or anti-Collagen I (Abcam) antibody diluted in blocking buffer for 1 hours at room temperature.

Alexa 647-donkey anti-rabbit antibody was used as a secondary antibody and nuclei were stained using DAPI. Images were obtained using an Olympus BX53 fluorescent microscope.

Cloning of shRNA-expressing vector and transient transfection of fibroblasts. To generate vectors expressing shRNA against *GDF15*, AgeI/EcoRI-digested pLKO.1-puro vector was ligated with 58-base pair annealed oligos. The sequence of the forward oligo was CCGGGCAAGAACTCAGGACGGTGAACTCGAGTTCACCGTCCTGAGTTCTTGCTTTTTG and sequence for the reverse oligo was AATTCAAAAAGCAAGAACTCAGGACGGTGAACTCGAGTTCACCGTCCTGAGTTCTTGC. Ligated plasmids were transformed into XL10 gold competent bacteria and selected on ampicillin-containing LB agar plates (100µg/ml). Single colonies were grown for 16 hours in LB broth and plasmids were isolated using a NucleoSpin® Plasmid QuickPure kit (Macherey-Nagel). The presence of each insert was tested by PCR (KAPA Biosystems) using pLKO.1 Forward primer: GGAATAGAAGAAGAAGGTGGA and GDF15 Reverse primer: GCAAGAACTCAGGACGGTGAA. Following verification by DNA sequencing (Macrogen, Netherlands), transient transfection of fibroblasts was performed with pLKO-shScrambled vector (or shSCR, used as a control) or pLKO-shGDF15 vector using Lipofectamine 2000 transfection reagent (Invitrogen) according to manufacturer's guidelines. Cells were allowed to grow overnight in antibiotics-free medium before the co-culture with cancer cells.

Wound Healing assay. A wound healing assay was performed on cancer cells co-cultured with compressed or uncompressed fibroblasts based on published protocols [88]. By the end of the co-culture period, fibroblasts were removed from the co-culture system, conditioned medium was collected, centrifuged to remove cell debris and stored at 4 ^{o}C until

use. Cancer cells were then washed twice with PBS followed by treatment with 10 μg/mL Mitomycin-C in 2 % FBS-containing medium 2 hours prior to the generation of the wound in order to avoid any effect of cell proliferation in wound closure. Cell-free space was then created by generating a wound on the monolayer with a 200 μL pipette tip and cells were washed twice with PBS to remove debris. Cells were subsequently stimulated with the corresponding conditioned medium for 24 hours, which is thought to include all secreted factors. Images from 4 different fields per condition were taken at 0 hours and 24 hours. The cell-free area from at least 2 independent experiments was quantified using the ImageJ software. Quantification was performed for each condition using the following formula:

(Width of the wound at 0 hours – Width of the wound at 24 hours) / (Width of the wound at 0 hours).

Enzyme-linked immunosorbent assay (ELISA). Enzyme-linked immunosorbent assay (ELISA) was performed in conditioned medium from the co-culture system upon completion of the co-culture period, using the Quantikine ELISA human GDF15 (R & D systems,) following the company's guidelines.

Statistical Analysis. Results are represented as mean ± standard error (SE). Significant changes were determined by Student's *t*-test using two-tail distribution. Differences with *p*-values <0.05 were considered as significant (indicated by an asterisk *).

2.3 Results

Solid stress regulates gene expression of normal pancreatic fibroblasts. In order to study the effect of solid stress on normal pancreatic fibroblasts, cells were subjected to a constant mechanical compression similar in magnitude to that

experienced by cells in the tumor interior [17], using an established transmembrane pressure device [57, 63, 64] (**Figure 2-1A**). Cells were exposed to a stress ranging from 1.0 to 6.0 mmHg [17] and the expression of several genes known to be upregulated in tumor-infiltrated activated fibroblasts was evaluated by qPCR. First, we tested the expression of *TGFβ* which has been shown to be implicated in ECM synthesis and mediates cancer cell proliferation and migration [89]. Moreover, we measured the mRNA expression of genes encoding proteins of the ECM, such as *Collagen I* and *Fibronectin I*, as well as *Periostin*, which has been shown to regulate matrix elasticity, stimulates the expression of ECM proteins and promotes cancer progression [44, 90-92]. Our results revealed a trend for increased mRNA expression in all these genes in response to increasing levels of mechanical compression (**Figure 2-2, dashed red line**). More specifically, a modest but significant increase in the expression of *TGFβ, Collagen I, Fibronectin I and Periostin* (**Figure 2-2A-2D**) was more pronounced when cells were subjected to stresses ranging from 2.0 to 6.0 mmHg. However, within the same range of compression, *GDF15* which regulates cellular responses to stress [79] exhibited the highest mRNA expression of all genes tested (**Figure 2-2E)**. Interestingly, *a-SMA*, one of the most established markers for fibroblast activation [4], was upregulated when cells were compressed from 1.0 to 6.0 mmHg (**Figure 2-2F**), suggesting that fibroblasts can immediately get activated, as early as 6 hours post application without any effects in cell viability (**Figure 2-3A**).

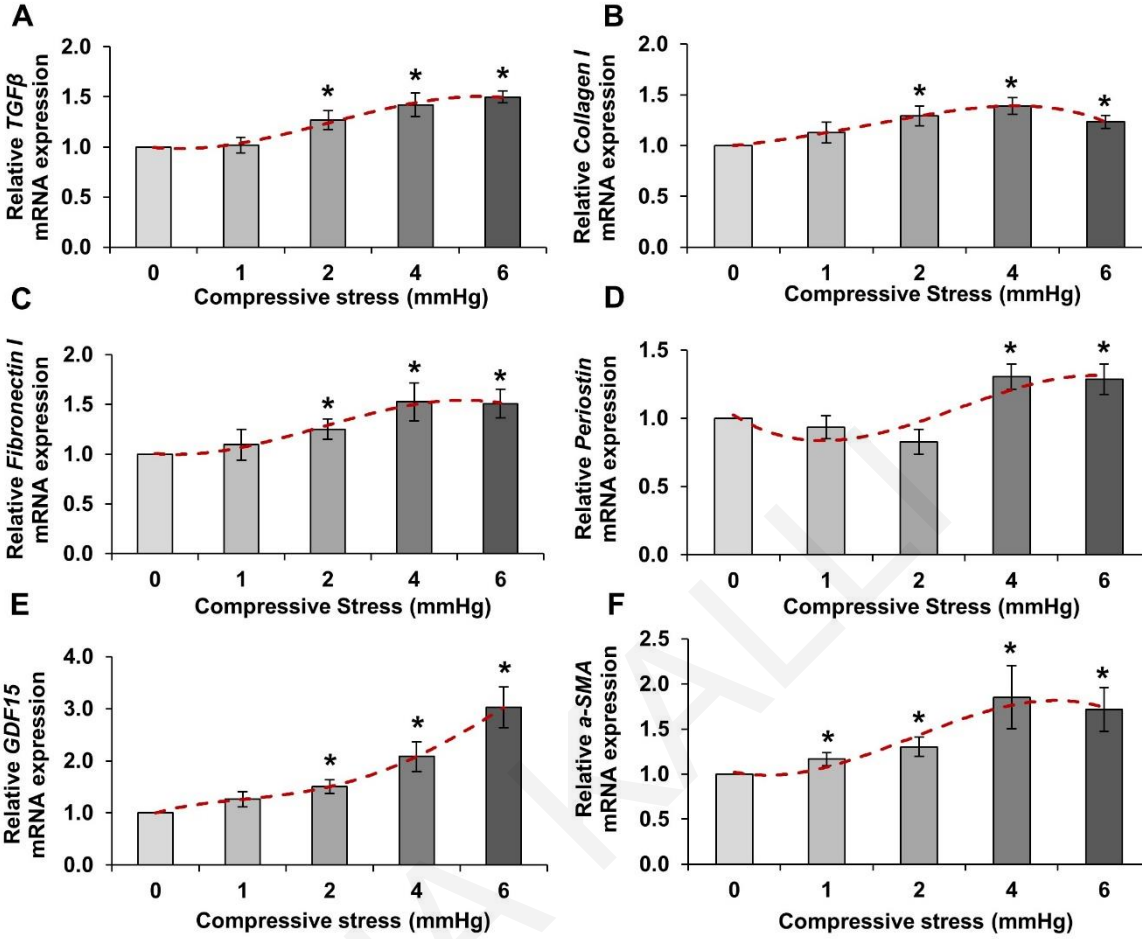

Figure 2-2. **Solid stress regulates gene expression of normal pancreatic fibroblasts**. Normal fibroblasts were subjected to 1.0, 2.0, 4.0 and 6.0 mmHg of compressive stress for 6 hours. qPCR was used to measure the mRNA expression of TGFβ (A), Collagen I (B), Fibronectin I (C), Periostin (D), GDF15 (E) and a-SMA (F). The expression in each sample was analyzed with the ΔΔCt method relative to the expression of control sample (cells compressed by the agarose cushion only). The mean fold change was calculated and plotted for each gene. Each bar indicates the mean fold change ±SE of two independent experiments (n=6). Asterisk (*) indicates a statistically significant difference ($p<0.05$).

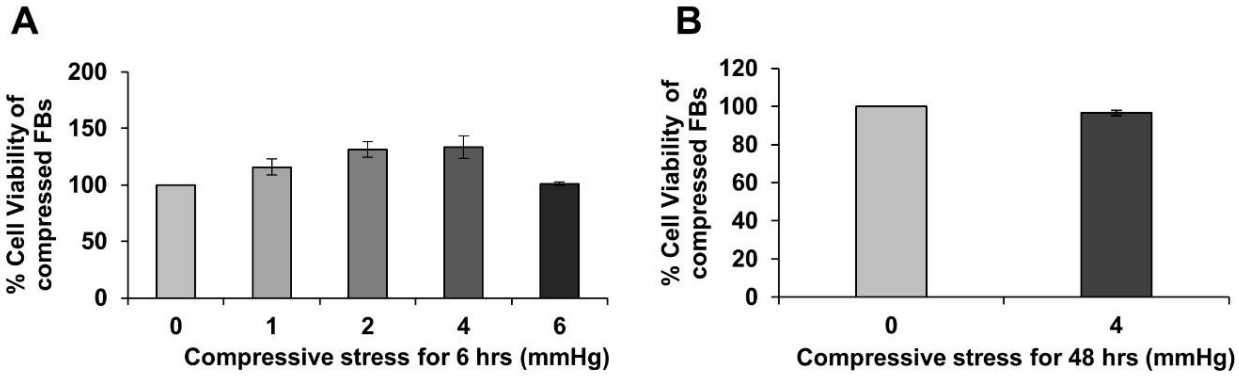

Figure 2-3. **Mechanical Compression does not affect the viability of fibroblasts. (A)** Fibroblasts were subjected to 1, 2, 4 and 6 mmHg of compressive stress for 6 hours, with the 0.0 mmHg sample be the negative control. Percentage of cell viability was quantified using the absorbance measured from Alamar Blue assay. No statistically significant differences were observed as compared with the negative control (n=3, *p<0.05). **(B)** Fibroblasts were subjected to 0.0 mmHg or 4.0 mmHg of compressive stress for 48 hours. By the end of the experiment absorbance was measured from Alamar Blue assay and cell viability was quantified using the uncompressed cells (0.0 mmHg) as a reference. No statistically significant difference was observed between uncompressed (0.0 mmHg) and compressed fibroblasts (4.0 mmHg) (n=3, *p<0.05).

Solid stress maintains fibroblasts activation, induces desmoplasia and upregulates the expression of GDF15. To examine whether fibroblasts remain activated after application of mechanical compression for longer time periods, we repeated the experiment for 48 hours using the 4.0 mmHg stress condition, as this was the minimum stress condition in which *a-SMA* exhibited the highest mRNA expression level (**Figure 2-2F**). Under these experimental conditions, *a-SMA*, *GDF15 and Collagen I* were upregulated, not only at the RNA (**Figure 2-3A-3C**) but also at the protein level (**Figure 2-3D-3F)**. Quantification of protein levels is shown in **Figure 2-3G-3I**. The expression of *a-SMA* and *Collagen I* was also evaluated by immunofluorescence staining, which confirmed that these proteins become upregulated in compressed compared to uncompressed cells (**Figure 2-3J**). Consistent with the data from the short-term application

of stress (**Figure 2-2**), the expression of *TGFβ, Fibronectin I* and *Periostin* exhibited a modest increase at the mRNA level (**Figure 2-5**), while cell viability showed no significant difference between compressed and uncompressed fibroblasts (**Figure 2-1B**). Collectively, our findings suggest that solid stress not only stimulates but also maintains the activation of fibroblasts, which subsequently can produce larger amounts of fibrillar proteins such as Collagen I. In addition, solid stress strongly upregulates the expression of *GDF15*, and to a lesser extent it induces the expression of genes implicated in ECM synthesis.

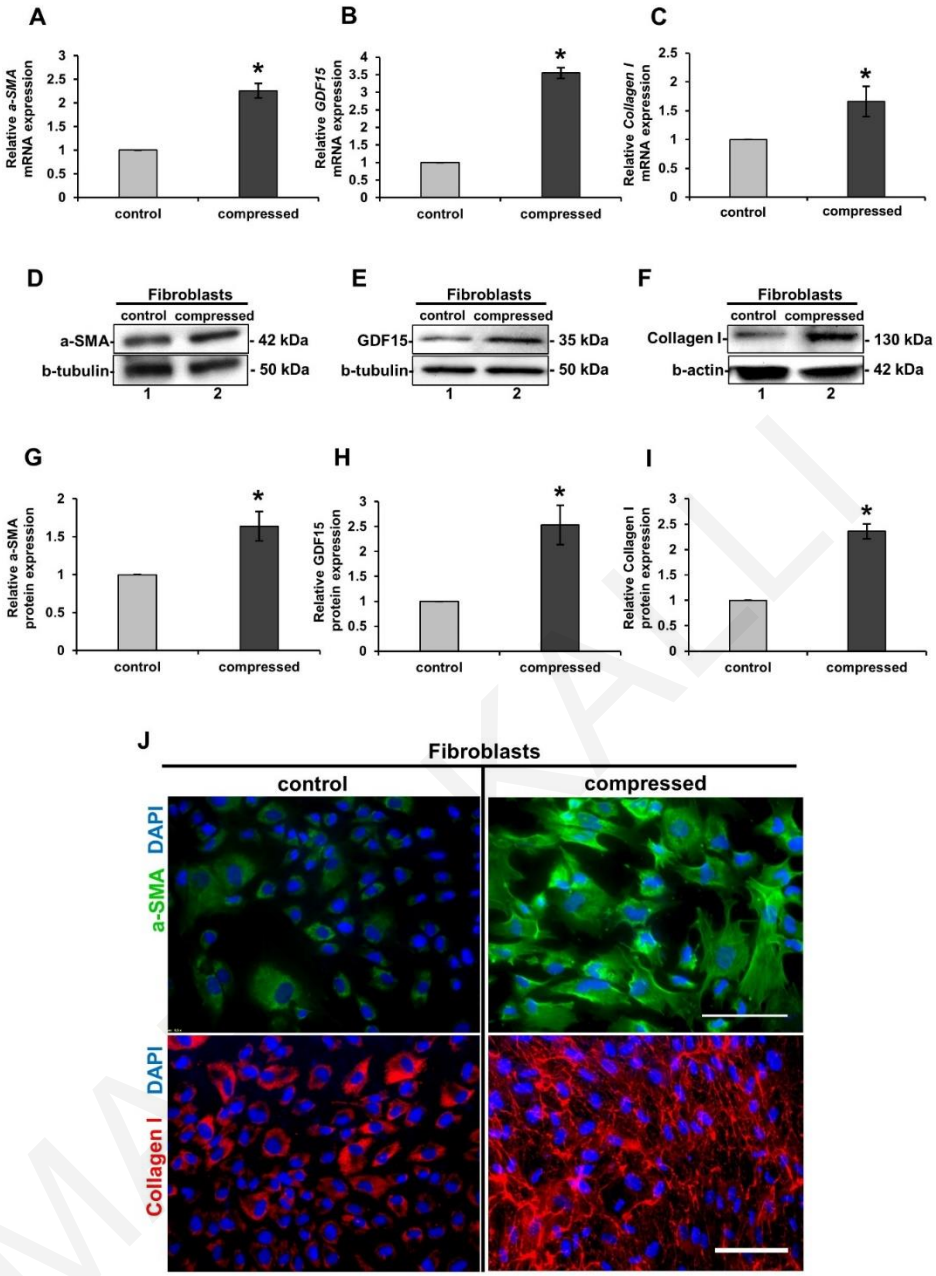

Figure 2-4. **Solid stress maintains fibroblasts activation, induces Collagen I expression and upregulates the expression of *GDF15*. (A-C)** Fibroblasts were compressed at 4.0 mmHg for 48 hours and total RNA and protein were extracted. qPCR was used to measure *a-SMA (A), GDF15 (B)* and *Collagen I (C)* mRNA expression. The expression in each sample was calculated with the ΔΔCt method using the expression of uncompressed cells as a reference. Each bar indicates the mean fold change ±SE of three independent experiments (n=9); **(D-F)** Representative western blot showing a-SMA (D), GDF15 (E) and Collagen I (F) protein expression. B-tubulin or β-actin was used as a loading control. **(G-I)** Quantification of a-SMA (G), GDF15 (H) and Collagen I (I) protein expression was normalized to the β-tubulin or β-actin loading control using the ImageJ software. The mean intensity was quantified from 3 immunoblots (n=3); **(J)** Representative immunofluorescent staining of fibroblasts with anti-a-SMA antibody (green), anti-Collagen I (red)

and DAPI (blue) for visualization of the nuclei. Pictures for a-SMA and Collagen I were taken under 40x and 20x objective respectively, using an Olympus BX53 fluorescent microscope. Scale bar: 0.1 mm. Asterisk (*) indicates a statistically significant difference ($p<0.05$).

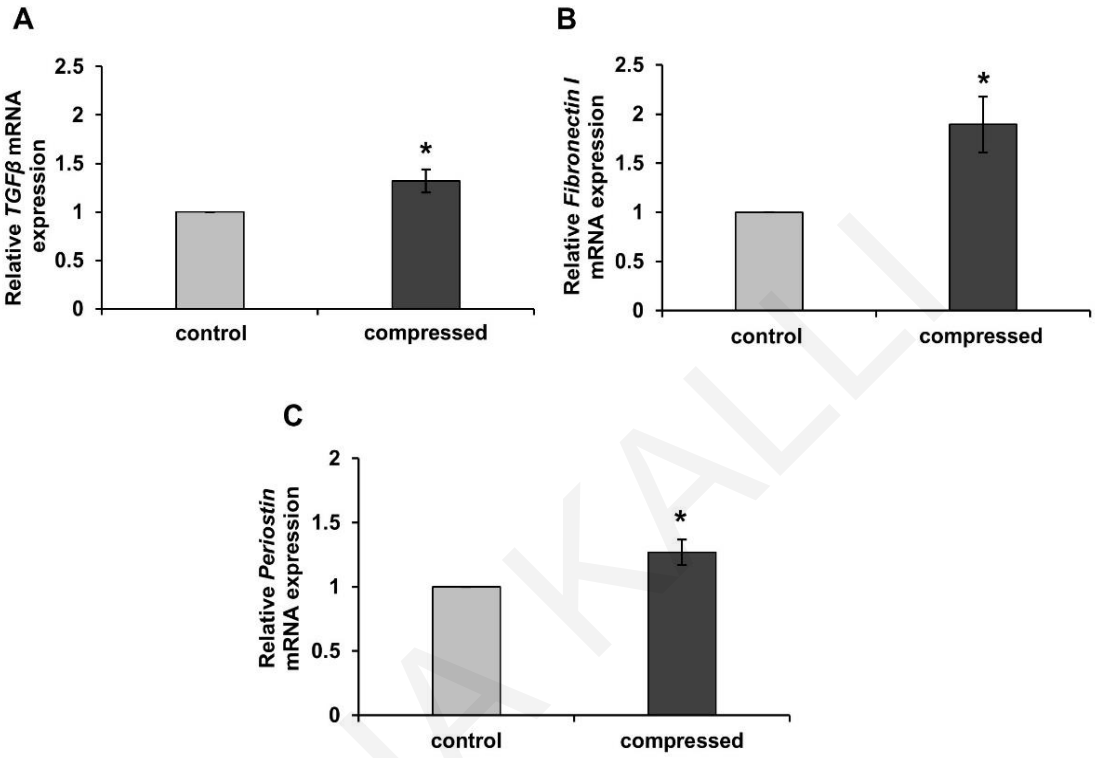

Figure 2-5. **Mechanical Compression upregulated the gene expression of fibroblasts after 48 hours of application.** Total RNA was isolated from uncompressed (0.0 mmHg) and compressed (4.0 mmHg) fibroblasts after 48 hours. RNA was reverse transcribed into cDNA and qPCR was used to measure the expression of *TGFβ* (A), Fibronectin *I* (B) and *Periostin* (C). The expression in each sample was analyzed with the ΔΔCt method relative to the expression of uncompressed fibroblasts. The mean fold change was calculated and plotted for each gene. Each bar indicates the mean fold change ±SE of two independent experiments (n=6); *$p<0.05$.

Mechanical compression activates normal fibroblasts to promote the migration of CFPAC-1 and MIA PaCa-2 pancreatic cancer cells. .

It has been proposed that tumor-infiltrated activated fibroblasts interact with cancer cells to promote tumor growth and invasion [87], hence we wanted to test whether fibroblasts

activation by mechanical compression affects adjacent cancer cells through fibroblasts-derived factors, such as GDF15[87]. To this end, we developed a novel co-culture system (**Figure 2-1B)** which consists of compressed fibroblasts and two distinct pancreatic cancer cell lines, CFPAC-1 or MIA PaCa-2 **(see Figure 2-6A for the experimental design**). In this setup, cells were allowed to interact for 48 hours and then a wound healing assay was performed on cancer cells. Both cell lines were pretreated with mitomycin-C, in order to avoid any effect on wound closure due to cancer cell proliferation. As presented in **Figure 2-7A**, both pancreatic cell lines exhibited higher migratory ability when co-cultured with compressed compared to uncompressed fibroblasts (**Figure 2-7A-7C**). Interestingly, this was associated with the higher *GDF15* mRNA expression in compressed fibroblasts co-cultured with CFPAC-1 and MIA PaCa-2 (**Figure 2-7D**). This result indicated that secreted GDF15 may act in a paracrine fashion to stimulate the migration of adjacent cancer cells. However, to eliminate the possibility that GDF15 could be secreted by cancer cells and act in an autocrine manner, we tested its expression in cancer cells. Real-time PCR analysis showed that *GDF15* mRNA levels were unchanged when both CFPAC-1 or MIA PaCa-2 were co-cultured with uncompressed or compressed fibroblasts (**Figure 2-7E**). Moreover, to verify whether GDF15 is produced and secreted by fibroblasts, we performed ELISA to quantify GDF15 protein levels in the conditioned medium. We found that GDF15 was present in higher concentration when MIA PaCa-2 cells were co-cultured with compressed fibroblasts compared to the system where cells were co-cultured with uncompressed fibroblasts (**Figure 2-7F**). Our results suggest that solid stress not only activates normal fibroblasts but it can also induce the secretion of GDF15 from them.

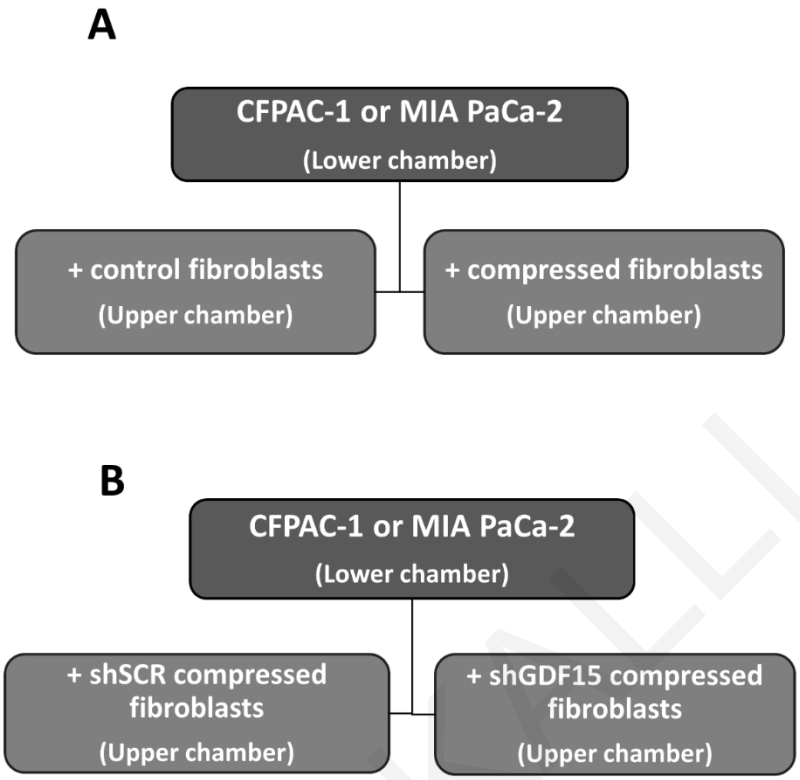

Figure 2-6. **Diagrammatic representation showing the experimental design of co-culture systems. (A)** CFPAC-1 or MIA PaCa-2 were co-cultured for 48 hours with compressed fibroblasts (4.0 mmHg) on the lower and upper chamber of a transwell insert, respectively. Co-culture of CFPAC-1 or MIA PaCa-2 with uncompressed fibroblasts (agarose cushion only) was used as a control condition. **(B)** CFPAC-1 or MIA PaCa-2 were co-cultured for 48 hours with compressed fibroblasts (4.0 mmHg) transfected with shGDF15 vector on the lower and upper chamber of a transwell insert, respectively. Co-culture of CFPAC-1 or MIA PaCa-2 with compressed fibroblasts transfected with shSCR vector (control) was used as a control.

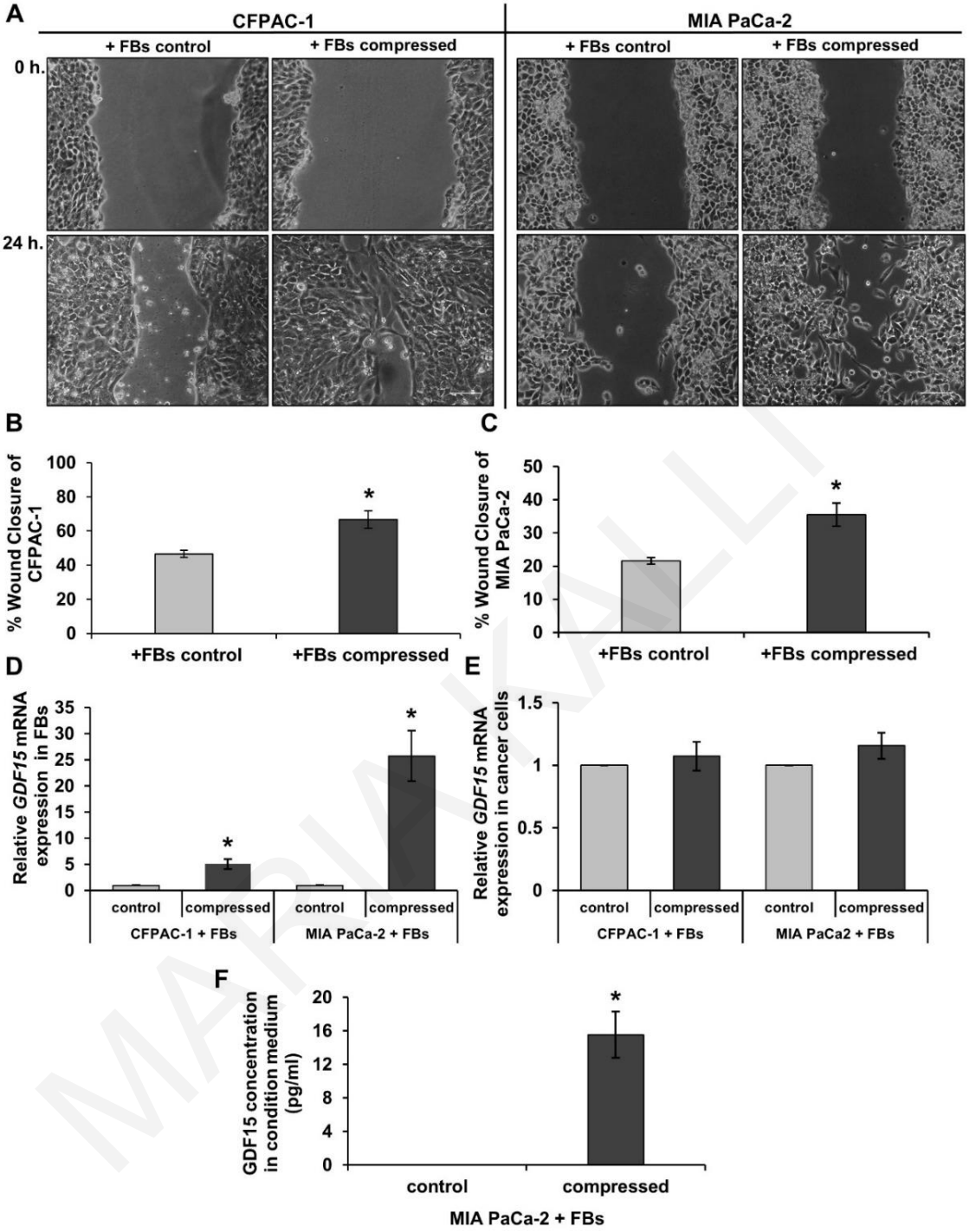

***Figure 2-7*. Compression-induced activated fibroblasts stimulate the migration of CFPAC-1 and MIA PaCa-2 pancreatic cancer cells**. **(A)** Control and compressed fibroblasts (FBs) were co-cultured with CFPAC-1 (A) and MIA PaCa-2 (B) in 2 % FBS containing DMEM for 48 hours. FBs were then removed, and cancer cells were subjected to wound healing assay for 24 hours. Pictures were taken with Nikon Eclipse TS100 optical microscope. Scale bar: 0. 1 mm. **(B-C)** Graphs show the percentage of wound closure of CFPAC-1 (B) and MIA PaCa-2 (C) as quantified with the ImageJ software. At least 3 different images from three independent experiments were

analyzed. Asterisk (*) indicates a statistically significant difference in wound closure of CFPAC-1 or MIA PaCa-2 co-cultured with compressed FBs compared with CFPAC-1 or MIA PaCa-2 co-cultured with control FBs ($p<0.05$). **(D-E)** RNA was extracted from both FBs (D) and cancer cells (E), reversed transcribed into cDNA and qPCR was used to measure the *GDF15* mRNA expression in all cell lines. The expression in each sample was calculated with the ΔΔCt method using the expression of cells from the co-culture system of CFPAC-1 or MIA PaCa-2 with control FBs as a reference. Each bar indicates the mean fold change ±SE of at least three independent experiments (n=9); **(F)** Human GDF15 protein (pg/ml) secreted in the conditioned medium (y-axis) was quantified using ELISA. Two independent experiments were performed. Asterisk (*) represents a statistically significant difference ($p < 0.05$).

GDF15 secreted by compressed fibroblasts is required for the migration of CFPAC-1 and MIA PaCa-2 pancreatic cancer cells.

Finally, we investigated whether GDF15 expression and secretion from fibroblasts is necessary for pancreatic cancer cells to migrate. For this purpose, we constructed a plasmid vector expressing shRNA against *GDF15,* and transiently transfected fibroblasts to inhibit its upregulation by solid stress. We then co-cultured compressed fibroblasts, transfected either with shRNA against *GDF15* or scrambled shRNA (control), with CFPAC-1 or MIA PaCa-2 for 48 hours (**see Figure 2-6B for the experimental design**). A wound healing assay showed that neither CFPAC-1 nor MIA PaCa-2 cells could migrate when co-cultured with sh*GDF15*-transfected compressed fibroblasts compared to pancreatic cancer cells co-cultured with sh*SCR*-transfected compressed fibroblasts (**Figure 2-8A-8C**). Finally, real time PCR analysis and Western Blotting verified that *GDF15* was successfully silenced by shGDF15-expressing construct (**Figure 2-8D-8G**). Our results suggest that the upregulation and the subsequent secretion of GDF15 from fibroblasts as a response to solid stress are necessary for the migration of pancreatic cancer cells *in vitro*.

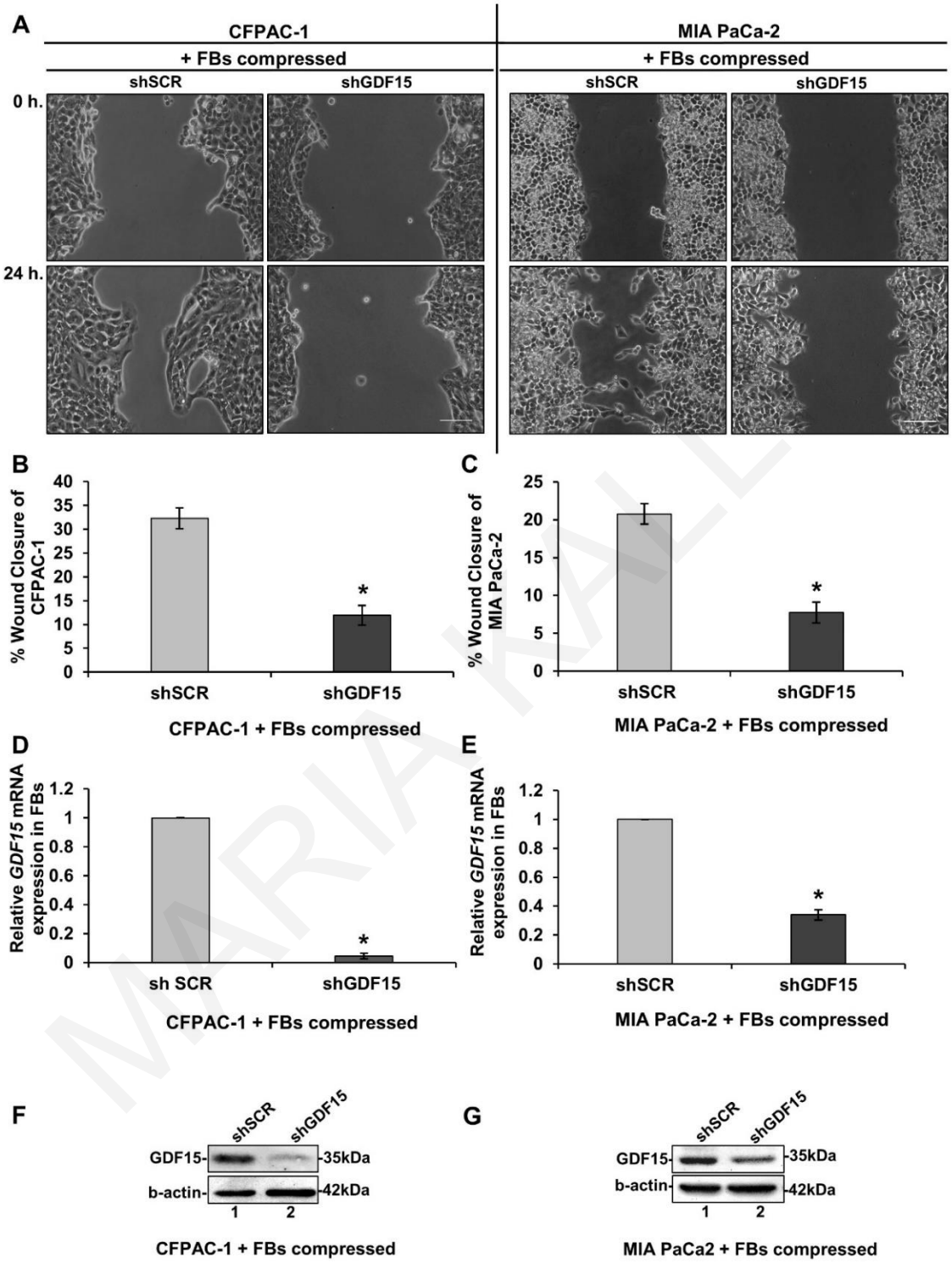

***Figure 2-8*. GDF15 secreted by compressed fibroblasts is required for the migration of CFPAC-1 and MIA PaCa-2 pancreatic cancer cells. (A)** Transfected fibroblasts (FBs) with shSCR (control) and shGDF15 vectors were compressed and co-cultured with CFPAC-1 (A) and

MIA PaCa-2 (B) in 2 % FBS containing DMEM for 48 hours. FBs were then removed and cancer cells were subjected to wound healing assay for 24 hours. Pictures were taken with Nikon Eclipse TS100 optical microscope. Scale bar: 0. 1 mm. **(B-C)** Graphs show the percentage of wound closure of CFPAC-1 (B) and MIA PaCa-2 (C) as quantified with the ImageJ software. At least 3 different images from three independent experiments were analyzed. Asterisk (*) indicates a statistically significant difference in wound closure of CFPAC-1 or MIA PaCa-2 co-cultured with compressed FBs knockdown for GDF15 (shGDF15) compared with CFPAC-1 or MIA PaCa-2 co-cultured with compressed shSCR FBs ($p<0.05$). **(D-E)** RNA was extracted from shGDF15-transfected FBs co-cultured with CFPAC-1 (D) and MIA PaCa-2 (E), reversed transcribed into cDNA and qPCR was used to measure the GDF15 mRNA expression. The expression in each sample was calculated with the ΔΔCt method using the expression of FBs transfected with shSCR vector as a reference. Each bar indicates the mean fold change ±SE of a representative experiment (n=3); Asterisk (*) represents a statistically significant difference ($p < 0.05$). **(F-G)** Representative western blot verifying succesfull knockdown of GDF15 at the protein level, between shGDF15 compressed fibroblasts and shSCR compressed fibroblasts. B-actin has been used as a loading control.

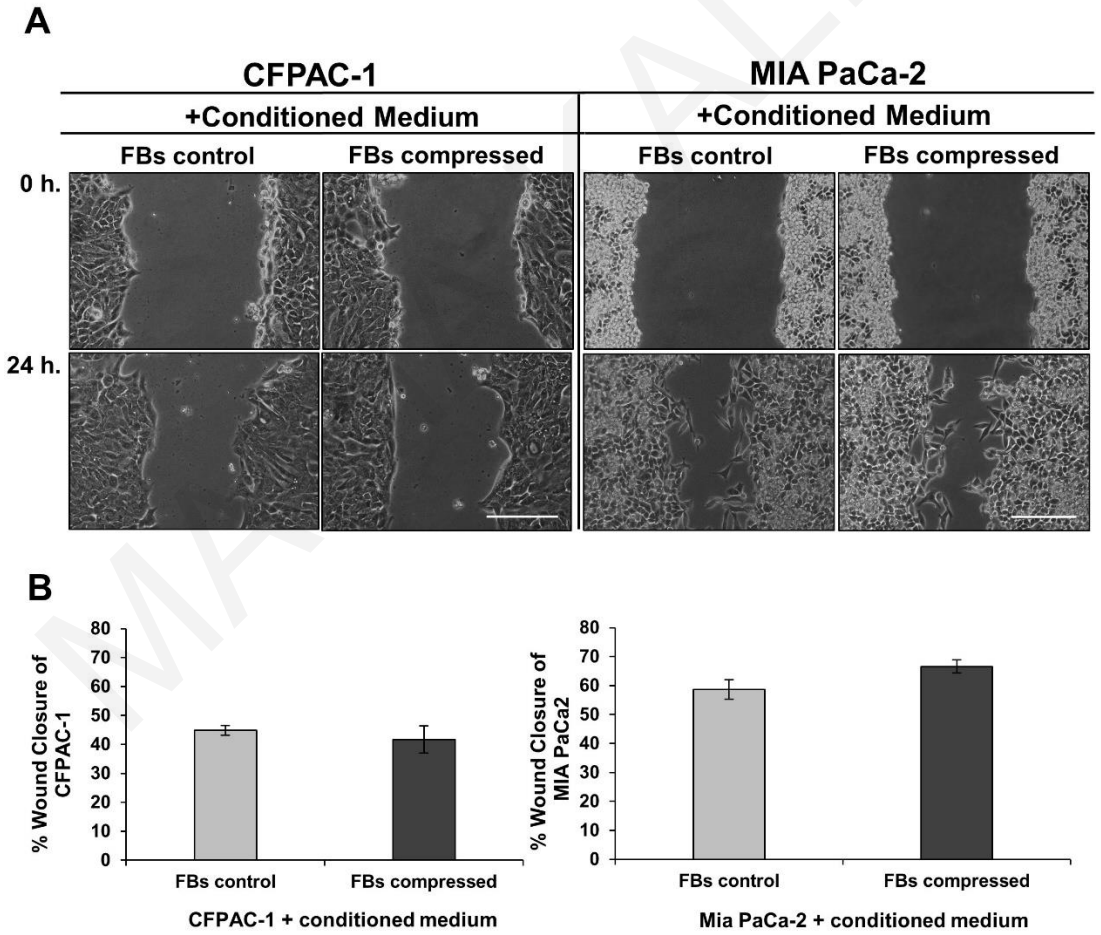

Figure 2-9. **Co-culture is necessary for compressed fibroblasts to induce the migratory ability of cancer cells. (A)** CFPAC-1 and MIA PaCa-2 cancer cells were serum starved in 2 %

FBS containing DMEM and then were subjected to a wound healing assay in the presence of conditioned medium derived from control and compressed fibroblasts (FBs). Scale bar: 0. 2 mm. **(B)** Graphs show the percentage of wound closure of CFPAC-1 and MIA PaCa-2 as quantified with the ImageJ software. At least 4 different images from two independent experiments were analyzed. No statistically significant difference was observed among treatments.

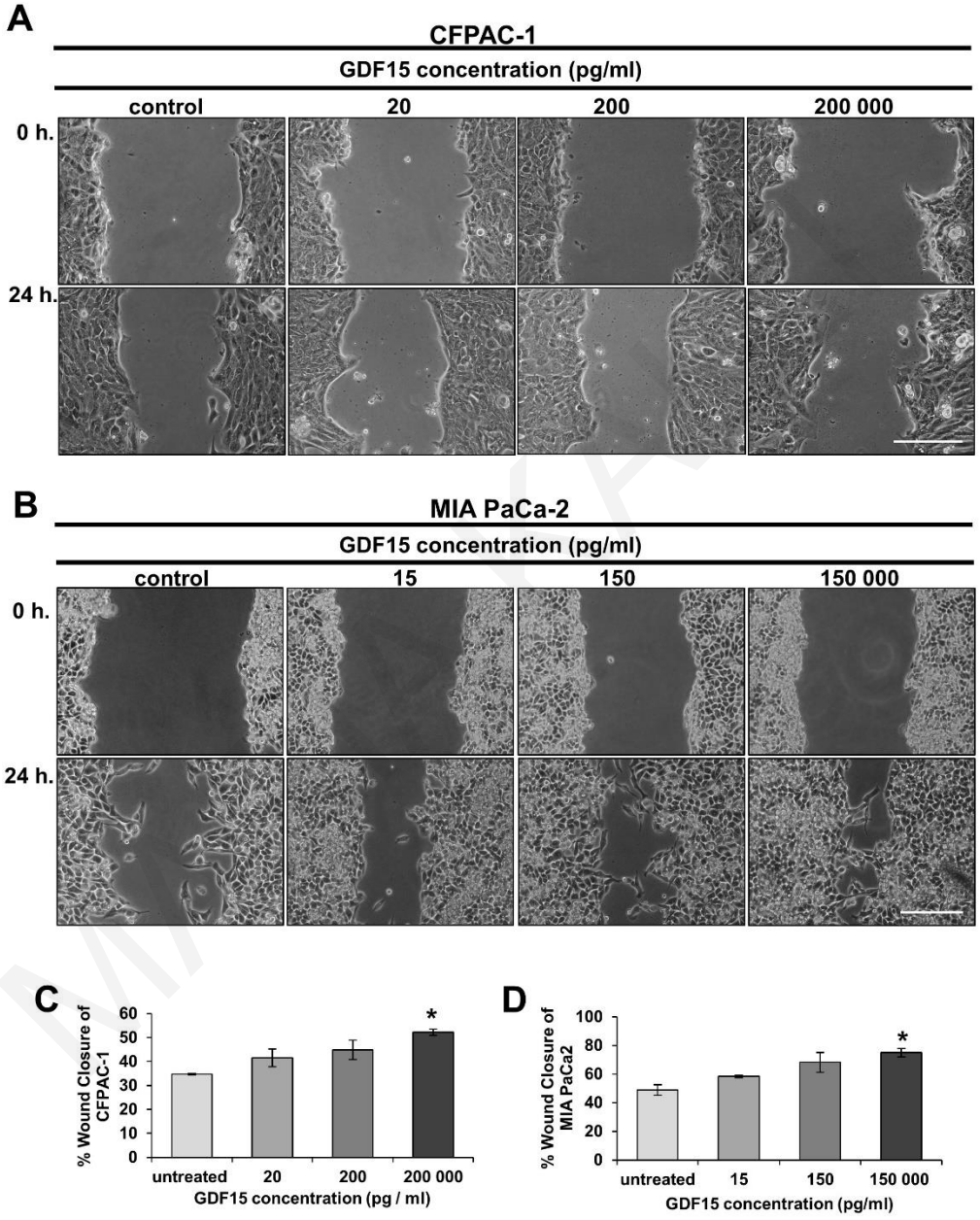

***Figure 2-10*. Recombinant GDF15 stimulates the migration of pancreatic cancer cells. (A-B)** CFPAC-1 and MIA PaCa-2 cancer cells were serum starved in 2 % FBS containing DMEM and then were subjected to a wound healing assay in the presence of recombinant GDF15 (rGDF15) for 24 hours. Scale bar: 0.2 mm. **(C-D)** Graphs show the percentage of wound closure of CFPAC-

1 (C) and MIA PaCa-2 (D) as quantified with the ImageJ software. At least 4 different images were analyzed and the asterisk (*) indicates a statistically significant difference ($p<0.05$).

2.4 **Discussion**

Solid stress developed within tumors, as a result of a highly dense ECM and uncontrolled cancer cell proliferation, has been shown to promote cancer cell migration *in vitro* [64]. However, solid stress is also exerted on other cellular components of the tumor microenviroenment, including fibroblasts, which aquire an activated phenotype fueling tumor progression[4].

In this study, we employed a previously described transmembrane pressure device [57, 63, 64] as a tool to apply compressive solid stress in a measurable and predefined manner, similar in magnitude to the stress applied on cells in the tumor interior [17]. The level of compressive stress used, ranged from 1.0 to 6.0 mmHg, which was in agreement with experimental measurements in pancreatic tumor models [11, 17].

Our results reveal that solid stress facilitates the activation of normal pancreatic fibroblasts as indicated by the upregulation of *a-SMA*, the most established marker of fibroblasts activation [4], and promote desmoplasia as revealed by the upregulation of Collagen I expression. Furthermore, we show that solid stress strongly upregulates the expression of *GDF15* in fibroblasts, which has been previously shown to be regulated by cellular stress, morphological or cytoskeletal changes [79, 93], but it has never been linked to solid stress. Finally, we demonstrate that both CFPAC-1 and MIA PaCa-2 pancreatic cancer cell lines exhibited higher migration rates when co-cultured with compressed fibroblasts, while this effect was not observed when cancer cells were independently treated with the conditioned medium of control and compressed fibroblasts (**Figure 2-9**). This phenomenon

indicates that compressed fibroblasts continously interact with cancer cells and induce cancer cell migration possibly through secretion of fibroblasts-derived factors. Notably, GDF15 levels in fibroblasts of both co-culture systems (CFPAC-1 or MIA PaCa-2) were elevated. In fact, it is of note that while compressed fibroblasts co-cultured with CFPAC-1 showed increased mRNA expression of GDF15, fibroblasts co-cultured with MIA PaCa-2 showed an even more dramatic increase in GDF15 expression (4 times that of fibroblasts co-cultured with CFPAC-1). We further verified the levels of secreted GDF15 from fibroblasts co-cultured with MIA PaCa-2 cells by ELISA and found an also dramatic elevation compared to the co-culture system of CFPAC-1. Next, to assess the direct effect of GDF15 on cancer cells, we treated both cancer cell lines with recombinant GDF15 (rGDF15) and we found that rGDF15 can induce pancreatic cancer cell migration in the absence of compressed fibroblasts (**Figure 2-10**). Nevertheless, the co-culture of cancer cells with fibroblasts, which is more physiologically relevant to the native tumor microenvironment, is necessary to enhance their GDF15-induced migratory ability. Strikingly, this effect was significanlty decreased when cancer cells were co-cultured with compressed fibroblasts in which *GDF15* had been silenced . Our findings suggest, for the first time, that compression-induced secretion of GDF15 by activated fibroblasts could be responsible for migration of cancer cells. Therefore, *GDF15* can be a promising target for prevention of compression-induced pancreatic cell migration.

Collectively, we propose that solid stress developed within tumors is able by itself to activate normal fibroblasts, which in turn produce excessive amounts of ECM proteins leading to desmoplasia. Desmoplasia along with the uncontrolled proliferation of cancer cells leads to the development of solid stress within the tumor, to create a feedback loop (**Figure 2-11**). To date, there is no pertinent study taking into account the effect of solid stress on fibroblasts and thus, this is the first study showing that solid stress directly activates

fibroblasts to promote pancreatic cancer cell migration. More importantly, we provide evidence that this effect is mediated, at least in part, by the secretion of high levels of GDF15 in response to mechanical stimuli (**Figure 2-11**). So far, it was only known that GDF15 stimulates cancer cell migration and invasion *in vitro* and *in vivo* [87], but the exact mechanisms by which GDF15 is upregulated in the tumor microenvironment were unclear. Therefore, our findings highlight the involvement of biophysical factors, such as solid stress, in tumor progression and malignancy, revealing a novel regulatory mechanism of *GDF15* expression. Further studies are needed in order to shed light upon the mechanisms by which fibroblast-derived GDF15 stimulates cancer cell migration. Since GDF15 belongs in the TGFβ superfamily of cytokines, it could regulate cellular responses via the ligand binding on TGFβ receptors type I and II. The activation of these receptors can recruit and phosphorylate downstream signaling molecules such as Smads, which create complexes that are subsequently translocated into the nucleus and act as transcription factors regulating the expression of genes implicated in the migration and invasion of cancer cells [78, 94]. GDF15, could also regulate cancer cell behavior by activating other signaling pathways such as PI3K-Akt[95], MEK-Erk1/2[96] and FAK-RhoA signaling pathways[81]. GDF15 was also shown to drive the invasiveness of breast cancer cells by binding to the Insulin Growth Factor Receptor (IGF-1R), while the exact activated intracellular pathways are yet to be determined[97]. In pancreatic cancer, it has been shown that Twist stimulates the expression of GDF15 through p38 MAPK signaling pathway to promote the invasiveness of pancreatic cancer cells and drug resistance, while treatment with an appropriate p38 MAPK inhibitor significantly reversed these effects [98]. Similarly, inhibitors against PI3K and ERK1/2 signaling pathways impaired GDF15-induced proliferation and invasion of liver and breast cancer stem-like cells[95, 96], while patients with multiple myeloma that were treated with cyclophosphamide showed decreased GDF15 serum levels and progression-free patient

survival[99]. Thus, using neutralizing antibodies or small molecules against GDF15 could serve as therapeutic targets for patients with pancreatic and other cancer types. Identification of the molecular pathways involved in GDF15-induced cancer cell migration will certainly provide information that could be exploited therapeutically.

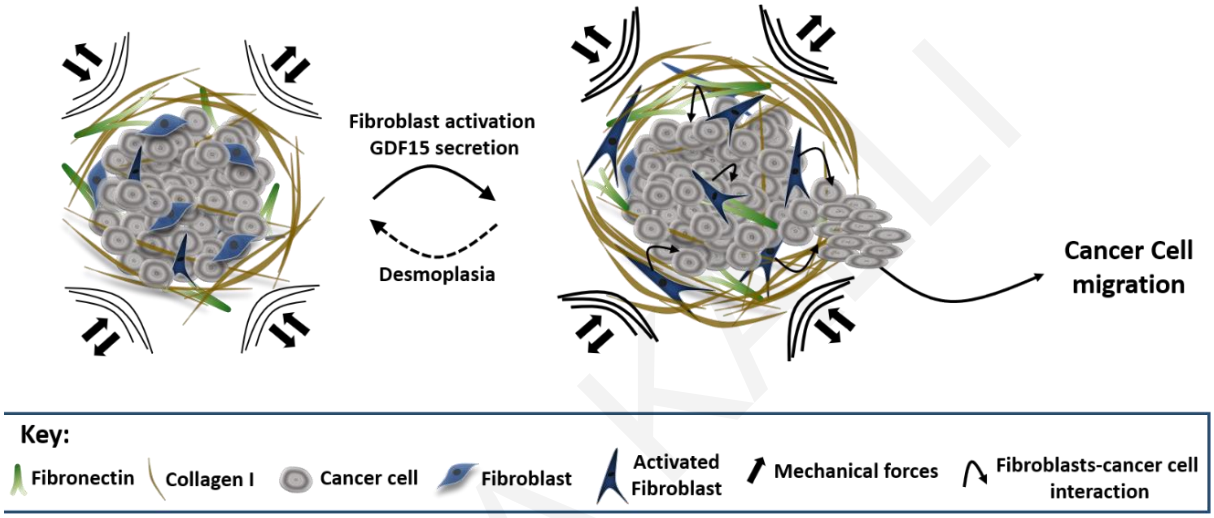

Figure 2-11. **Diagram showing the working hypothesis of the present study.** Mechanical forces in the tumor microenvironment activate normal fibroblasts, which in turn produce excessive amounts of ECM proteins (such as Collagen I and fibronectin), leading to desmoplasia. Desmoplasia along with the uncontrolled proliferation of cancer cells in the confined space of the host tissue, leads to the development of compressive stress within the tumor, thus creating a feedback loop. At the same time, mechanical compression upregulates GDF15 expression in activated fibroblasts, which is secreted to the ECM and stimulates the migration of adjacent cancer cells.

3 *Chapter 3: Solid stress-induced migration is mediated by GDF15 through Akt pathway activation in pancreatic cancer cells*

This research has been published in Scientific Reports: **Maria Kalli**, Angeliki Minia, Vaia Pliaka, Christos Fotis, Leonidas G Alexopoulos, Triantafyllos Stylianopoulos. Solid stress-induced migration is mediated by GDF15 through Akt pathway activation in pancreatic cancer cells. *Scientific Reports* volume 9, Article number: 978 (2019) [doi: 10.1038/s41598-018-37425-6].

3.1 **Introduction**

It is well known that solid stress inhibits tumor growth, induces cell apoptosis and regulates tumor morphology [54, 57-59], while a limited number of studies has shown that solid stress can also enhance the metastatic potential of cancer cells [59, 61, 64, 73]. As also mentioned in **Section 1.2.2**, mechanical compression of about 6.0 mmHg has been found to promote the invasion of mammary carcinoma cells through a subset of "leader cells" that have the capacity of forming filopodia at the leading edge of the cell sheet[64]. In a more recent study, it was shown that peripheral cells growing under confined conditions within multicellular spheroids, were more proliferative and migratory, suggesting that mechanical stimuli from the surrounding microenvironment might promote cancer cell invasion[59]. Moreover, an exogenously-induced predefined mechanical compression of about 9.0 mmHg applied on colon crypts has been found to stimulate Ret/β-catenin/Myc pathway *in vivo*, contributing to the growth and spread of the tumor[61]. Recently, it has also been proposed that mechanical compression (5.0 mmHg) in combination with Interleukin-6 (IL-6) treatment activates the Akt/Gsk-3β/β-catenin signaling pathway to induce epithelial-to-mesenchymal transition

(EMT) in renal cell carcinoma[100]. However, data regarding the exact mechanism by which solid stress promotes cellular responses, especially in pancreatic cancer, are limited.

In this chapter, we aimed to investigate the effect of solid stress on the migration of two distinct pancreatic cancer cell lines, MIA PaCa-2 and BxPC-3, using the *in vitro* transmembrane pressure device that was used in our previous study, in the absence of pancreatic fibroblasts. Next, through a phosphoproteomic screening we identified a mechanism by which solid stress is transmitted through cells in order to regulate cellular behavior, such as cell migration. Similarly to our previous findings, we show the important role of GDF15 for cancer cell migration under mechanical compression, further suggesting that this molecule could serve as molecular target for the treatment of patients with pancreatic cancer.

3.2 **Methods**

Cell culture. Pancreatic cancer cell lines, MIA PaCa-2 and BxPC-3, were obtained from American Type Culture Collection (ATCC) and were incubated at 37 ^{o}C and 5 % CO_2 in a humidified incubator. MIA PaCa-2 cells were maintained in Dulbecco's Modified Eagle's Medium (DMEM) and BxPC-3 cells in Roswell Park Memorial Institute 1640 (RPMI) medium, both supplemented with 10 % Fetal Bovine Serum (FBS) and 1 % antibiotics.

In vitro compression device. In order to apply a defined and controlled compressive solid stress on cancer cells, we used the previously described experimental setup (**Figure 2-1A**). In this study the cells were compressed by 4.0 mmHg for 16 hours or to 4.0 mmHg stress for 3, 6 and 16 hours. Uncompressed cells (control) were covered with

an agarose cushion only (i.e., 0.0 mmHg). The solid stress level used in this study was selected according to the levels estimated in pancreatic tumors [17].

Transient transfection of pancreatic cancer cells with shRNA against GDF15. To deplete *GDF15* from pancreatic cancer cells, we generated vectors that express shRNA against *GDF15* (shGDF15) and control vectors (sh-Scrambled or shSCR) as described in detail in **Section 2.2**. Cells were tran–siently transfected with each shRNA using Lipofectamine 2000 transfection reagent (Invitrogen) according to manufacturer's guidelines.

In vitro Scratch assay. Cancer cells were grown to form a monolayer and a cross-like wound was created using a 200 μL pipette tip. Cells were then washed with Phosphate Buffered Saline (PBS) and treated as indicated in each figure caption for 16 hours. Pictures from four different fields per condition were captured at 0 and 16 hours. The wound area was calculated by the ImageJ software and quantification was performed using the following equation:

((Wound area at 0 hours – Wound area at 16 hours) / (Wound area at 0 hours)) x 100.

Cell treatments. In order to examine the effect of GDF15 on the migratory ability of pancreatic cancer cells under 4.0 mmHg solid stress condition, MIA PaCa-2 cells lacking *GDF15 (*shGDF15) or control cells (shSCR) were grown in transwell inserts and were subjected to a scratch wound healing assay in the presence or absence of 10 ng/ml of human recombinant GDF15 (rhGDF15, R&D systems) under mechanical compression in 2 % FBS-containing medium for 16 hours. Control cells were treated with equal volume of the solvent used to dissolve rhGDF15 (4 mM HCl supplemented with 0.1 % Bovine Serum Albumin-BSA). In order to study the role of Akt pathway in pancreatic cancer cell migration under mechanical compression, a PI3K inhibitor (BKM120 or Buparlisib, MedChemExpress) was

selected to block the Akt pathway. Cells were grown in transwell inserts with 2 % FBS-containing medium for 24 hours and were then pre-treated with 10 μM BKM120 or equal volume of DMSO for 1 hour. The concentration of BKM120 was selected according to the manufacturer's guidilines. Mechanical compression (4.0 mmHg) was then applied and a wound healing assay was performed. To study the role of Akt pathway and GDF15 on the migration of pancreatic cancer cells, MIA PaCa-2 cells were pre-treated with 10 μM BKM120 or equal volume of DMSO for 1 hour and subjected to a scratch wound healing assay under mechanical compression (4.0 mmHg) in the presence of 10 ng/ml rhGDF15 or equal volume of solvent.

Cell Viability Assay. Cell viability of cancer cells was assesed using Alamar Blue reagent (Invitrogen Life Technologies) following compression with or without treatment with BKM120 inhibitor, following the manufacturer's instructions.

Gene expression analysis. RNA isolation from cancer cells and gene expression analysis was performed as described in **Section 2.2**. The primers used for each target gene are shown in **Table 1, in Appendices**.

Phosphoproteomics. 24 custom dual-antibody Luminex assays were developed using ProtATonce (Athens, Greece) multiplex assay service. Briefly, 2 to 5 antibodies were selected and tested pair-wise as capture and as detection antibody. For each protein, the optimal capture/detection antibody pair was selected based on signal-to-noise ratio measurement. Assays were then multiplexed and concentration of detection antibody was evaluated based on its signal and its noise (off-target signal) in the panel.

Sample preparation and phosphoprotein's measurements. Cells were plated in transwell inserts and were compressed with 4.0 mmHg stress for 3, 6 and 16

hours in 2 % FBS-containing DMEM. Protein isolation was performed using radio immunoprecipitation assay (RIPA) buffer containing a protease inhibitor cocktail tablet (Sigma). The BCA protein assay kit (Pierce) was used to determine protein concentration and 200 μg/ml of cell lysates were used for phosphoprotein measurements. 24 capture antibodies coupled to Luminex magnetic beads and 24 biotinylated detection antibodies were multiplexed to create the bead mix and the detection mix, respectively. 50ul of the coupled beads (bead mix) were incubated with the samples on a flat bottom 96-well plate on a shaker at 900 rpm for 90 minutes at room temperature. Then, detection mix was added, and the samples incubated on a shaker at 900rpm for 60 minutes at room temperature. The final step was the addition of freshly prepared SAPE solution (Streptavidin, R-Phycoerythrin conjugate, Cat Nr: S866, Invitrogen) for the detection of the signal. 15 minutes after the incubation with SAPE, samples were measured with the Luminex FlexMAP 3D instrument.

Western Blotting. Whole protein cell lysates were extracted as described in **Section 2.2**. However, to determine GDF15 secretion, conditioned medium (~4 ml) was collected after each experiment, filtered through 0.2 μm pores, concentrated 40 X using 10K protein concentrators (Pierce) and stored at -80^{o}C until use. Protein concentration was determined using the BCA protein assay kit (Pierce) and about 20-40 μg of protein were separated on a 12 % SDS-PAGE as described in **Section 2.2**. The membrane was incubated with anti-Growth Differentiation Factor 15 (GDF15) (Cell Signalling), anti-phospho-Akt (Ser 473) (Cell signalling), anti-Akt total (Cell Signalling), anti-phospho-CREB1 (Ser 133) (Abcam) or anti-CREB1 total (Abcam) antibodies overnight. A Coomassie staining (Sigma), for blots with conditioned medium, or antibodies against β-tubulin or β-actin, for blots with cell extracts, were used as loading controls. The detection of antibodies was performed as mentioned in **Section 2.2**.

3.3 **Results**

Mechanical Compression promotes pancreatic cancer cell migration.

It has been previously reported that mechanical compression promotes breast and colon cancer cell migration and invasion [59, 61, 64], whereas there is no information on the effect of it on pancreatic cancer cells. In the present study, we used MIA PaCa-2 and BxPC-3 pancreatic cancer cell lines to study their migratory ability as a response to mechanical compression. Cells were compressed at 4.0 mmHg, which is similar in magnitude to the stress levels measured *in* situ by Nia et al., (Figure 1D in Ref [17]), and subjected to a scratch wound healing assay. Although this experimental approach presents some technical hurdles involving critical steps such as generation of the wound, placement of the agarose cushion, application of mechanical pressure, and removal of the agarose cushion without damaging the cells, it proved to be ideal for our study as it offered the advantage of allowing us to accurately assess the migratory ability of cancer cells under mechanical compression. As shown in **Figure 3-1**, both cell lines exhibited increased migratory ability as a response to mechanical compression.

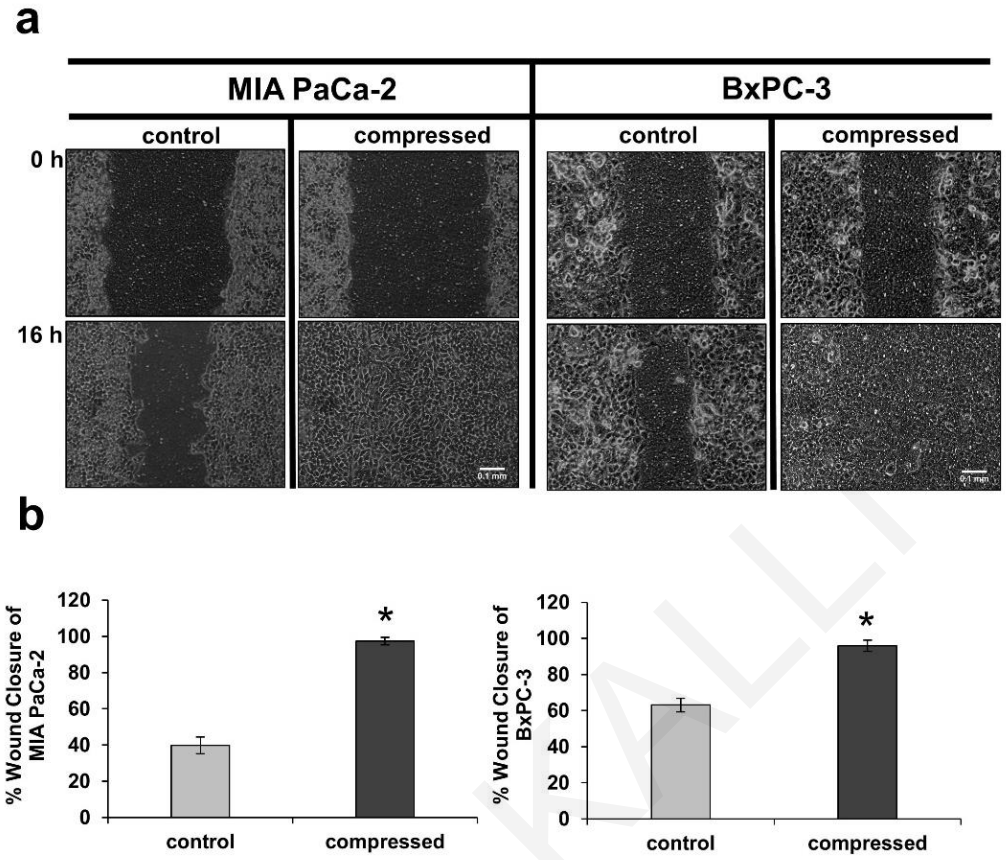

Figure 3-1. **Mechanical Compression promotes pancreatic cancer cell migration. (a)** MIA PaCa-2 (left) and BxPC-3 (right) pancreatic cancer cells were subjected to a scratch-wound assay under 4.0 mmHg of compressive solid stress for 16 hours. Uncompressed cells (control) were covered with an agarose layer only. Scale bar: 0. 1 mm. **(b)** Graphs represent the wound closure of MIA PaCa-2 (left) and BxPC-3 (right) as analyzed by ImageJ software. In each condition, at least four different images from two independent experiments were analyzed. Statistically significant differences ($p<0.05$) between compressed and uncompressed MIA PaCa-2 or BxPC-3 are indicated with asterisk (*).

Mechanical Compression stimulates GDF15 secretion and upregulation of Rho GTPases mRNA expression. Intrigued by our previous work, showing that GDF15 is strongly upregulated in normal pancreatic fibroblasts as a response to mechanical compression [101], and knowing that GDF15 as well as Rho GTPases are upregulated in response to mechanical stretch or cytoskeleton disruption [79, 102, 103], we examined the gene expression of these genes in compressed MIA PaCa-2 and BxPC-

3 cells. We observed a strong increase in *GDF15* and *RhoB* mRNA expression (**Figure 3-2a, Figure 3-3b, Figure 3-4a**) and elevated GDF15 secretion in the conditioned medium (**Figure 3-2b, Figure 3-4b**) of both cell lines with MIA PaCa-2 cells exhibiting the most dramatic changes.

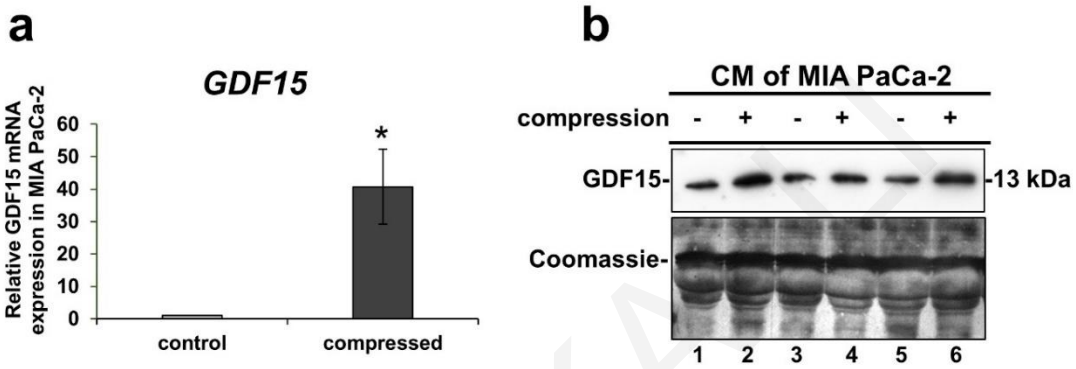

***Figure 3-2*. Mechanical Compression stimulates the mRNA expression and secretion of GDF15 in MIA PaCa-2 cells. (a)** MIA PaCa-2 cells were subjected to 4.0 mmHg of compressive stress for 16 hours and the expression of *GDF15* was measured by qPCR. The mRNA expression in each sample was quantified by the ΔΔCt method using the expression in uncompressed cells as a reference. Bar graphs represent the mean fold change ±SE of four biological replicates (n=12). Statistically significant changes between compressed and uncompressed cells are indicated by an asterisk (*) ($p<0.05$). **(b)** Western blot showing the secretion of GDF15 in the conditioned medium (concentrated by 40X) of compressed MIA PaCa-2 from three independent experiments. Coomassie staining was used to verify equal protein loading.

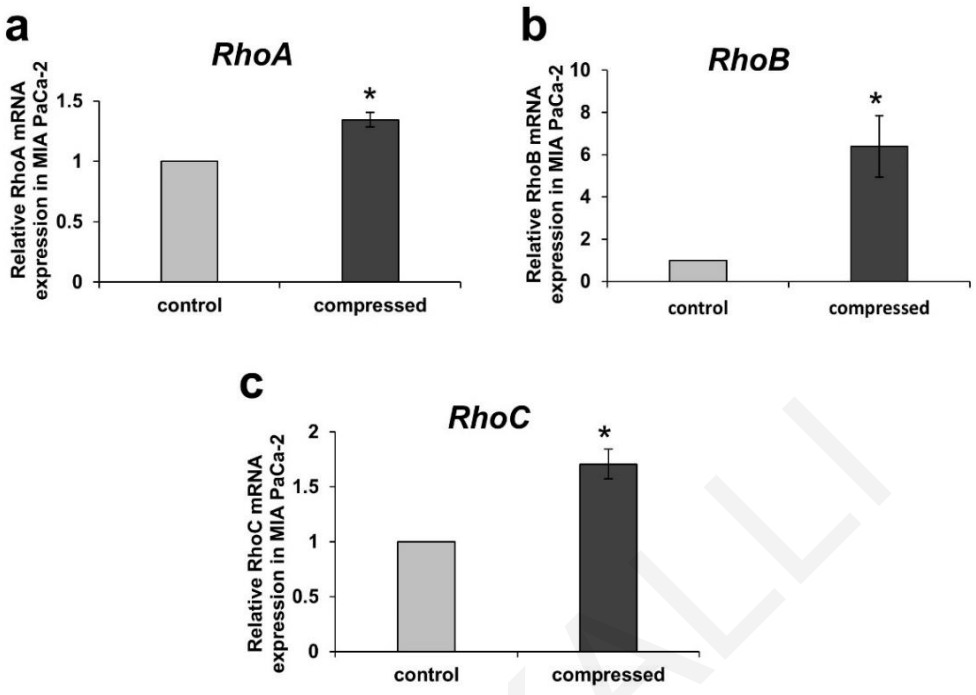

***Figure 3-3*. Mechanical Compression stimulates the mRNA expression of Rho GTPases in MIA PaCa-2 cells.** MIA PaCa-2 were compressed by 4.0 mmHg for 16 hours and qPCR was used to measure the expression *RhoA* **(a)**, *RhoB* **(b)** and *RhoC* **(c)**. The expression in each sample was analyzed with the ΔΔCt method relative to the expression of control sample (cells compressed by the agarose cushion only). The mean fold change was calculated and plotted for each gene. Each bar indicates the mean fold change ±SE of two independent experiments (n=6). Asterisk (*) indicates a statistically significant difference ($p<0.05$).

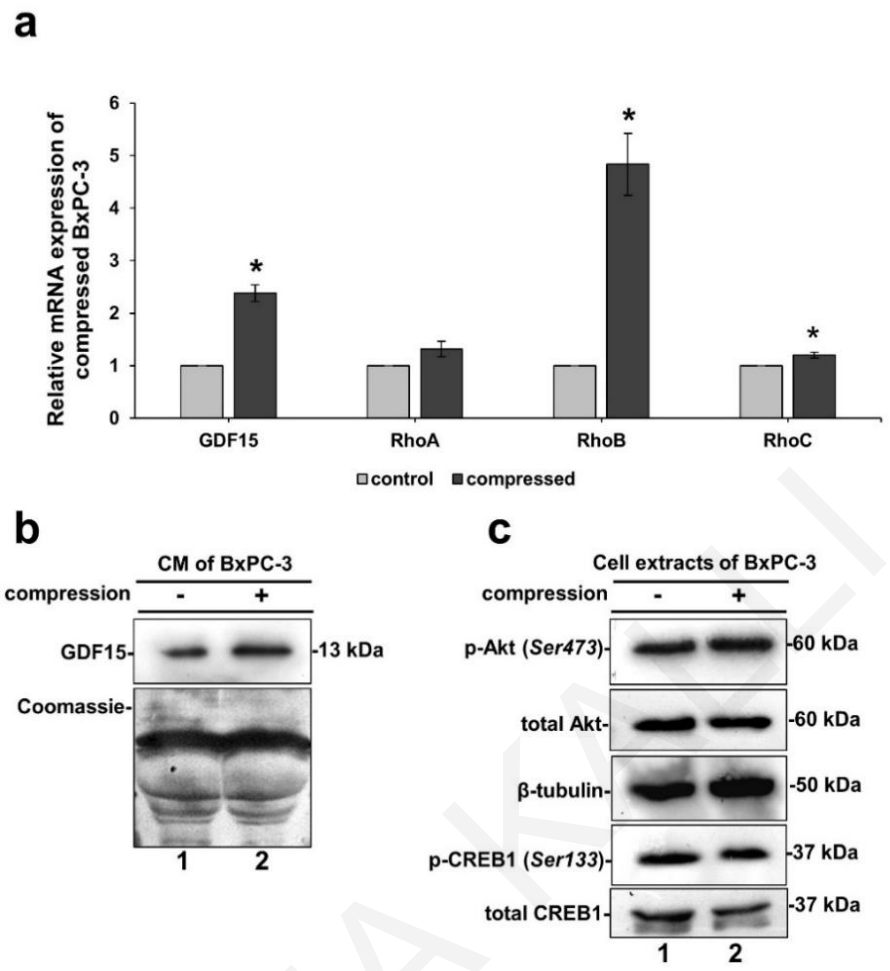

***Figure 3-4*. Mechanical Compression stimulates the mRNA expression and secretion of GDF15 in BxPC-3 cells. (a)** BxPC-3 were compressed by 4.0 mmHg for 16 hours and qPCR was used to measure the expression of *GDF15, RhoA, RhoB* and *RhoC.* The expression in each sample was analyzed with the ΔΔCt method relative to the expression of control sample (cells compressed by the agarose cushion only). The mean fold change was calculated and plotted for each gene. Each bar indicates the mean fold change ±SE of two independent experiments (n=6). Asterisk (*) indicates a statistically significant difference ($p<0.05$). **(b)** Western blot showing GDF15 protein levels in the conditioned medium (concentrated by 40 X) of compressed BxPC-3. Coomassie staining was used to verify equal protein loading. **(c)** Western Blotting showing phosphorylated Akt (Ser 473), total Akt, phosphorylated CREB1 (Ser 133) and total CREB1 levels in compressed BxPC-3.

GDF15 is a key regulator for solid stress-induced pancreatic cancer cell migration. In order to identify how GDF15 is implicated in cancer cell migration under solid stress conditions, it was transiently silenced using an shRNA or siRNA-mediated silencing approach. Mechanical compression was then applied for 16

hours. As shown in **Figures 3-5 and Figure 3-6**, *GDF15* was effectively depleted both at the mRNA and protein level following each silencing approach (shRNA or siRNA). With regard to cell migration, our results show that MIA PaCa-2 cells lacking GDF15 have reduced migratory ability **(Figure 3-5c&d, Figure 3-6c&d)** indicating that *GDF15* is critically involved in solid stress-induced pancreatic cancer cell migration. Interestingly, however, treatment with rhGDF15 managed to completely reverse this inhibitory effect (**Figure 3-5c&d**), clearly suggesting that *GDF15* plays a crucial role in solid stress-induced pancreatic cancer cell migration.

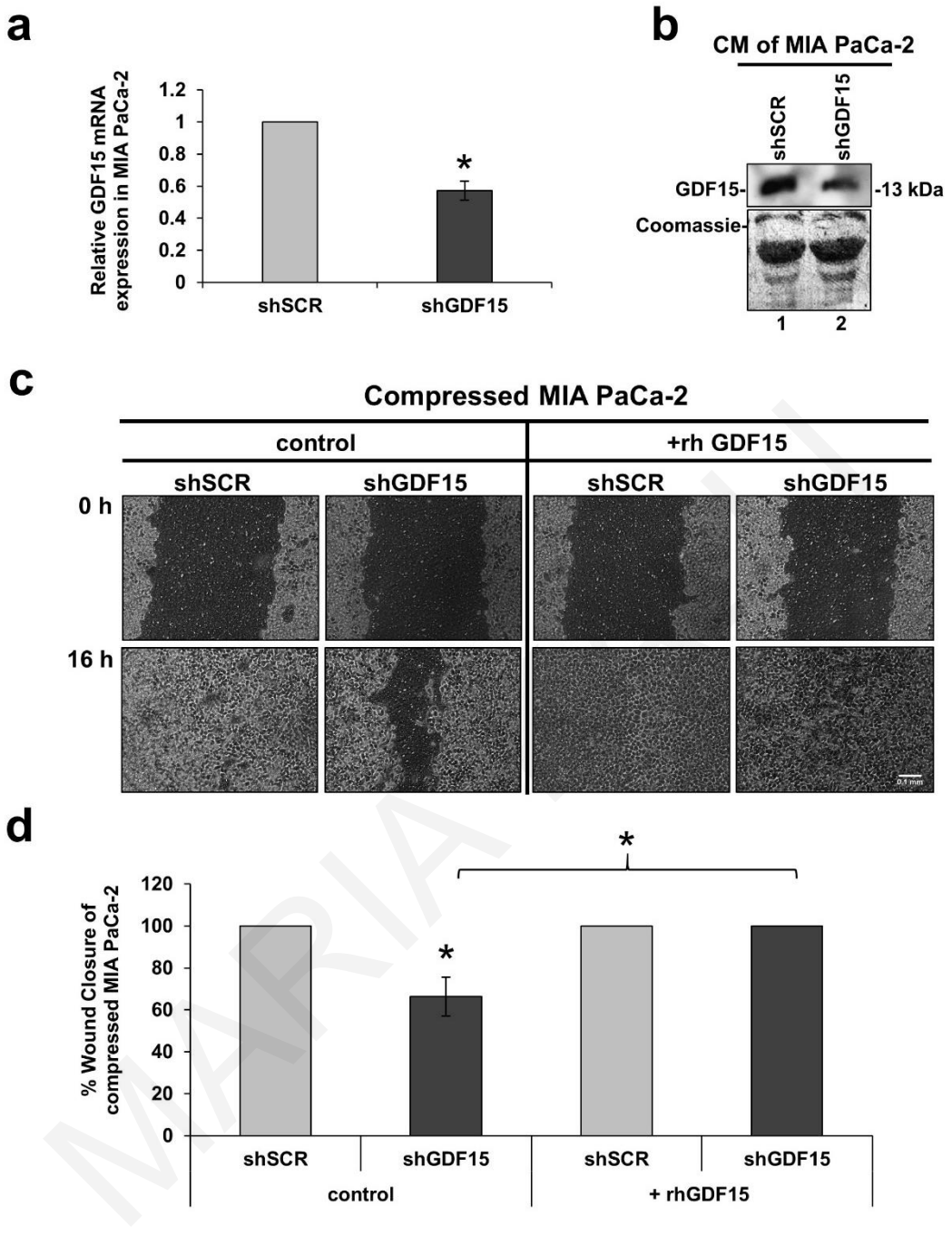

Figure 3-5. **GDF15 is a key regulator for solid stress-induced pancreatic cancer cell migration.** **(a)** MIA PaCa-2 cancer cells were transiently transfected with shSCR- and shGDF15- expressing vectors and were compressed by 4.0 mmHg in 2 % FBS containing DMEM. Total RNA was then isolated and *GDF15* mRNA expression was quantified by qPCR. Each bar indicates the mean fold change ±SE of a representative experiment (n=3). Asterisk (*) indicates a statistically significant difference ($p<0.05$). **(b)** Representative Western Blotting showing that GDF15 secretion has been succesfully reduced in the conditioned medium (40X concentrated) of compressed shGDF15-treated MIA PaCa-2 cells (lane 2) compared to compressed shSCR cells (lane 1). **(c)** MIA PaCa-2 cells knockdown for GDF15 were compressed by 4.0 mmHg in low-serum medium and then subjected to a scratch wound healing assay stimulated by 10 ng/ml rhGDF15 for 16 hours. Control cells (shSCR)

were treated with solvent (indicated as control). Scale bar: 0.1 mm. **(d)** Graph showing the percentage wound closure as quantified using ImageJ software. Statistical significant difference in wound closure of shGDF15 MIA PaCa-2 cells compared to shSCR MIA PaCa-2 cells both treated with solvent (control) is indicated with an asterisk (*) (n=4; $p<0.05$).

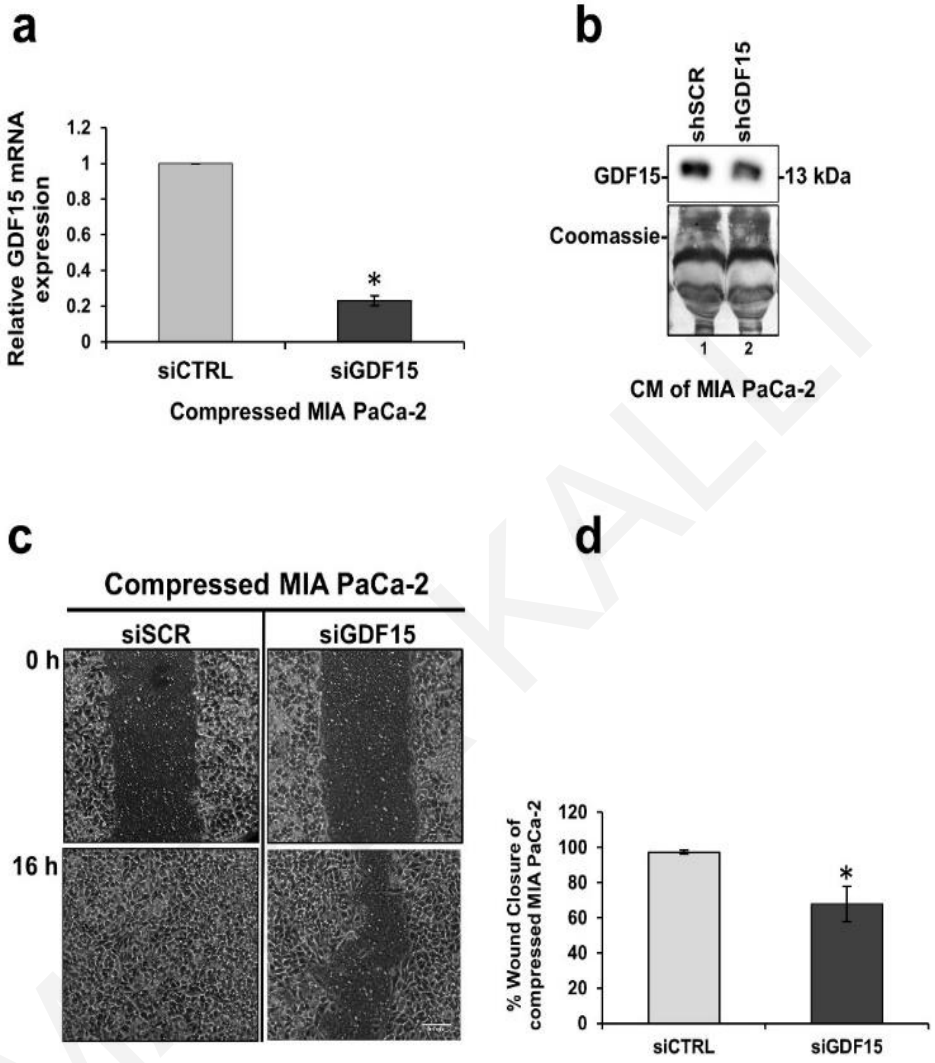

***Figure 3-6*. Knockdown of GDF15 using siRNA impaired pancreatic cancer cell migration. (a)** MIA PaCa-2 cancer cells were transfected with control siRNA (siCTRL) or siRNA against GDF15 (siGDF15) and were compressed by 4.0 mmHg in 2 % FBS containing DMEM. Total RNA was then isolated and *GDF15* mRNA expression was quantified by qPCR. Each bar indicates the mean fold change ±SE of a representative experiment (n=3). Asterisk (*) indicates a statistically significant difference ($p<0.05$). **(b)** Representative Western blotting showing that GDF15 secretion has been successfully reduced in the conditioned medium (40X concentrated) of compressed siGDF15-treated MIA PaCa-2 cells (lane 2) compared to compressed siCTRL cells (lane 1). **(c)** MIA PaCa-2 cells knockdown for GDF15 were compressed by 4.0 mmHg in low-serum medium and then subjected to a scratch wound healing assay for 16 hours. Scale bar: 0.1 mm. **(d)** Graph showing the percentage of wound closure as quantified using ImageJ software. Statistically significant difference in wound closure of siGDF15-treated MIA PaCa-2 cells compared to siCTRL-treated MIA PaCa-2 cells is indicated with an asterisk (*) (n=4; $p<0.05$).

Screening for the identification of solid stress signal transduction mechanisms. Since mechanical compression regulates gene expression of pancreatic cancer cells, we investigated the mechanism by which the extracellular mechanical stimuli are transmitted into the cell nucleus ultimately regulating cellular responses. To that regard, we applied mechanical compression on MIA PaCa-2 cells, that exhibited the most dramatic changes, for different time points, and whole cell lysates were screened for the identification of activated signaling pathways by using Multiplex Assay designed to detect 24 influential phospho-proteins. Analysis of the Multiplex Assay findings showed that Akt was strongly upregulated by mechanical compression as early as 3 hours post compression, as indicated by the increased phosphorylation level of Akt (Ser473 residue) (**Figure 3-7**). Strikingly, among all phosphoproteins tested in this screen, Cyclic AMP-responsive element-binding protein-1 (CREB1), which is directly linked to Akt phosphorylation as a widely known transcription factor downstream of Akt [104-106], was also found to be activated in compressed cells (phosphorylation on Ser133 residue) (**Figure 3-7a**). Akt and CREB1 activation was verified by Western Blotting with the maximum increase observed at 16 hours (**in Figure 3-7b&c compare lane 4 to lane 1**), which corresponds to the time point at which cells closed the wound in the wound healing assay (**Figure 3-1a**). To validate the results of our initial screen and time-point experiment, we ran an independent experiment where MIA PaCa-2 and BxPC-3 were compressed for 16 hours and confirmed that Akt/CREB1 pathway gets activated in response to mechanical compression at the specific time point (**Figure 3-7d&e,** for MIA PaCa-2 and **Figure 3-4c**, for BxPC-3). Our data suggest that this pathway mediates a solid stress signal transduction mechanism that could regulate cancer cell migration [107, 108].

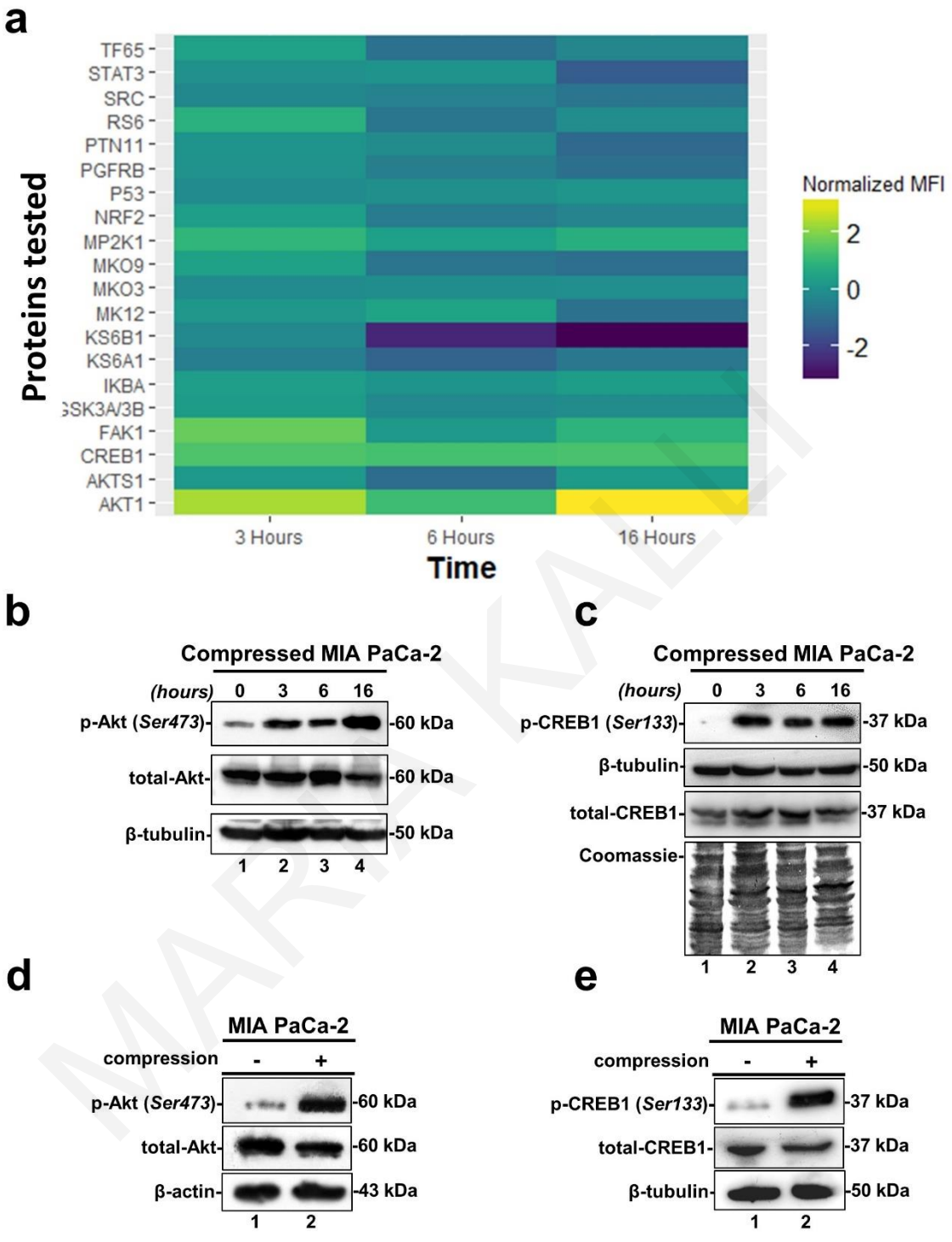

***Figure 3-7*. Screening for identification of solid stress signal transduction mechanisms. (a)** The heatmap depicts the change of the normalized Median Fluorescent Intensity (MFI) for the compressed cells at 3, 6 and 16 hours compared to the MFI for the uncompressed cells**. (b-c)** Validation of Akt phosphorylation (Ser473) and CREB1 phosphorylation (Ser133). B-tubulin (b) or a Coomassie staining (c) have been used as loading controls. **(d-e)** Western Blotting showing

Akt and CREB1 phosphorylation levels in MIA PaCa-2 compressed by 4.0 mmHg for 16 hours. B-actin (d) or β-tubulin (e) were used as loading controls.

Akt pathway is required for solid stress-induced pancreatic cancer cell migration. The Akt pathway is a well characterized signaling pathway known to play a crucial role in cell survival and inhibition of apoptosis[108]. Interestingly however, several studies have also shown that this pathway can be responsible for cancer cell migration and invasion [95, 100, 104, 109-111]. Nevertheless, the involvement of the Akt pathway in solid stress-induced pancreatic cancer cell metastasis has not been described yet. To this end, we used an inhibitor of Phosphoinositide 3-kinase (PI3K), which is directly upstream of Akt to test the solid stress-induced migration with or without activated Akt. BKM120 (NVP-BKM120 or Buparlisib), is a PI3K inhibitor that has been previously used to inhibit Akt activation *in vitro* and *in vivo* [112-116]. Thus, we applied mechanical compression on MIA PaCa-2 and BxPC-3 cells treated with BKM120 and we verified that Akt phosphorylation was successfully inhibited in both cell lines (**Figure 3-8a**). Moreover, we observed that the migratory ability of both cell lines was also blocked (**Figure 3-8b&c**) suggesting a critical involvement of Akt in this process. Finally, we wanted to test whether rhGDF15, which is shown to promote pancreatic cancer cell migration, could rescue the Akt inhibitory effect. We observed that while BKM120 blocked MIA PaCa-2 migration, treatment with rhGDF15 partially reversed this phenotype **(Figure 3-9a&b)**. The same effect was observed in the activation of Akt pathway, since rhGDF15 was able to rescue Akt phosphorylation levels blocked by BKM120 (**Figure 3-9c**). These results suggest that GDF15 could activate Akt pathway and act synergistically to promote pancreatic cancer cell migration under mechanical compression.

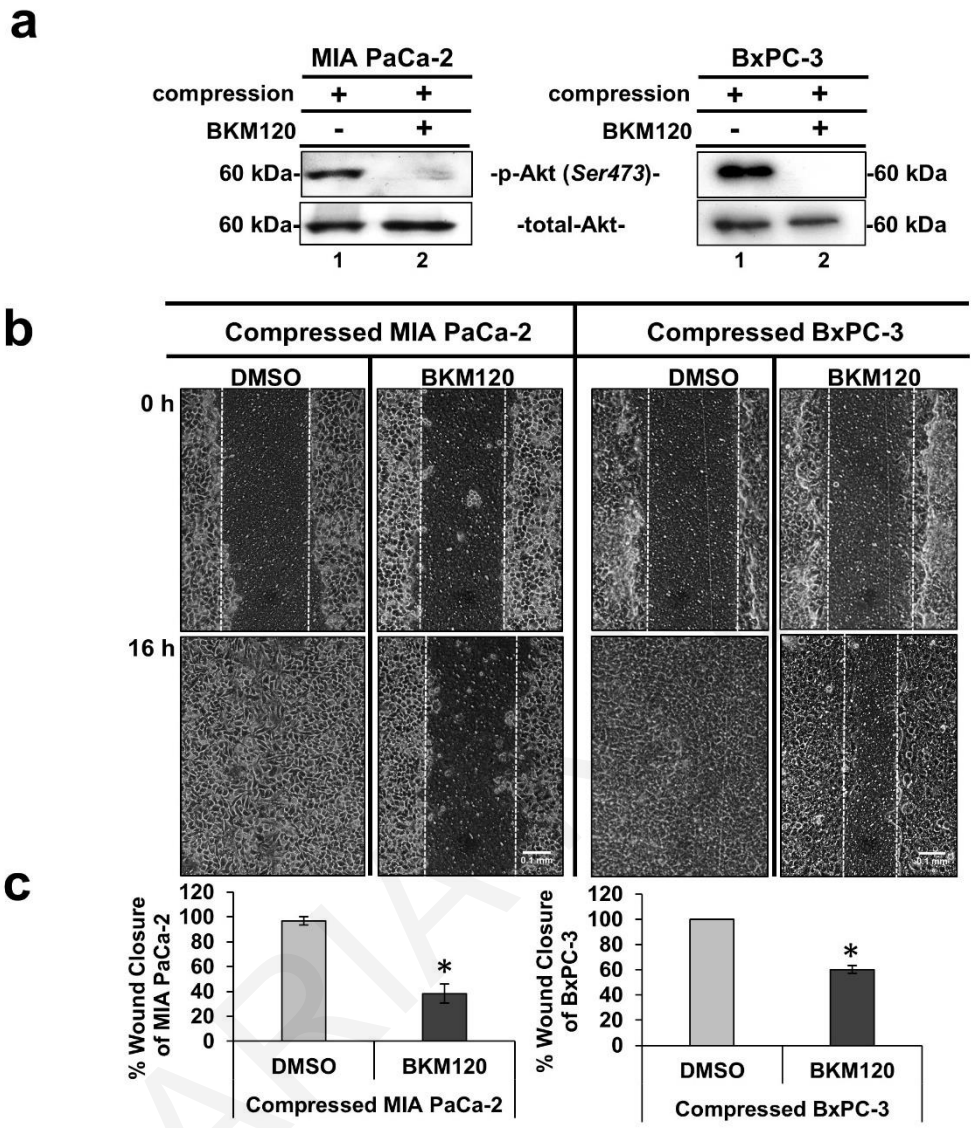

***Figure 3-8*. Akt pathway is required for solid stress-induced pancreatic cancer cell migration. (a)** MIA PaCa-2 and BxPC-3 were pre-treated with 10 μM BKM120 for 1 hour and then were compressed by 4.0 mmHg for 16 hours in 2% FBS-containing medium. Control cells were treated with equal volume of DMSO. Proteins were extracted and Western Blotting represents the levels of Akt phosphorylation (Ser473) in MIA PaCa-2 (left) and BxPC-3 (right). **(b)** MIA PaCa-2 and BxPC-3 were pre-treated with 10 μM BKM120 for 1 hour, and then were subjected to a scratch wound assay under 4.0 mmHg in 2% FBS-containing medium for 16 hours. Control cells were treated with equal volume of DMSO. Scale bar: 0.1 mm. White dashed line indicates the difference in wound closure between 0 and 16 hours. **(c)** Graphs represent the wound closure between compressed MIA PaCa-2 (left) or BxPC-3 (right) treated with DMSO compared to compressed cells treated with 10 μM BKM120 as quantified using the ImageJ software. Two independent experiments were performed and at least four different images were analyzed. Statistical significant differences are indicated with an asterisk (*) ($p<0.5$).

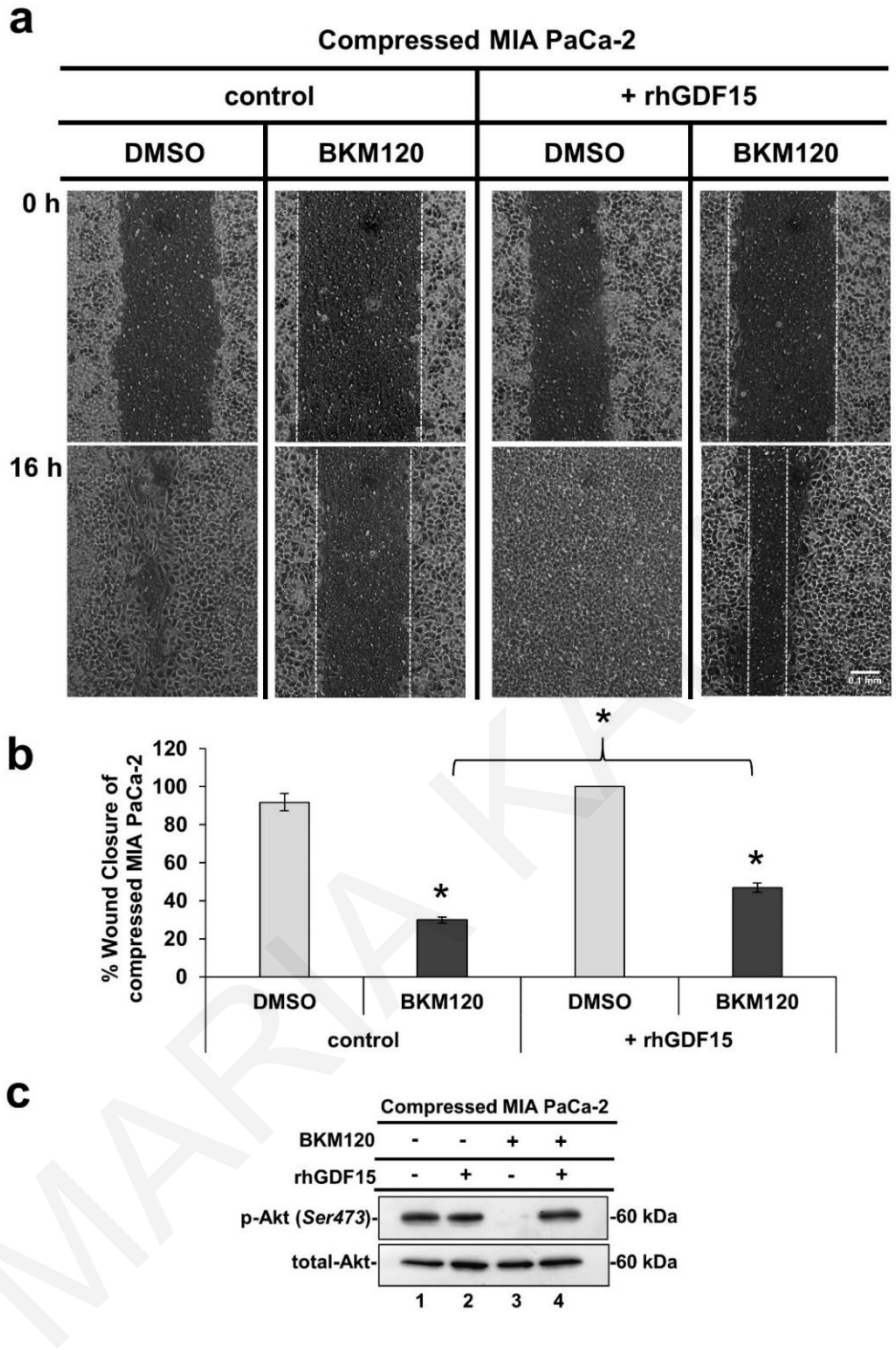

***Figure 3-9*. Treatment with rhGDF15 can overcome the blockade of solid stress-induced migration caused by Akt inhibition. (a)** MIA PaCa-2 were pre-treated with 10 μM BKM120 or equal quantity of DMSO and subjected to a scratch wound healing assay under 4.0 mmHg of compression in the presence of 10 ng/ml rhGDF15 or equal quantity of the respective solvent (control). Pictures from 4 different fields were taken from two independent experiments. Scale bar: 0.1 mm. White dashed line shows the difference in wound closure between 0 and 16 hours. **(b)** Graph showing the perentage wound closure of compressed MIA PaCa-2 treated with DMSO or 10 μM BKM120 in the presence of 10 ng/ml rhGD15 or solvent (control). Asterisk (*) indicates a statistical significant difference between compressed MIA PaCa-2 treated with BKM120 compared to compressed MIA PaCa-2 treated with BKM120 in the presence of rhGDF15

($p<0.05$). **(c)** Representative Western Blot showing phosphorylated Akt (Ser 473) and total Akt levels in compressed MIA PaCa-2 cells treated with 10 ng/ml rhGDF15 or solvent in combination with 10 μM BKM120 or DMSO.

Solid stress signal transduction is mediated by Akt/CREB1 pathway to regulate GDF15 expression. We next wondered whether Akt regulates the expression of factors responsible for pancreatic cancer cell migration through CREB1 phosphorylation. As presented in **Figure 3-10a,** CREB1 phosphorylation was also inhibited in compressed MIA PaCa-2 in the presence of BKM120, suggesting that Akt activation is necessary for the subsequent CREB1 activation. Hence, to determine whether CREB1 regulates the expression of factors responsible for pancreatic cancer cell migration, we searched for CREB1-binding sequences using the MatInspector tool (Genomatix) [117], which identifies transcription-factor-binding sites in nucleotide sequences using a large library of weight matrices (Matrix Family Library version 11.0). We found that CREB1 can bind at two sites on the 5' promoter region of *GDF15* exhibiting a perfect match getting a matrix similarity of 1.00 (which is translated to 100% match between Transcription factor-binding site and nucleotide sequences) (**Figure 3-10b**). Thus, we analyzed the mRNA expression of *GDF15* in compressed MIA PaCa-2 cells treated with BKM120. Interestingly, qPCR analysis revealed that *GDF15* mRNA expression as well as GDF15 secretion were downregulated when Akt/CREB1 pathway was blocked by BKM120 (**Figure 3-10c&d**). This result suggests that the Akt/CREB1 pathway is activated by solid stress in order to regulate the expression of *GDF15* mediating pancreatic cancer cell migration.

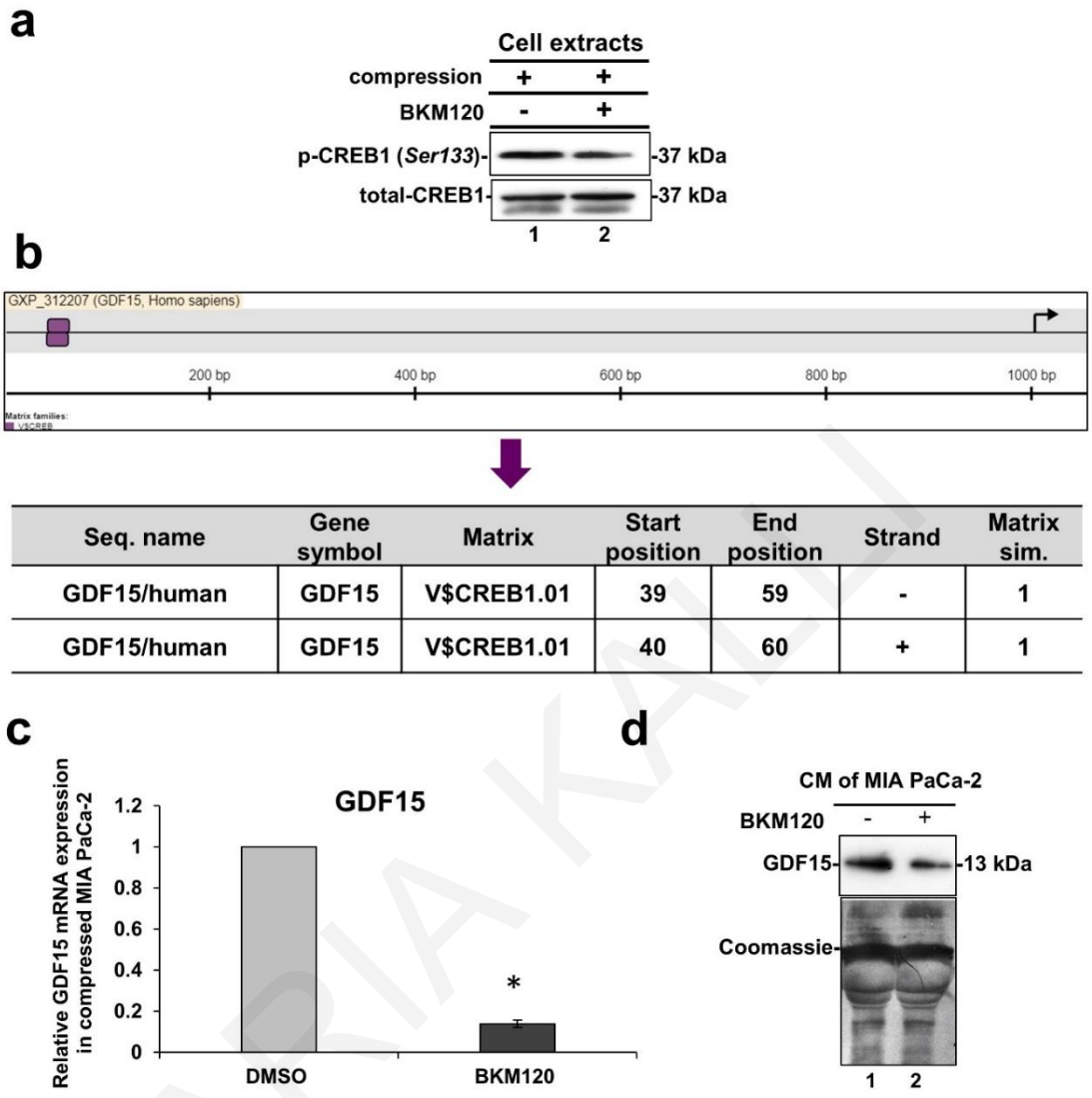

Seq. name	Gene symbol	Matrix	Start position	End position	Strand	Matrix sim.
GDF15/human	GDF15	V$CREB1.01	39	59	-	1
GDF15/human	GDF15	V$CREB1.01	40	60	+	1

***Figure 3-10*. Solid stress signal transduction is mediated by Akt/CREB1 to regulate GDF15 expression. (a)** Representative western Blotting showing phosphorylated CREB1 (Ser 133) and total CREB1 levels in compressed MIA PaCa-2 cells treated with 10 μM BKM120 or DMSO. **(b)** Prediction of CREB1 (Matrix) transcription factor-binding sites on the nucleotide sequence of GDF15 (Seq. name) as predicted by MatInspector tool. **(c)** qPCR was used to quantify the mRNA levels of *GDF15* in compressed MIA PaCa-2 cells treated with 10 μM BKM120 compared to compressed cells treated with DMSO. ΔΔCt method was used to quantify the gene expression in each sample using as a reference the expression in compressed and treated with DMSO cells (control). Bar graphs represent the mean fold change ±SE of two independent experiments (n=6) and statistical changes are indicated with an asterisk (*) ($p<0.05$). **(d)** Western blotting showing that GDF15 secretion in the conditioned medium (concentrated by 40X) of compressed MIA PaCa-2 cells treated with BKM120 (lane 2) is reduced compared to compressed cells treated with DMSO (lane 1). Coomassie staining was used to ensure equal protein loading.

3.4 **Discussion**

In the current study, we used an *in vitro* compression device to apply predefined and measurable compressive solid stress, similar in magnitude to the stress applied on cells in the tumor interior. The level of compressive stress used in this study (4.0 mmHg) was in agreement with experimental estimations of solid stress in pancreatic tumor models [17], and it is used herein to enhance the metastatic potential of MIA PaCa-2 and BxPC-3 pancreatic cancer cell lines, as indicated by a scratch wound assay, and to upregulate *GDF15* expression and secretion, as indicated by qPCR and Western Blotting. Furthermore, we show that compressed MIA PaCa-2 cells lacking *GDF15* (either after shGDF15 or siGDF15 treatment) exhibited reduced migratory ability while treatment with rhGDF15 reversed this effect, suggesting that GDF15 plays a crucial role in solid stress-induced pancreatic cancer cell migration. These novel findings could possibly give an explanation for the elevated *GDF15* levels observed in the serum of patients with solid tumors, such as in the case of breast, prostate and pancreatic cancer that exhibit high solid stress levels [10, 17].

In order to identify possible solid stress signal transduction mechanisms that regulate gene expression in cancer cells, we screened compressed MIA PaCa-2 cells, which showed the most robust mRNA changes, for activated signaling pathways implicated in mechanical stimuli signal transduction. We found that, from the pathways tested, the Akt pathway was activated as a response to solid stress as early as 3 hours post-compression, suggesting that solid stress could by itself activate this pathway. Furthermore, we demonstrated that inhibition of Akt pathway by the PI3K inhibitor, BKM120, completely blocked the compression-induced migration of cancer cells. It should be noted that PI3K/Akt has been found upregulated in 59% of patients with pancreatic cancer, while BKM120 has been already used in studies employing mouse models or is currently being administered in phase

I clinical trials for the treatment of patients with solid tumors, such as pancreatic, colon and breast tumors [113-116], where GDF15 serum levels are found elevated [78].

Based on the phosphoproteins screen, the compression-induced Akt activation could be directly linked to CREB1 activation, as it is an already known downstream transcription factor of Akt pathway [104-106]. This hypothesis was verified by the inhibition of CREB1 phosphorylation in compressed MIA PaCa-2 cells treated with BKM120. Interestingly, by using the MatInspector tool, we also found that CREB1 has two binding sites on *GDF15* promoter. To this end, we showed that GDF15 mRNA expression and secretion is downregulated in compressed MIA PaCa-2 cells treated with BKM120, suggesting a novel regulatory mechanism of GDF15 by Akt/ CREB1 pathway under compression. In order to examine whether there is a positive feedback loop between GDF15 and Akt/CREB1 pathway, we treated uncompressed MIA PaCa-2 cells with rhGDF15 and found that Akt/ CREB1 pathway is activated, while in the absence of GDF15 Akt is blocked without any change in CREB1 phosphorylation levels as previously shown [95, 118, 119]. Notably, compressed MIA PaCa-2 lacking GDF15 showed increased phosphorylation levels of Akt, but not of CREB1, suggesting that other pathways are activated in the absence of GDF15, in order to regulate Akt pathway either in compressed or uncompressed conditions.

In conclusion, we propose a model suggesting that solid stress signal transduction is mediated by Akt/CREB1 pathway to transcriptionally regulate *GDF15* expression. Subsequently, GDF15 is secreted and acts in an autocrine manner to promote pancreatic cancer cell migration possibly through Akt activation (**Figure 3-11**). Although many questions still remain regarding the exact molecular mechanism involved in solid stress-induced migration, this is the first study actually connecting solid stress-induced migratory profile of cells with GDF15 upregulation and secretion through Akt/CREB1 activation,

bringing GDF15 to the centre of solid tumor biology and rendering it a potential target for future anti-metastatic therapeutic innovations.

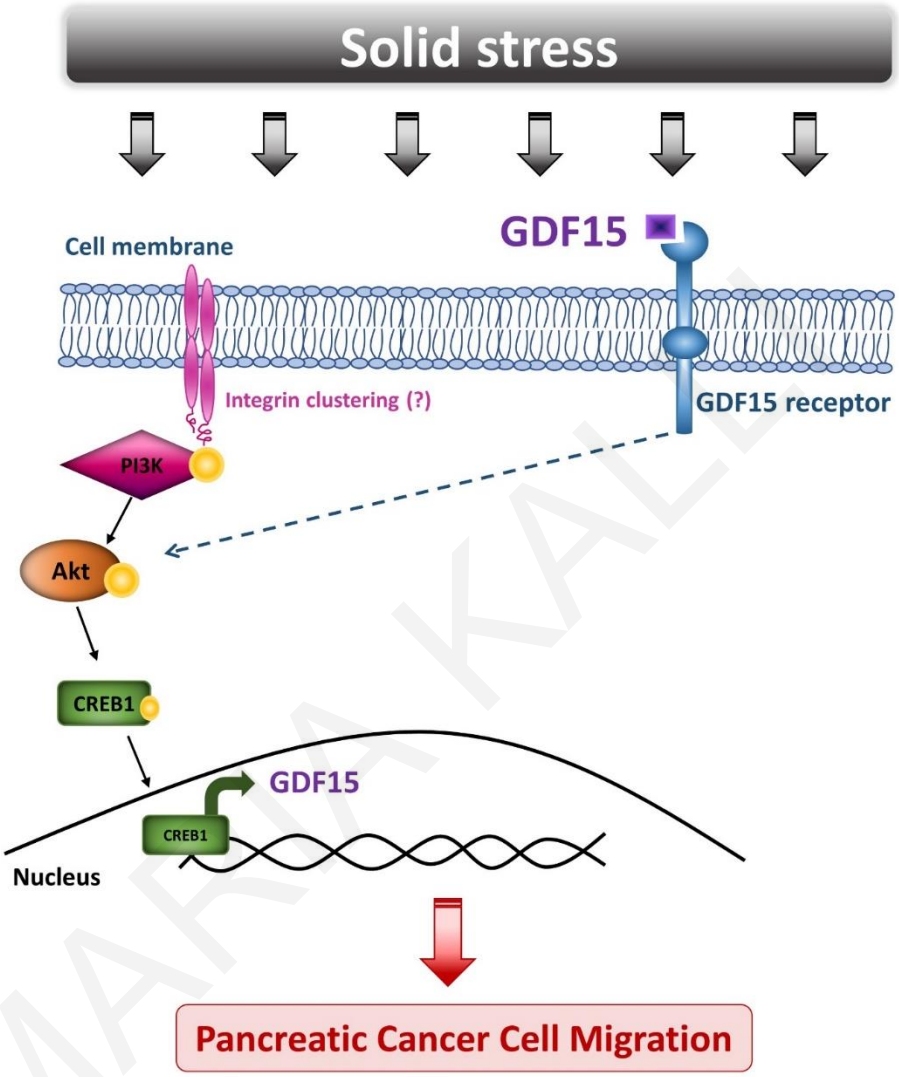

***Figure 3-11*. Proposed mechanism of how solid stress signal transduction via Akt pathway regulates GDF15 expression to induce pancreatic cancer cell migration.** The development of solid stress during the growth of several solid tumors, such as pancreatic cancer, activates Akt pathway which in turn phosphorylates CREB1. Subsequently, the activated CREB1 acts as transcription factor by a direct binding onto the promoter region of GDF15. GDF15 is then secreted and acts in an autocrine manner to promote pancreatic cancer cell migration.

4 Chapter 4: Solid stress differentially regulates the proliferative and migratory ability of brain cancer cells according to their aggressiveness

4.1 Introduction

In the previous chapters, we described our work on the effects of solid stress on pancreatic cancer cells and fibroblasts. Here, we extend the work to study brain cancer cells that also experience mechanical compression during their growth in the very confined space of the brain. Glioma is the most common primary malignant brain tumor and arises from glial cells, a type of supporting tissue for the brain cells. A glioma can be differentiated into low grade or benign glioma (grade I-III) and a high grade or malignant glioma, such as glioblastoma (Grade IV), also termed Glioblastoma multiforme (GBM), that is found to be highly cancerous containing a very high blood supply and comprising a necrotic and cystic tissue [120, 121].

A common characteristic and a major cause of the clinical symptoms seen in patients suffering from brain cancer, is the compression of brain tissue by the primary tumor mass. As the tumor grows in the cranium, it must displace the surrounding tissue and this tumor growth-induced deformation of the brain can cause severe disabilities to patients, representing a negative prognostic factor [122]. Specifically, shift of the cranial midline is a common finding among patients diagnosed with GBM and patients with midline shift tend to have significant brain compression with associated rapidly developing and pronounced neurologic deficits[123] (**Figure 4-1**). It has been previously found that the presence of midline shift adversely affects survival in patients able to undergo a biopsy, but not in those patients

able to undergo resection [123], suggesting that resection and the subsequent alleviation of compressive forces generated by the tumor growth could be very effective [123, 124].

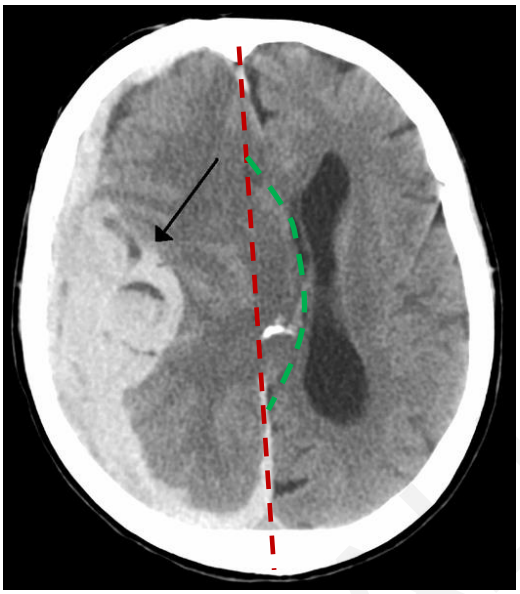

***Figure 4-1*. Midline shift is a typical symptom of patients with brain tumors.** As indicated with the black arrow, when a tumor mass is formed in the left hemisphere of the brain, it causes a midline (red dashed line that separates brain in two hemispheres) shift to the right (green dashed line).
Source:https://commons.wikimedia.org/wiki/File:Intracranial_bleed_with_significant_midline_shift.png .

Despite the importance of mechanical compression in brain tumors, there is no study examining the effects of compressive solid stress on brain cancer cells. We used the non-metastatic glioma H4 cell line and the highly malignant and metastatic GBM cell line A172, in order to investigate how brain tumor cells, respond to mechanical compression by examining their proliferative and migratory abilities. Given the fact that there is a limited number of studies estimating the levels of the compressive solid stress in brain tumors [122, 125], we used mathematical modelling in order to calculate *in vitro* the magnitude of solid stress developed during the growth of multicellular spheroids (MCS) embedded in an agarose matrix. The estimation of solid stress levels enabled us to apply a controlled and

predefined mechanical compression on cell monolayers in order to investigate the mechanism by which solid stress regulates cellular behavior. In particular, it is well established that in gliomas, there is an overexpression of the Epidermal Growth Factor Receptor (EGFR) and a downregulation or mutations of the tumor suppressor TP53 transcription factor [126]. EGFR can regulate a variety of signaling pathways including Ras/Raf/MEK/Erk, PI3K/Akt/mTOR or Jak/STAT that are implicated in cell survival, proliferation and migration (**Figure 4-2**) [127]. Indeed, Ras guanosine triphosphate (Ras-GTP) has been documented in cell lines and primary brain tumors, and is able to translate extrinsic signals into the Raf-MEK-Erk, or into either the PI3K-PKB or the PI3K-Rac-Rho pathways, which influence cell survival and migration [127] [126] [128]. Notably, almost all GBMs show increased activity of PI3K pathway, while its negative regulator PTEN, that is implicated in survival, proliferation and migration, is usually downregulated [127] [126]. Moreover, the signaling pathway regulated by cytosolic tyrosine kinase Janus kinase (JAK)-family proteins and transcription factor signal transducer and activator of transcription (STAT)-family proteins is efficiently activated, especially downstream of cytokine receptors, while the expression of retinoblastoma-associated protein (RB1) which controls the transition from G1 into S-phase of the cell cycle is also altered in GBM [127] [126]. Finally, TGFβ-mediated signaling is suggested to play crucial roles in regulating the highly malignant phenotype of gliomas, which could be considered, at least in part, TGFβ-dependent [127]. Based on these data, we expect that solid stress could alter a combination of these pathways in order to regulate cellular responses, such cell proliferation and migration. Through a phospho-proteomic screening, we set out to identify a possible molecular mechanism by which solid stress can regulate brain cellular responses, similarly to the mechanism identified for pancreatic cancer cells [129].

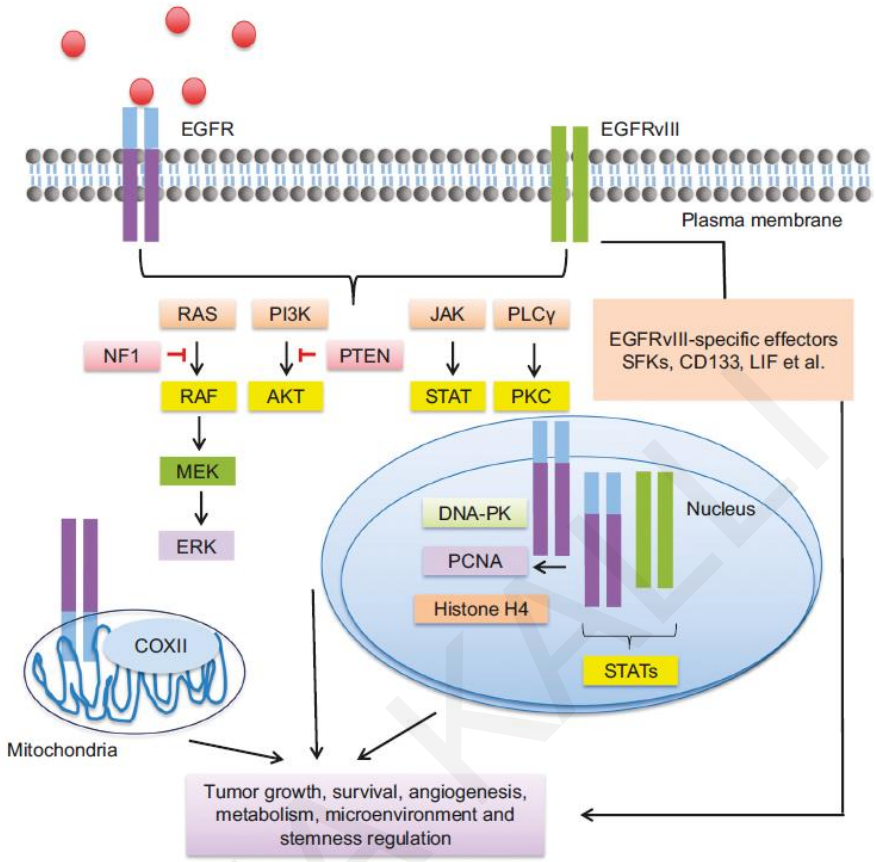

Figure 4-2. **Schematic showing the pleiotropic functions of EGFR in GBM.** Mutations causing an overexpression of the *EGFR* gene is one of the most common characteristic of patients with GBM. Overexpressed EGFR can mediate signal transduction through several pathways including Ras/Raf/MEK, PI3K/Akt and JAK/STAT. All these pathways can regulate tumor growth, survival and metastasis and are also found to be de-regulated in patients diagnosed with GBM [130].

4.2 Methods

Cell culture. Brain neuroglioma (H4) and glioblastoma (A712) cell lines, were obtained from American Type Culture Collection (ATCC) and were cultured in Dulbecco's Modified Eagle's Medium (DMEM) supplemented with 10 % Foetal Bovine Serum (FBS) and 1 % antibiotics. Cells were maintained at 37 ^{o}C and 5 % CO_2 in a humidified incubator.

Multicellular Spheroid (MCS) Formation. H4 and A172 multicellular spheroids were formed using the "hanging drop" technique [131-133]. Briefly, cells were counted and put in suspension at a concentration of 2-2.5×10^4 cells/ml. Hanging drops (20 μl) containing 500 cells were placed on the inside of the cover of a 100-mm culture dish. Drops were left for 48 h and the formed spheroids were transferred into a 96-well plate, which was pre-coated with 50 μl of 1% low-melting agarose (concentration was obtained by mixing stock solution of 4% agarose in DMEM). Culture medium, for free spheroids, or 1% low-melting agarose was then added, and pictures were taken after 24 h using a Nikon Eclipse optical microscope. Spheroids were incubated at 37 °C for a total period of 21 days and pictures were taken every 2-3 days. Spheroid size (area) was measured using the ImageJ software and difference in spheroids' size was compared to the initial size at Day 1 according to the following formula:

((Spheroid size at Day 21 – Spheroid size at Day 1) / (Spheroid size at Day 1)) x 100.

Estimation of solid stress. To mathematically model the growth and mechanical behavior of tumor spheroids, the multiplicative decomposition of the deformation gradient tensor, **F**, was used [134], a methodology that has been applied successfully to solid tumors [135-140] as well as to other soft tissues [141, 142]. The model considered only the solid phase of the spheroid and accounted for tumor growth and mechanical interactions between the spheroid and the surrounding agarose matrix. Therefore, **F** was divided into two components:

$$\mathbf{F}=\mathbf{F_e}\mathbf{F_g} \qquad (4.1)$$

where $\mathbf{F_e}$ is the elastic component of the deformation gradient tensor that accounts for mechanical interactions with the surrounding matrix or with any other external stimulus and $\mathbf{F_g}$ is the component that accounts for spheroid growth.

Tumor spheroid growth was considered to be isotropic and the growth component $\mathbf{F_g}$ was given by:

$$\mathbf{F}_g = \lambda_g \mathbf{I} \tag{4.2}$$

where λ_g is the growth stretch ratio. The growth stretch ratio was described by a linear equation expressed in differential form as [135]:

$$\frac{d\lambda_g}{dt} = -a\lambda_g \tag{4.3}$$

where *t* is the time and α describes the growth rate of the spheroids, the value of which was estimated experimentally for each cell line.

Finally, we used the constitutive equation for the compressible neo-Hookean material to describe the elastic response of the agarose matrix. The strain energy density function, *W*, of the neo-Hookean equation is:

$$W = 0.5\mu\left(-3+\mathrm{II}_1\right)+0.5\kappa\left(-1+J_e\right)^2 \tag{4.4}$$

where the mechanical properties of the model are the shear modulus, μ and bulk modulus, κ. J_e is the determinant of the elastic deformation gradient tensor $\mathbf{F_e}$ and $II_1 = I_1 J_e^{-2/3}$. I_1, I2 and I_3 are the invariants of the right Cauchy-Green deformation tensor, which is evaluated from the elastic part of the deformation gradient tensor, $\mathbf{F_e}$.

The Cauchy stress tensor, $\boldsymbol{\sigma}$, was calculated by the strain energy density function as [143]:

$$\boldsymbol{\sigma} = J_e^{-1}\mathbf{F}_e \frac{\partial W}{\partial \mathbf{F}_e^T} \tag{4.5}$$

Finally, the linear momentum balance was solved assuming a quasi-static problem in the absence of body forces:

$$\nabla \cdot \boldsymbol{\sigma} = \mathbf{0} \tag{4.6}$$

A finite element model was constructed in COMSOL to solve the system of Eqs.(4.1)-(4.6).

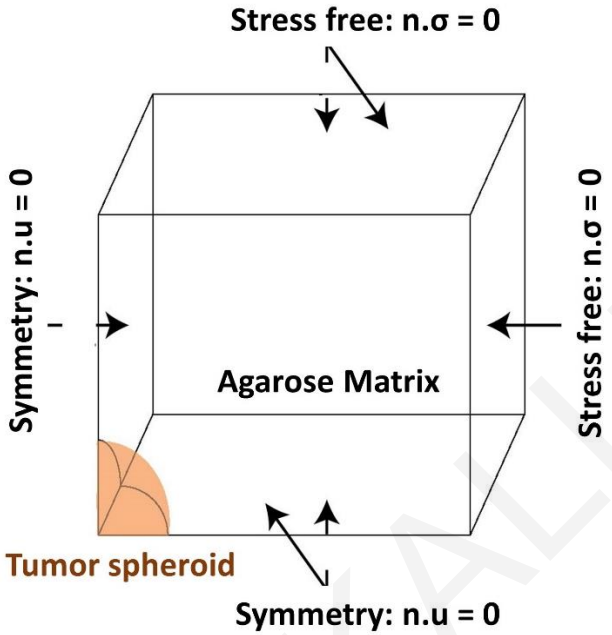

Figure *4-3.* Boundary conditions employed. Due to symmetry the one eight of the domains was solved. **n** is the unit normal vector and **u** is the displacement vector. The continuity of the displacements and the normal stress at the spheroid-matrix interface is implemented automatically by the software.

Material properties of the agarose gel. In order to estimate the material properties of the agarose gel (i.e., elastic modulus or stiffness) stress-strain experiments were performed. Unconfined compression, stress-strain experiments were carried out using a commercial high precision mechanical testing system (Instron 5944, Norwood, MA, USA). Agarose (1%) specimens were cut in an orthogonal shape with approximate dimensions 3×3×2 mm (length × width × thickness). According to the stress-strain protocol the specimens were placed between two parallel platens and they were compressed to a final strain of 15% with a strain rate of 0.05mm/min, the minimum rate the system can apply in order to avoid any transient, poroelastic effects. Stress was calculated as the force measured on the load cell divided by the initial surface area of the specimen (i.e., 1st Piola-Kirchhoff

stress), and displacement data were converted to strain as $\varepsilon = \Delta l / l_0$, where Δl is the change in the length of the specimen in the direction of compression and l_0 the initial, undeformed length. The elastic modulus was calculated from the slope of the stress-strain curve at 30% strain.

In vitro compression of cell monolayer. In order to apply mechanical compression on cancer cell monolayers, the procedure described in **Section 2.2** was followed [144, 145].

In vitro Scratch assay. A scratch wound assay was performed as described in **Section 3.2.**

Cell Viability Assay. Cell viability of cancer cells, indicative of the total cell number, was assesed using Alamar Blue reagent (Invitrogen Life Technologies) prior- and post- compression following the manufacturer's instructions.

Gene expression analysis. RNA isolation from brain cancer cells and gene expression analysis was performed as described in **Section 2.2**. The primers used for each target gene are shown in **Table 1 in Appendices**.

Immunoblotting. Whole protein cell lysates were extracted as mentioned in **Section 2.2**. Membranes were incubated with anti-Growth Differentiation Factor 15 (GDF15) (Cell Signaling), or anti-RhoB total (Abcam) antibodies overnight. Antibody against β-actin was used as loading control. The detection of antibodies was performed as previously described (**Section 2.2**).

Statistics. Data are expressed as mean ± standard error (SE). Statistical significance was examined by Student's *t*-test using two-tail distribution. Tests with *p*-values <0.05 were considered as significantly different and are nominated in each figure with an asterisk (*).

4.3 **Results**

The growth of brain cancer MCS is hindered by compression from a surrounding agarose matrix.

To evaluate the effect of mechanical compression on brain tumor growth *in vitro*, MCS composed of H4 or A172 cells, were formed and embedded in 1% agarose matrix or grown in free- suspension for 21 days. We found that the presence of agarose strongly impaired the growth of MCS, with H4 spheroids presenting a delay of growth compared to the respective control spheroids, and A172 spheroids exhibiting a complete cease of their growth as compared to the free spheroids (**Figure 4-4A&B**). Our results are in accordance with previously published studies employing colon and breast cancer cells [54, 57, 58] and data from *in vivo* measurements of brain tissue pressure in patients or animal models with brain tumors [17, 125].

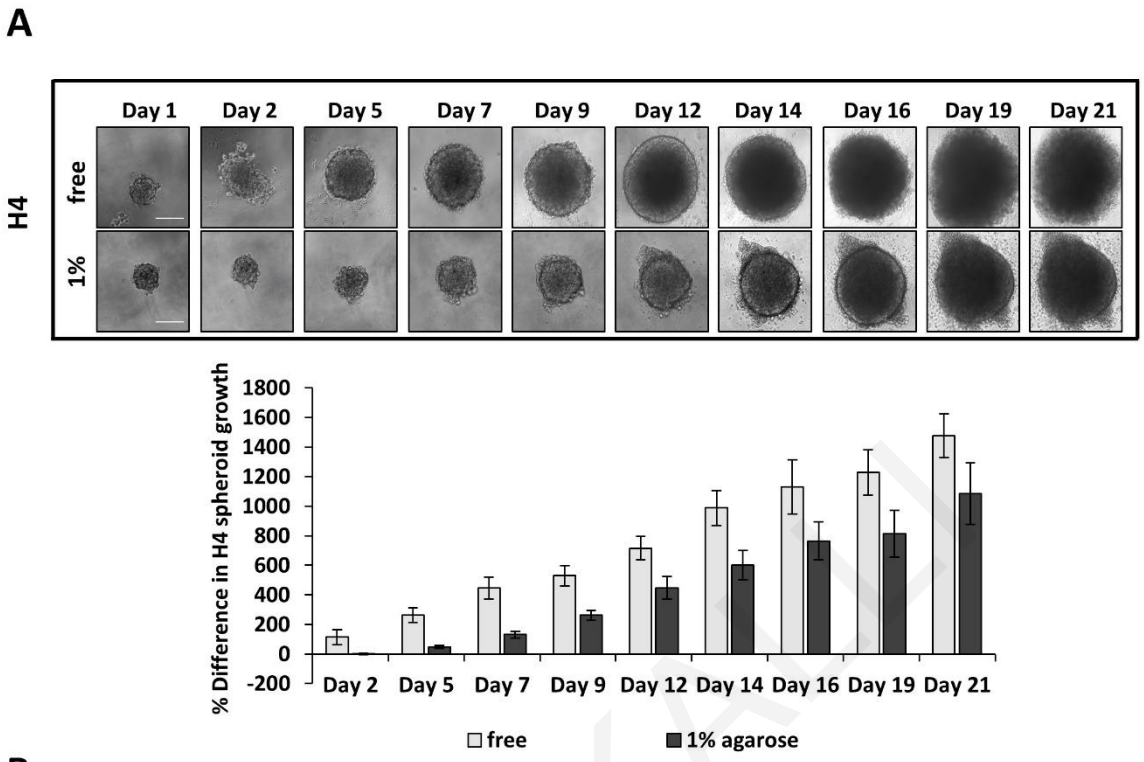
A
H4
Day 1
Day 2
Day 5
Day 7
Day 9
Day 12
Day 14
Day 16
Day 19
Day 21
free
1%
% Difference in H4 spheroid growth
1800
1600
1400
1200
1000
800
600
400
200
0
-200
Day 2
Day 5
Day 7
Day 9
Day 12
Day 14
Day 16
Day 19
Day 21
free
1% agarose

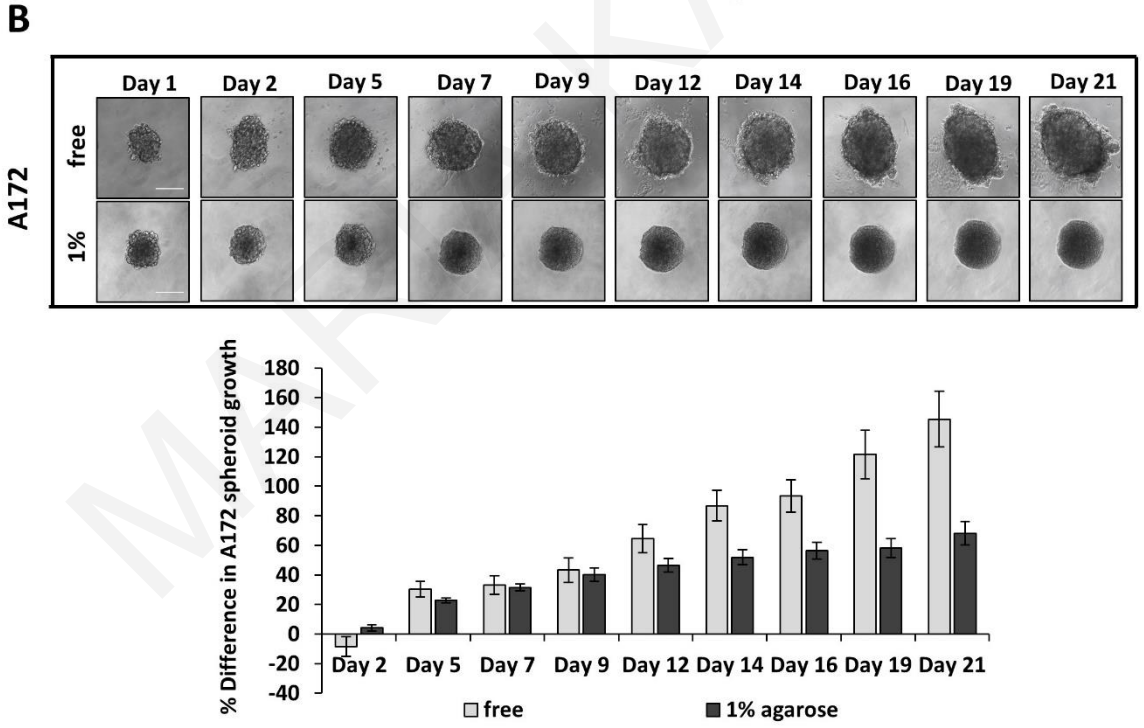
B
A172
Day 1
Day 2
Day 5
Day 7
Day 9
Day 12
Day 14
Day 16
Day 19
Day 21
free
1%
% Difference in A172 spheroid growth
180
160
140
120
100
80
60
40
20
0
-20
-40
Day 2
Day 5
Day 7
Day 9
Day 12
Day 14
Day 16
Day 19
Day 21
free
1% agarose

***Figure 4-4*. The growth of brain cancer MCS is hindered by a surrounding agarose matrix. A-B** Multicellular spheroids (MCS) composed by H4 (A) or A172 (B) cells, were embedded in 1% agarose matrix or in free suspension and grew for 21 days. Images were taken every 2-3 days with an optical microscope and the area of each spheroid was quantified using ImageJ. The average % difference in each spheroid size was calculated and plotted for each cell line (n=12-18). Scale bar: 0. 15 mm.

Estimation of solid stress generated during the growth of brain cancer MCS in agarose matrix.

In order for the MCS to grow in size, they should displace the surrounding matrix similar to the physiological growth of tumors in brain, however, we observed a delay on the growth of MCS compared to those in free-suspension (**Figure 4-4**). To estimate the compressive force that is exerted from the agarose on the spheroids to resist their expansion, we employed mechanical testing experiments and mathematical modelling. We first measured the elastic modulus of the agarose gel in unconfined compression and found it to be equal to 75 ±3.75 mmHg (10.47±0.5 kPa). Subsequently, we employed the neo-Hookean constitutive equation to fit the experimentally derived stress-strain results and to derive the value of the shear modulus μ and bulk modulus κ in (equation *4.4*) assuming a Poisson's ratio of 0.2 (**Figure 4-5)**. Then, the growth of the MCS was simulated and the predicted by the mathematical model growth curves were fitted to the experimental data (**Figure 4-6A-B**) by varying the parameter α in equation 4.3 and the developed solid stress was calculated from the model (**Figure 4-6C-D**). The Figure 4-2C, D presents the bulk stress at the centre of the MCS, calculated as the average of the diagonal components of the Cauchy stress tensor (radial σ_{rr} and circumferential $\sigma_{\theta\theta}$, $\sigma_{\varphi\varphi}$) , i.e., $\bar{\sigma} = (\sigma_{rr} + \sigma_{\theta\theta} + \sigma_{\varphi\varphi})/3$. The compressive solid stress was calculated in the range of ~0-60 mmHg (~0.0-8 kPa). In particular, the level of solid stress developed during the growth of H4 spheroids (~0-60 mmHg/ 0.0-8 kPa) was much higher than that of A172 spheroids (~0-26 mmHg/0.0-3.5 kPa), which would be expected as the H4 spheroids grew to a much higher volume than that of A172. However, the estimated

levels of solid stress in both cell lines was in accordance with previous *in situ* (2.8-60.1 mmHg/0.37-8.0 kPa), *in vivo* (4-28 mmHg/ 0.53-3.53 kPa) and *in vitro* estimations (28-120 mmHg/3.7-16.0 mmHg) [10, 17, 54, 57, 125] of solid stress.

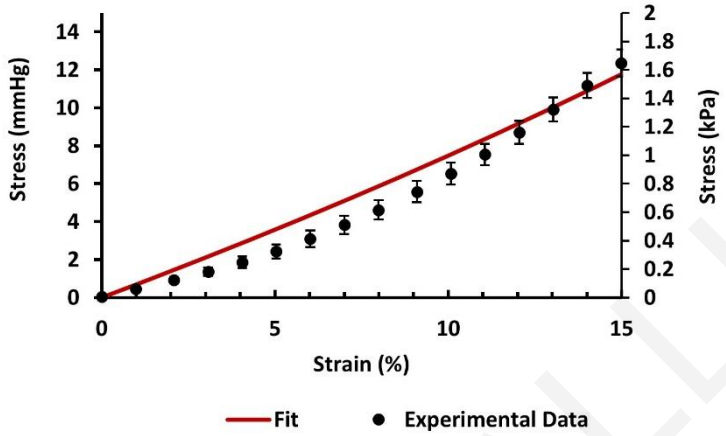

Figure 4-5. Representative fitting of the neo-Hookean equation to the experimentally measured stress-strain response of 1% agarose gel.

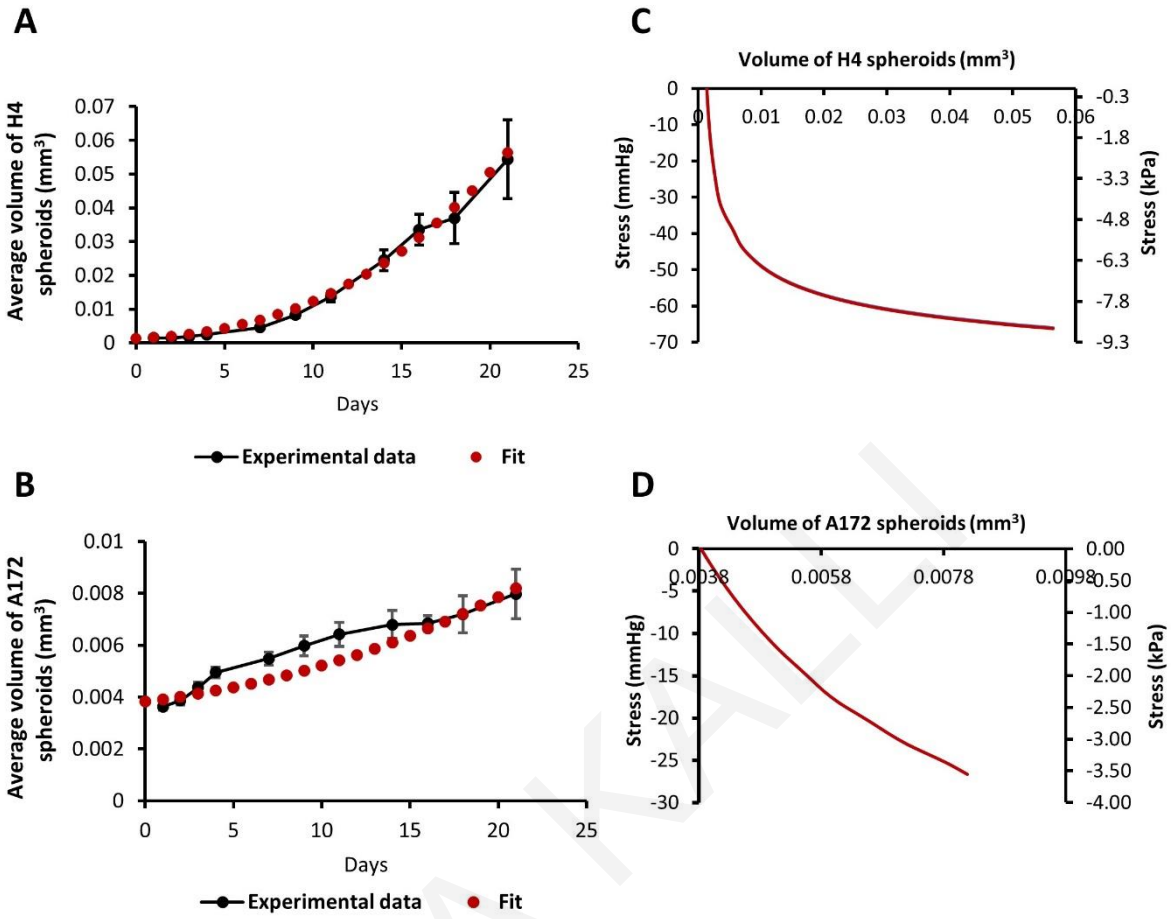

Figure 4-6. **Estimation of solid stress generated during the growth of brain cancer MCS within an agarose matrix. A-B,** Fit of the mathematical model to the experimental data of the growth of H4 (A) and A172 (B) spheroids. **C-D,** The calculated by the model bulk solid stress generated during the growth of H4 (C) and A172 (D) spheroids.

Solid stress differentially regulates the migration and proliferation of brain cancer cells.

To determine how solid stress affects the cellular behaviour of brain cancer cells, we used our previously described transmembrane pressure device [101, 129101, 129101, 129101, 129101, 129,101, 129,73, 101,73, 101,73, 101] in order to compress cell monolayers[73, 101]. Based on the estimations of solid stress, we employed 2.0 and 4.0 mmHg (0.26 and 0.53 kPa) of stress, as these levels can be generated in the first 2 days of spheroid's growth in the agarose matrix and are supposed to be an early-transmitted solid stress stimulus in brain cancer cells, at least *in*

vitro. We found that while the 2 mmHg stress did not cause any significant change in the migratory ability of brain cancer cells, the 4 mmHg solid stress was able to enhance the migration of glioma H4 cells and impair that of GBM A172 cells (**Figure 4-7A-B**). Moreover, we observed that mechanical compression strongly reduced the cell number of H4 cells without any effect on A172 cells, as indicated by Alamar Blue assay (**Figure 4-7C**), suggesting that solid stress can differentially regulate the migratory and proliferative ability of brain cancer cells, depending on their metastatic potential.

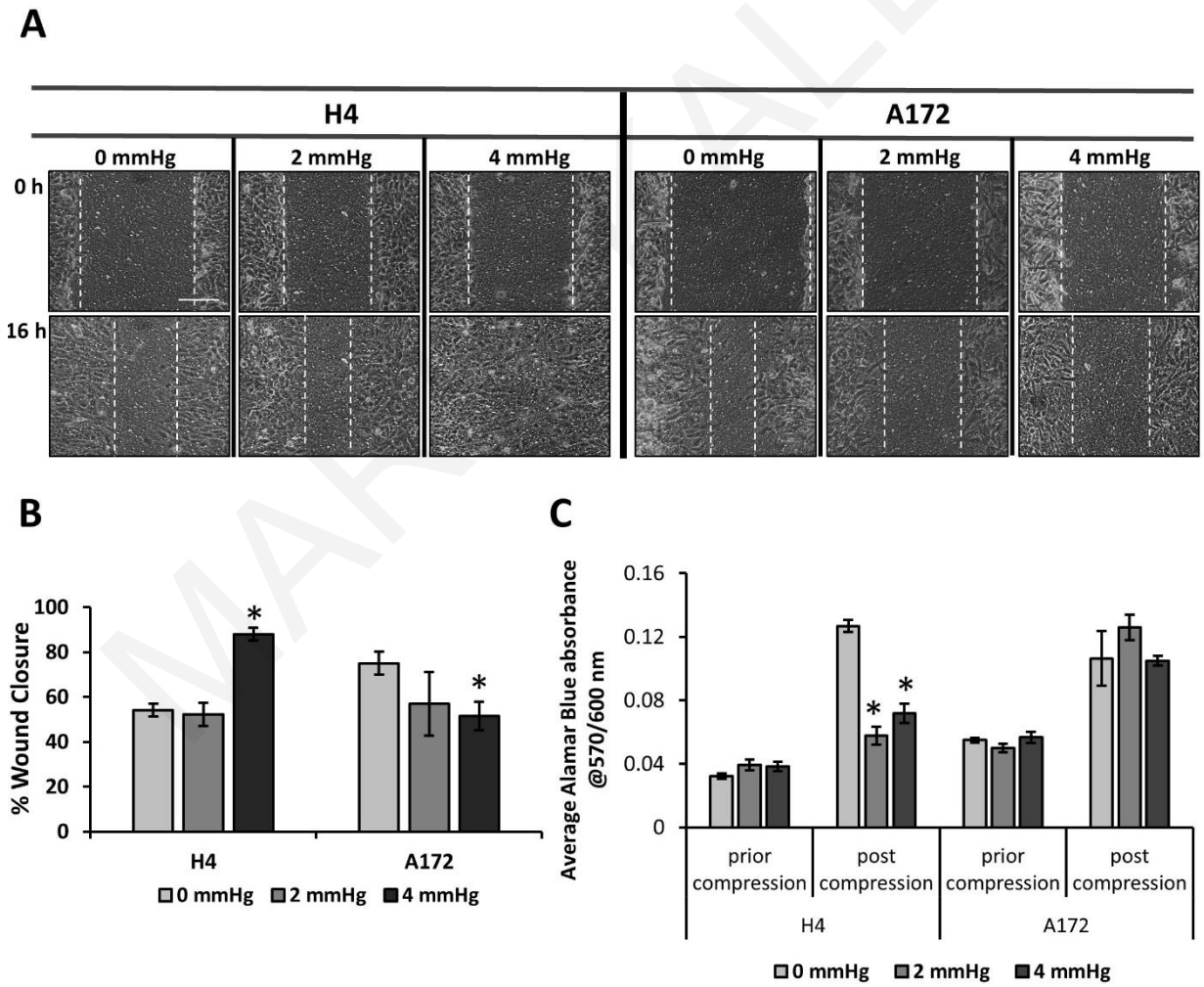

Figure 4-7. **Solid stress differentially regulates the migration and proliferation of brain cancer cells according to their aggressiveness. A,** Brain cancer cells, H4 (left) and A172 (right) were grown in transwell inserts to form a monolayer. A scratch wound was then introduced and compression (0, 2 and 4 mmHg) was applied for 16 hours. Pictures from at least 3 different fields per condition were taken with an optical microscope (10X magnification) prior and post compression. Scale bar: 0.15 mm. **B**, Cell-free area was quantified using ImageJ software and the average percentage of wound closure from at least two independent experiments was plotted for each cell line (n=6-9). **C**, Brain cancer cells lines were counted and seeded with equal density in 6-well transwell inserts. Alamar Blue was added in culture medium (10%) and absorbance was measured prior- and post- comperssion at 570/600 nm. Absorbance of Alamar Blue is indicative of the total cell number.

Solid stress differentially regulates the gene expression profile of brain cancer cells.

Based on the data described above suggesting that solid stress can differentially regulate the migration and growth of brain cancer cells, we proceeded to analyze the gene expression profile of both cell lines in order to further investigate the cellular behavior that was observed in response to compression. To this end, we compressed H4 and A172 cells at 4 mmHg, as this level of compression caused significant changes in the migration of both cell lines, and we then examined the expression profile of several migration-related genes, such as Rho GTPases, Fibronectin I, Vimentin, as well as the expression of GDF15 which was found to be consistently upregulated as a response to compression [101, 129]. Real-time PCR and Western Blotting revealed a strong increase in the expression of *RhoB GTPase* in H4 cells, while a slight decrease was observed in A172 cells (**Figure 4-8A&4-8C**). In addition, *GDF15* exhibited a dramatic increase in both cell lines at both the mRNA and protein level (**Figure 4-8A&4-8B**). Notably, the rest of the genes tested showed negligible changes as compared to the changes showed for *RhoB* and *GDF15,* which was in agreement with our previous study employing pancreatic cancer cells [101]. Knowing that the expression of GDF15 is systematically upregulated in response to compression, these results allowed us to form the hypothesis that the differential response of brain cancer cells to mechanical compression could possibly be explained by the differential expression of RhoB GTPase. Thus, future

experiments are needed to identify how this Rho GTPase is implicated in solid stress-induced brain cancer cell migration.

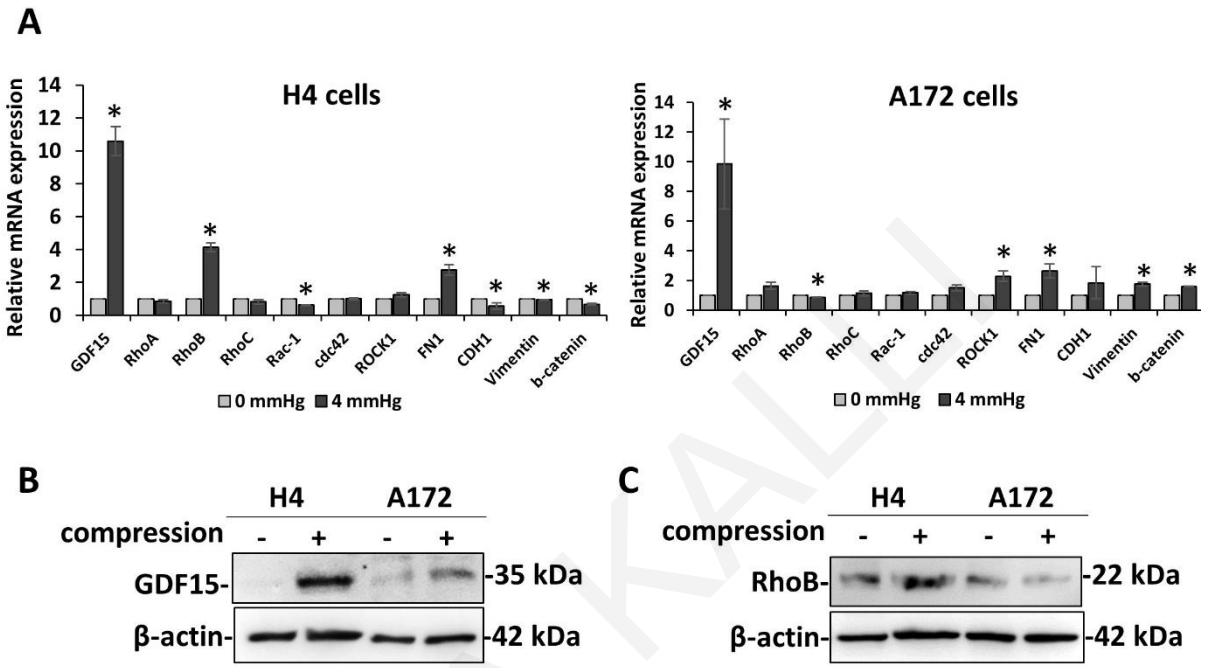

***Figure 4-8*. Solid stress differentially regulates the gene expression profile of brain cancer cells.** **A,** Brain cancer cells, H4 (left) and A172 (right) were subjected to 4.0 mmHg of compressive stress for 16 hours and the expression of several migration-related genes was measured by qPCR. The mRNA expression in each sample was quantified by the ΔΔCt method using the expression in uncompressed cells as a reference. Bar graphs represent the mean fold change ±SE of three biological replicates (n=9). Statistically significant changes between compressed and uncompressed cells are indicated by an asterisk (*) ($p<0.05$). **B-C**, Representative Western blotting showing the expression of GDF15 (B) and RhoB (C) in the compressed H4 and A172 cells. B-actin was used to verify equal protein loading.

4.4 **Discussion**

Mechanical compression is a common abnormality of brain tumors that has been shown to be responsible for the severe neurological defects of brain cancer patients [122]. It is of note that patients that undergo resection – that can effectively alleviate solid stress - exhibit higher survival rates than those subjected to biopsy only [123], suggesting that

compressive forces generated during brain tumor growth play a key role in tumor progression [123,96].

In order to investigate the role of these compressive forces in brain tumor progression *in vitro*, we first examined their effect on MCS composed of two distinct brain cancer cell lines embedded in an agarose matrix. The agarose matrix is supposed to mimic the confinement of the normal host tissue that resists to tumor expansion, resulting in the development of compressive forces in the tumor interior. We found that the presence of the surrounding matrix impaired MCS growth as compared to spheroids grown in free suspension (**Figure 4-4**). With the use of computational analysis, we estimated that the level of the resultant compressive solid stress in MCS is in the range of ~0-60 mmHg (0-8 kPa) (**Figure 4-6**), which is in accordance with previously established *in vitro* and *in vivo* studies [10, 17, 25, 28, 97].

Next, by using our established transmembrane pressure device for the compression of cell monolayers, we analysed the migratory and proliferative abilities of brain cancer cells in response to a predefined and controlled mechanical compression, which was selected based on our computational analysis. We found that compression can differentially regulate the migration and proliferation of brain cancer cells according to their metastatic potential. More specifically, mechanical compression induced the migration and decreased the proliferation of the non-metastatic H4 cell line, while the opposite effect was observed for the highly aggressive A172 cells (**Figure 4-7**). By further analysing the gene expression of these cells, emphasizing on migration-related genes, we found that GDF15 is consistently upregulated in response to compression in both cell lines, while the expression of RhoB GTPase was differentially regulated following the migratory pattern of cells under compression (**Figure 4-8**). Specifically, RhoB was strongly increased in compressed H4

cells and decreased in A172 cells, suggesting that this molecule could be responsible for their differential migratory ability. It is of note that Rho A/B/C GTPases can get activated by growth and stress stimuli and are important regulators of cell and tissue morphology and function, acting mainly through actin cytoskeleton reorganization [103]. Although it has been clearly shown that Rho A and Rho C can promote cancer cell migration, invasion and adhesion, the effect of RhoB on cell migration is proposed to be cell type and context-dependent, probably because it affects both intracellular protein trafficking and actin organization[146]. Interestingly, RhoB has been found to be expressed in high-grade glioma, while depletion of this molecule impaired proliferation and survival of GBM cells through a STAT3-dependent regulation of p53 and p21 expression, and that knockdown of RhoB found to impair the *in vivo* tumorigenic potential of GBM cells[147]. Moreover, RhoB was found to control different mechanisms involved in brain tumor radioresistance, thus inhibition of RhoB could be an important therapeutic intervention employing an adjuvant treatment combined with radiotherapy in GBM to improve the response of this tumor to treatment [148]. Indeed, Tipifarnib, a Farnesyltransferase inhibitor (FTI), has been administered in Phase I clinical trial showing a positive effect on patients with brain tumor by inhibiting the farnesylated (activated) form of RhoB [149].

Based on these studies, further experiments, including validation of the activated form of the endogenous RhoB by a pull-down assay or knockdown of RhoB expression in H4 cells and an overexpression in A172 cells will reveal the role of this molecule in the differential regulation of compression-induced migration of brain cancer cells. Moreover, a phosphoprotein screening will contribute to the identification of a molecular mechanism by which solid stress regulates brain tumor progression and whether this solid stress-induced mechanism can also regulate the differential expression of RhoB GTPase. By combining all

these data, we will contribute to the identification of possible therapeutic targets for the treatment of patients with brain cancer, rendering mechanical compression and the resultant solid stress as key regulators for brain tumor progression and malignancy.

5 Conclusions and Future Directions

5.1 Conclusions

In this work, we investigated the effect of solid stress on normal pancreatic fibroblasts, and how it affects their interaction with adjacent pancreatic cancer cells. Moreover, we examined how pancreatic and brain cancer cell behavior is altered under mechanical compression. For our experiments, we employed a custom-made transmembrane pressure device used in pertinent studies as a tool to apply compressive solid stress in a measurable and predefined manner, similar in magnitude to the stress applied on cells in the tumor interior [17]. The level of compressive stress used in this study ranged from 1.0 to 6.0 mmHg (0.13-0.8 kPa), which was in agreement with experimental measurements in pancreatic, breast and brain tumor models [10, 11, 17]. Moreover, we developed a 3D experimental setup composed of multicellular spheroids embedded in an agarose matrix to study how solid stress affects brain tumor growth and metastasis *in vitro*.

By applying 4.0 mmHg compressive stress on normal pancreatic fibroblasts we observed that several genes were upregulated in response to the applied stress. In particular, we found that normal pancreatic fibroblasts are get activated as a response to mechanical compression, as indicated by elevated expression of the fibroblast-activation marker a-SMA and Collagen I. Moreover, we observed a significant upregulation of GDF15, which has been shown to be regulated by cytoskeletal changes but has never been linked to solid stress. We next used a novel co-culture system comprised by compressed fibroblasts and uncomrpessed cancer cells and found that compression-induced activated fibroblasts promote the migration of pancreatic cancer cells through GDF15 secretion. Our results further suggest that this

fibroblast-derived cytokine is fundamentally responsible for migration of cancer cells under solid stress, which has not been shown previously.

We next studied the direct effect of solid stress on pancreatic cancer cells using a similar experimental setup in the absence of fibroblasts. We found that solid stress stimulate GDF15 expression not only in fibroblasts but also in cancer cells, which ultimately promotes pancreatic cancer cell migration. Moreover, through a phosphoproteomic screen we identified that solid-stress signal transduction is mediated through Akt pathway activation, which is responsible for the regulation of GDF15 expression in order to induce pancreatic cancer cell migration under compression.

Finally, using multicellular spheroids embedded in agarose matrix, we found that solid stress impaired the growth of brain tumor spheroids *in vitro*, while mechanical compression applied on cell monolayer differentially regulates the proliferation, migration, as well as the gene expression of brain cancer cells. More importantly, we observed a strong upregulation of GDF15 in compressed brain cancer cells, as similarly observed in compressed fibroblasts and pancreatic cancer cells. The expression of RhoB GTPase was found to be differentially regulated in compressed glioma and glioblastoma cell lines, allowing us to hypothesize that this molecule is a key regulator for brain cancer cell migration. However, further experiments including silencing of *RhoB* gene in combination with a phosphoproteomic screening will identify the molecular mechanism by which solid stress regulates brain cancer cell behaviour.

5.2 **Future Directions**

Collectively, our data revealed that solid stress can regulate the progression of solid tumors, suggesting that targeting the transduction of its signal in cancer cells or fibroblasts could be promising for the treatment of patients with tumors characterized by high solid stress levels.

Apart from our future experiments regarding the role of RhoB GTPase in solid stress-induced brain cancer cell migration, we could also enhanced our research by our recent data extrapolated from a Reverse Phase Protein Assay (RPPA) performed on compressed pancreatic cancer cells by MD Anderson Cancer Center, University of Texas (**Figure 5-1A**). RPPA represents an antibody-based functional proteomic analysis that characterizes the basal protein expression and modification levels, growth factor- or ligand-induced effects. Using this assay we were able to test approximately 300 different proteins that are differentially expressed or modified in cancer cells in response to compression. Through this screen, we identified about 15 proteins that are regulated by mechanical compression in pancreatic cancer cells, including tumor suppressors (such as Retinoblastoma-related protein 1 (or Rb1) and p53), Akt and Heat Shock Protein 27 (HSP27) (**Figure 5-1B**). HSP27 is an oxidative or heat stress sensor that interacts with actin cytoskeleton [150, 151], and it has been found to be upregulated in the serum of patients with pancreatic cancer, similarly with GDF15 [152, 153]. Moreover, HSP27 is suggested to be responsible for the gemcitabine resistance in patients with pancreatic cancer and targeting this molecule by siRNAs has already been used in Phase II clinical trials in combination with gemcitabine for the treatment of patients with pancreatic cancer [154-157] . However, data regarding the mechanism by which this protein is up-regulated in cancer and how could be correlated with solid stress are not elucidated yet.

It is already suggested that Akt pathway can regulate or being regulated by HSP27 in response to cellular stress [158-163], and knowing that both are upregulated by mechanical compression in pancreatic cancer cells, a plausible hypothesis is that these molecules are connected to each other in order to regulate the solid stress-induced cancer cell migration. Indeed HSP27 has been implicated in cancer cell invasion and migration in several tumor types, including prostate, breast, melanoma and brain cancer, however data regarding its role in pancreatic cancer are limited [164-167]. Thus, future experiments would contribute to the

identification of the molecular mechanism by which HSP27 interacts or synergistically acts with the already known solid stress-induced molecules or signaling pathways, such as GDF15, RhoB and PI3K/Akt, in order to regulate pancreatic tumor progression.

In conclusion, by combining our results, we will be able to suggest novel serum biomarkers indicating the presence of solid stress in solid tumors, such as GDF15, HSP27 or even RhoB. This could suggest a therapeutic intervention that employs a conventional therapy or/and a stress alleviation strategy, such as tranilast or pirfenidone [168, 169], in order to suppress tumor growth and at the same time, to block the *de novo* solid stress-induced expression of genes that could promote tumor progression avoiding a targeted therapy against each gene (**Figure 5-2).**

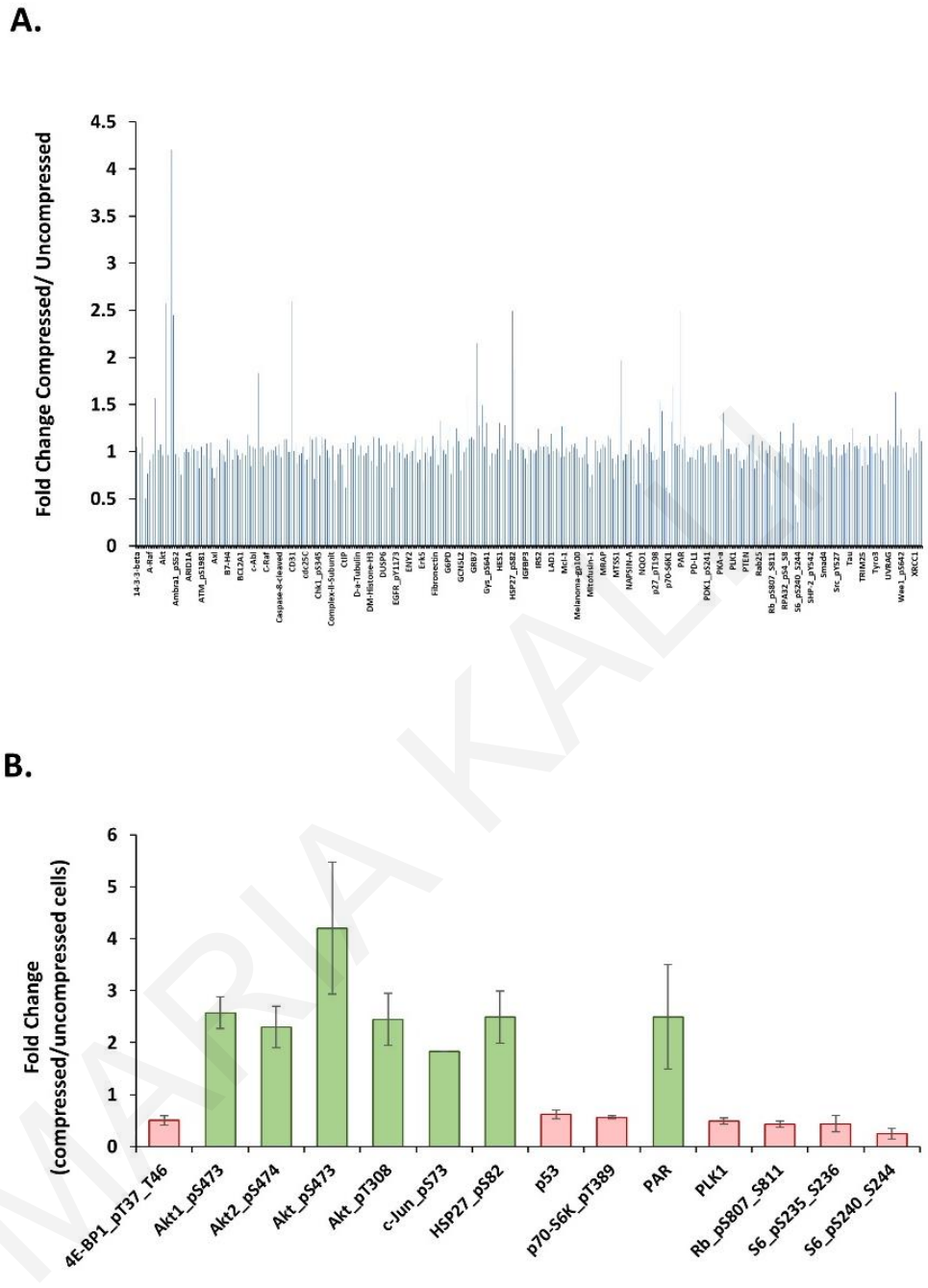

***Figure 5-1*. A, RPPA analysis of compressed pancreatic cancer cells. A,** Signal intensities were normalized to uncompressed cells and the mean fold change from three independent experiments was plotted for each gene. **B**, RPPA hits with an average fold change ≥ 2.0 or ≤ 0.5 were selected and plotted for each gene. Red and green colors indicate downregulation or upregulation of each RPPA signal, respectively.

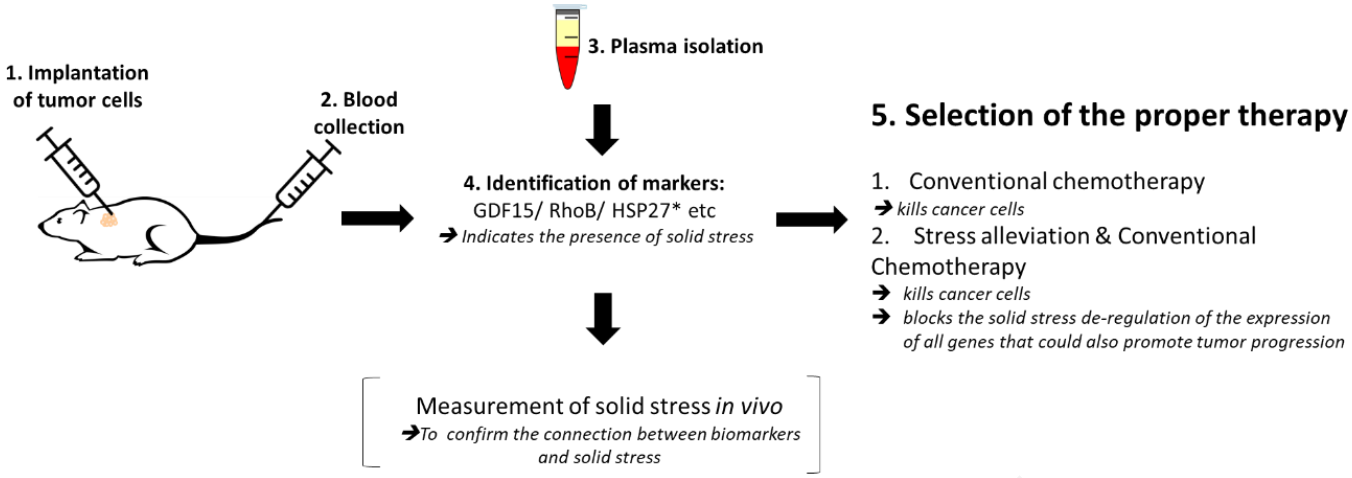

***Figure 5-2*. Diagram showing the future perspective of this PhD study.** Based on our *in vitro* data, we could move on *in vivo* studies employing animal models that are implanted with pancreatic or brain cancer cells (1). After tumor is formed, we could collect animals' blood (2) in order to examine the levels of markers indicating the presence of high solid stress levels such as GDF15, RhoB and HSP27 (3-4). As we have shown, these genes are upregulated in response to solid stress and can be found in the serum of cancer patients being implicated in tumor progression by triggering cancer cell migration and proliferation. Alleviating stresses from the tumor microenvironment would block their *de novo* solid-stress induced upregulation and by combining a stress alleviation strategy with a conventional chemotherapeutic agent we could suggest a novel therapeutic intervention without the limitation of using a targeted therapy against a selected gene target (5).

List of Tables

List of Figures

References

1. Pecorino, L. Molecular biology of cancer: mechanisms, targets, and therapeutics. (Oxford university press, 2012).
2. Quail, D.F. & Joyce, J.A. Microenvironmental regulation of tumor progression and metastasis. *Nature medicine* **19**, 1423-1437 (2013).
3. Kalluri, R. & Zeisberg, M. Fibroblasts in cancer. *Nature reviews. Cancer* **6**, 392-401 (2006).
4. Kalluri, R. The biology and function of fibroblasts in cancer. *Nature reviews. Cancer* **16**, 582-598 (2016).
5. Jain, R.K., Martin, J.D. & Stylianopoulos, T. The role of mechanical forces in tumor growth and therapy. *Annual review of biomedical engineering* **16**, 321-346 (2014).
6. Acerbi, I. et al. Human breast cancer invasion and aggression correlates with ECM stiffening and immune cell infiltration. *Integrative biology : quantitative biosciences from nano to macro* **7**, 1120-1134 (2015).
7. Rath, N. & Olson, M.F. Regulation of pancreatic cancer aggressiveness by stromal stiffening. *Nature medicine* **22**, 462-463 (2016).
8. Paszek, M.J. & Weaver, V.M. The tension mounts: mechanics meets morphogenesis and malignancy. *Journal of mammary gland biology and neoplasia* **9**, 325-342 (2004).
9. Butcher, D.T., Alliston, T. & Weaver, V.M. A tense situation: forcing tumour progression. *Nature reviews. Cancer* **9**, 108-122 (2009).
10. Stylianopoulos, T. et al. Causes, consequences, and remedies for growth-induced solid stress in murine and human tumors. *Proceedings of the National Academy of Sciences of the United States of America* **109**, 15101-15108 (2012).
11. Voutouri, C., Polydorou, C., Papageorgis, P., Gkretsi, V. & Stylianopoulos, T. Hyaluronan-Derived Swelling of Solid Tumors, the Contribution of Collagen and Cancer Cells, and Implications for Cancer Therapy. *Neoplasia* **18**, 732-741 (2016).
12. McGrail, Daniel J. et al. Osmotic Regulation Is Required for Cancer Cell Survival under Solid Stress. *Biophysical journal* **109**, 1334-1337 (2015).
13. Tomasek, J.J., Gabbiani, G., Hinz, B., Chaponnier, C. & Brown, R.A. Myofibroblasts and mechano-regulation of connective tissue remodelling. *Nature reviews. Molecular cell biology* **3**, 349-363 (2002).
14. Wipff, P.J., Rifkin, D.B., Meister, J.J. & Hinz, B. Myofibroblast contraction activates latent TGF-beta1 from the extracellular matrix. *The Journal of cell biology* **179**, 1311-1323 (2007).
15. Voutouri, C., Mpekris, F., Papageorgis, P., Odysseos, A.D. & Stylianopoulos, T. Role of constitutive behavior and tumor-host mechanical interactions in the state of stress and growth of solid tumors. *PloS one* **9**, e104717 (2014).
16. Stylianopoulos, T. et al. Coevolution of solid stress and interstitial fluid pressure in tumors during progression: implications for vascular collapse. *Cancer research* **73**, 3833-3841 (2013).
17. Nia, H.T. et al. Solid stress and elastic energy as measures of tumour mechanopathology. *Nature Biomedical Engineering* **1**, 0004 (2016).
18. Kalli, M. & Stylianopoulos, T. Defining the Role of Solid Stress and Matrix Stiffness in Cancer Cell Proliferation and Metastasis. *Frontiers in oncology* **8**, 55 (2018).

19. Stylianopoulos, T. The Solid Mechanics of Cancer and Strategies for Improved Therapy. *J Biomech Eng-T Asme* **139** (2017).
20. Polacheck, W.J. & Chen, C.S. Measuring cell-generated forces: a guide to the available tools. *Nature methods* **13**, 415-423 (2016).
21. De Pascalis, C. & Etienne-Manneville, S. Single and collective cell migration: the mechanics of adhesions. *Molecular biology of the cell* **28**, 1833-1846 (2017).
22. Chen, C.S. Mechanotransduction – a field pulling together? *Journal of cell science* **121**, 3285 (2008).
23. Trimis, G., Chatzistamou, I., Politi, K., Kiaris, H. & Papavassiliou, A.G. Expression of p21waf1/Cip1 in stromal fibroblasts of primary breast tumors. *Human molecular genetics* **17**, 3596-3600 (2008).
24. Gilkes, D.M. & Wirtz, D. Tumour mechanopathology: Cutting the stress out. *Nature Biomedical Engineering* **1** (2017).
25. Yeung, T. et al. Effects of substrate stiffness on cell morphology, cytoskeletal structure, and adhesion. *Cell Motility and the Cytoskeleton* **60**, 24-34 (2005).
26. Li, Z. et al. Transforming growth factor-beta and substrate stiffness regulate portal fibroblast activation in culture. *Hepatology* **46**, 1246-1256 (2007).
27. Ulrich, T.A., de Juan Pardo, E.M. & Kumar, S. The mechanical rigidity of the extracellular matrix regulates the structure, motility, and proliferation of glioma cells. *Cancer research* **69**, 4167-4174 (2009).
28. Friedland, J.C., Lee, M.H. & Boettiger, D. Mechanically activated integrin switch controls alpha5beta1 function. *Science* **323**, 642-644 (2009).
29. Lutolf, M.P. et al. Synthetic matrix metalloproteinase-sensitive hydrogels for the conduction of tissue regeneration: engineering cell-invasion characteristics. *Proceedings of the National Academy of Sciences of the United States of America* **100**, 5413-5418 (2003).
30. Paszek, M.J. et al. Tensional homeostasis and the malignant phenotype. *Cancer cell* **8**, 241-254 (2005).
31. Pedersen, J.A. & Swartz, M.A. Mechanobiology in the third dimension. *Annals of biomedical engineering* **33**, 1469-1490 (2005).
32. Kaufman, L.J. et al. Glioma expansion in collagen I matrices: analyzing collagen concentration-dependent growth and motility patterns. *Biophysical journal* **89**, 635-650 (2005).
33. Zaman, M.H. et al. Migration of tumor cells in 3D matrices is governed by matrix stiffness along with cell-matrix adhesion and proteolysis. *Proceedings of the National Academy of Sciences of the United States of America* **103**, 10889-10894 (2006).
34. Van Goethem, E., Poincloux, R., Gauffre, F., Maridonneau-Parini, I. & Le Cabec, V. Matrix architecture dictates three-dimensional migration modes of human macrophages: differential involvement of proteases and podosome-like structures. *Journal of immunology* **184**, 1049-1061 (2010).
35. Kraning-Rush, C.M. & Reinhart-King, C.A. Controlling matrix stiffness and topography for the study of tumor cell migration. *Cell adhesion & migration* **6**, 274-279 (2012).
36. Gkretsi, V., Stylianou, A., Louca, M. & Stylianopoulos, T. Identification of Ras suppressor-1 (RSU-1) as a potential breast cancer metastasis biomarker using a three-dimensional in vitro approach. *Oncotarget* **8**, 27364-27379 (2017).

37. Szot, C.S., Buchanan, C.F., Freeman, J.W. & Rylander, M.N. 3D in vitro bioengineered tumors based on collagen I hydrogels. *Biomaterials* **32**, 7905-7912 (2011).
38. Mason, B.N., Starchenko, A., Williams, R.M., Bonassar, L.J. & Reinhart-King, C.A. Tuning three-dimensional collagen matrix stiffness independently of collagen concentration modulates endothelial cell behavior. *Acta biomaterialia* **9**, 4635-4644 (2013).
39. Samuel, M.S. et al. Actomyosin-mediated cellular tension drives increased tissue stiffness and beta-catenin activation to induce epidermal hyperplasia and tumor growth. *Cancer cell* **19**, 776-791 (2011).
40. Northey, J.J., Przybyla, L. & Weaver, V.M. Tissue Force Programs Cell Fate and Tumor Aggression. *Cancer discovery* **7**, 1224-1237 (2017).
41. Lansman, J.B., Hallam, T.J. & Rink, T.J. Single stretch-activated ion channels in vascular endothelial cells as mechanotransducers? *Nature* **325**, 811-813 (1987).
42. Defilippi, P., Di Stefano, P. & Cabodi, S. p130Cas: a versatile scaffold in signaling networks. *Trends in cell biology* **16**, 257-263 (2006).
43. Levental, K.R. et al. Matrix crosslinking forces tumor progression by enhancing integrin signaling. *Cell* **139**, 891-906 (2009).
44. Kharaishvili, G. et al. The role of cancer-associated fibroblasts, solid stress and other microenvironmental factors in tumor progression and therapy resistance. *Cancer cell international* **14**, 41 (2014).
45. Gehler, S. et al. Filamin A-beta1 integrin complex tunes epithelial cell response to matrix tension. *Molecular biology of the cell* **20**, 3224-3238 (2009).
46. Shi, Q. & Boettiger, D. A novel mode for integrin-mediated signaling: tethering is required for phosphorylation of FAK Y397. *Molecular biology of the cell* **14**, 4306-4315 (2003).
47. Ross, T.D. et al. Integrins in mechanotransduction. *Current opinion in cell biology* **25**, 613-618 (2013).
48. Polacheck, W.J., Zervantonakis, I.K. & Kamm, R.D. Tumor cell migration in complex microenvironments. *Cellular and molecular life sciences : CMLS* **70**, 1335-1356 (2013).
49. Lawson, C.D. & Burridge, K. The on-off relationship of Rho and Rac during integrin-mediated adhesion and cell migration. *Small GTPases* **5**, e27958 (2014).
50. Wei, S.C. et al. Matrix stiffness drives epithelial-mesenchymal transition and tumour metastasis through a TWIST1-G3BP2 mechanotransduction pathway. *Nature cell biology* **17**, 678-688 (2015).
51. Gkretsi, V., Stylianou, A. & Stylianopoulos, T. Vasodilator-Stimulated Phosphoprotein (VASP) depletion from breast cancer MDA-MB-231 cells inhibits tumor spheroid invasion through downregulation of Migfilin, beta-catenin and urokinase-plasminogen activator (uPA). *Exp Cell Res* (2017).
52. Wipff, P.J. & Hinz, B. Myofibroblasts work best under stress. *Journal of bodywork and movement therapies* **13**, 121-127 (2009).
53. Zhang, K. et al. Mechanical signals regulate and activate SNAIL1 protein to control the fibrogenic response of cancer-associated fibroblasts. *Journal of cell science* **129**, 1989-2002 (2016).
54. Helmlinger, G., Netti, P.A., Lichtenbeld, H.C., Melder, R.J. & Jain, R.K. Solid stress inhibits the growth of multicellular tumor spheroids. *Nature biotechnology* **15**, 778-783 (1997).

55. Koike, C. et al. Solid stress facilitates spheroid formation: potential involvement of hyaluronan. *British journal of cancer* **86**, 947-953 (2002).
56. Roose, T., Netti, P.A., Munn, L.L., Boucher, Y. & Jain, R.K. Solid stress generated by spheroid growth estimated using a linear poroelasticity model. *Microvascular research* **66**, 204-212 (2003).
57. Cheng, G., Tse, J., Jain, R.K. & Munn, L.L. Micro-environmental mechanical stress controls tumor spheroid size and morphology by suppressing proliferation and inducing apoptosis in cancer cells. *PloS one* **4**, e4632 (2009).
58. Delarue, M. et al. Compressive stress inhibits proliferation in tumor spheroids through a volume limitation. *Biophysical journal* **107**, 1821-1828 (2014).
59. Alessandri, K. et al. Cellular capsules as a tool for multicellular spheroid production and for investigating the mechanics of tumor progression in vitro. *Proceedings of the National Academy of Sciences of the United States of America* **110**, 14843-14848 (2013).
60. Desmaison, A., Frongia, C., Grenier, K., Ducommun, B. & Lobjois, V. Mechanical stress impairs mitosis progression in multi-cellular tumor spheroids. *PloS one* **8**, e80447 (2013).
61. Fernández-Sánchez, M.E. et al. Mechanical induction of the tumorigenic β-catenin pathway by tumour growth pressure. *Nature* **523**, 92 (2015).
62. Demou, Z.N. Gene expression profiles in 3D tumor analogs indicate compressive strain differentially enhances metastatic potential. *Annals of biomedical engineering* **38**, 3509-3520 (2010).
63. Mitsui, N. et al. Effect of compressive force on the expression of MMPs, PAs, and their inhibitors in osteoblastic Saos-2 cells. *Life sciences* **79**, 575-583 (2006).
64. Tse, J.M. et al. Mechanical compression drives cancer cells toward invasive phenotype. *Proceedings of the National Academy of Sciences of the United States of America* **109**, 911-916 (2012).
65. Karagiannis, G.S. et al. Cancer-associated fibroblasts drive the progression of metastasis through both paracrine and mechanical pressure on cancer tissue. *Molecular cancer research : MCR* **10**, 1403-1418 (2012).
66. Masamune, A. & Shimosegawa, T. Pancreatic stellate cells: A dynamic player of the intercellular communication in pancreatic cancer. *Clinics and research in hepatology and gastroenterology* **39 Suppl 1**, S98-103 (2015).
67. Dimanche-Boitrel, M.T. et al. In vivo and in vitro invasiveness of a rat colon-cancer cell line maintaining E-cadherin expression: an enhancing role of tumor-associated myofibroblasts. *International journal of cancer* **56**, 512-521 (1994).
68. Hwang, R.F. et al. Cancer-associated stromal fibroblasts promote pancreatic tumor progression. *Cancer research* **68**, 918-926 (2008).
69. Olumi, A.F. et al. Carcinoma-associated fibroblasts direct tumor progression of initiated human prostatic epithelium. *Cancer research* **59**, 5002-5011 (1999).
70. Orimo, A. et al. Stromal fibroblasts present in invasive human breast carcinomas promote tumor growth and angiogenesis through elevated SDF-1/CXCL12 secretion. *Cell* **121**, 335-348 (2005).
71. Ilic, M. & Ilic, I. Epidemiology of pancreatic cancer. *World journal of gastroenterology* **22**, 9694-9705 (2016).
72. Bhowmick, N.A., Neilson, E.G. & Moses, H.L. Stromal fibroblasts in cancer initiation and progression. *Nature* **432**, 332 (2004).
73. Paul, C.D., Mistriotis, P. & Konstantopoulos, K. Cancer cell motility: lessons from migration in confined spaces. *Nature Reviews Cancer* **17**, 131 (2016).

74. Egeblad, M., Rasch, M.G. & Weaver, V.M. Dynamic interplay between the collagen scaffold and tumor evolution. *Current opinion in cell biology* **22**, 697-706 (2010).
75. Kikuta, K. et al. Pancreatic stellate cells promote epithelial-mesenchymal transition in pancreatic cancer cells. *Biochemical and Biophysical Research Communications* **403**, 380-384 (2010).
76. Vonlaufen, A. et al. Pancreatic Stellate Cells and Pancreatic Cancer Cells: An Unholy Alliance. *Cancer research* **68**, 7707-7710 (2008).
77. Mahadevan, D. & Von Hoff, D.D. Tumor-stroma interactions in pancreatic ductal adenocarcinoma. *Molecular cancer therapeutics* **6**, 1186-1197 (2007).
78. Mimeault, M. & Batra, S.K. Divergent molecular mechanisms underlying the pleiotropic functions of macrophage inhibitory cytokine-1 in cancer. *Journal of cellular physiology* **224**, 626-635 (2010).
79. Aw Yong, K.M. et al. Morphological effects on expression of growth differentiation factor 15 (GDF15), a marker of metastasis. *Journal of cellular physiology* **229**, 362-373 (2014).
80. Li, P.X. et al. Placental transforming growth factor-beta is a downstream mediator of the growth arrest and apoptotic response of tumor cells to DNA damage and p53 overexpression. *The Journal of biological chemistry* **275**, 20127-20135 (2000).
81. Senapati, S. et al. Overexpression of macrophage inhibitory cytokine-1 induces metastasis of human prostate cancer cells through the FAK-RhoA signaling pathway. *Oncogene* **29**, 1293-1302 (2010).
82. Welsh, J.B. et al. Large-scale delineation of secreted protein biomarkers overexpressed in cancer tissue and serum. *Proceedings of the National Academy of Sciences of the United States of America* **100**, 3410-3415 (2003).
83. Brown, D.A. et al. Measurement of serum levels of macrophage inhibitory cytokine 1 combined with prostate-specific antigen improves prostate cancer diagnosis. *Clinical cancer research : an official journal of the American Association for Cancer Research* **12**, 89-96 (2006).
84. Shnaper, S. et al. Elevated levels of MIC-1/GDF15 in the cerebrospinal fluid of patients are associated with glioblastoma and worse outcome. *International journal of cancer* **125**, 2624-2630 (2009).
85. Li, C. et al. Growth differentiation factor 15 is a promising diagnostic and prognostic biomarker in colorectal cancer. *Journal of cellular and molecular medicine* **20**, 1420-1426 (2016).
86. Danta, M. et al. Macrophage inhibitory cytokine-1/growth differentiation factor-15 as a predictor of colonic neoplasia. *Alimentary pharmacology & therapeutics* **46**, 347-354 (2017).
87. Bruzzese, F. et al. Local and systemic protumorigenic effects of cancer-associated fibroblast-derived GDF15. *Cancer research* **74**, 3408-3417 (2014).
88. Gardner, J.A., Ha, J.H., Jayaraman, M. & Dhanasekaran, D.N. The gep proto-oncogene Galpha13 mediates lysophosphatidic acid-mediated migration of pancreatic cancer cells. *Pancreas* **42**, 819-828 (2013).
89. Papageorgis, P. & Stylianopoulos, T. Role of TGFbeta in regulation of the tumor microenvironment and drug delivery (review). *International journal of oncology* **46**, 933-943 (2015).
90. Sidhu, S.S. et al. Roles of epithelial cell-derived periostin in TGF-beta activation, collagen production, and collagen gel elasticity in asthma. *Proceedings of the*

National Academy of Sciences of the United States of America **107**, 14170-14175 (2010).
91. Hu, Q. et al. Periostin Mediates TGF-beta-Induced Epithelial Mesenchymal Transition in Prostate Cancer Cells. *Cellular physiology and biochemistry : international journal of experimental cellular physiology, biochemistry, and pharmacology* **36**, 799-809 (2015).
92. Lv, Y.J. et al. Association between periostin and epithelial-mesenchymal transition in esophageal squamous cell carcinoma and its clinical significance. *Oncology letters* **14**, 376-382 (2017).
93. Albertoni, M. et al. Anoxia induces macrophage inhibitory cytokine-1 (MIC-1) in glioblastoma cells independently of p53 and HIF-1. *Oncogene* **21**, 4212-4219 (2002).
94. Li, C. et al. GDF15 promotes EMT and metastasis in colorectal cancer. *Oncotarget* **7**, 860-872 (2016).
95. Xu, Q. et al. Growth differentiation factor 15 induces growth and metastasis of human liver cancer stem-like cells via AKT/GSK-3beta/beta-catenin signaling. *Oncotarget* **8**, 16972-16987 (2017).
96. Sasahara, A. et al. An autocrine/paracrine circuit of growth differentiation factor (GDF) 15 has a role for maintenance of breast cancer stem-like cells. *Oncotarget* **8**, 24869-24881 (2017).
97. Peake, B.F., Eze, S.M., Yang, L., Castellino, R.C. & Nahta, R. Growth differentiation factor 15 mediates epithelial mesenchymal transition and invasion of breast cancers through IGF-1R-FoxM1 signaling. *Oncotarget* **8**, 94393-94406 (2017).
98. Ji, H. et al. Twist promotes invasion and cisplatin resistance in pancreatic cancer cells through growth differentiation factor 15. *Molecular medicine reports* **12**, 3841-3848 (2015).
99. Tanno, T. et al. Growth differentiating factor 15 enhances the tumor-initiating and self-renewal potential of multiple myeloma cells. *Blood* **123**, 725-733 (2014).
100. Chen, Q. et al. Growth-induced stress enhances epithelial-mesenchymal transition induced by IL-6 in clear cell renal cell carcinoma via the Akt/GSK-3beta/beta-catenin signaling pathway. *Oncogenesis* **6**, e375 (2017).
101. Kalli, M., Papageorgis, P., Gkretsi, V. & Stylianopoulos, T. Solid Stress Facilitates Fibroblasts Activation to Promote Pancreatic Cancer Cell Migration. *Annals of biomedical engineering* (2018).
102. Prendergast, G.C. Actin' up: RhoB in cancer and apoptosis. *Nature reviews. Cancer* **1**, 162-168 (2001).
103. Vega, F.M. & Ridley, A.J. The RhoB small GTPase in physiology and disease. *Small GTPases*, 1-10 (2016).
104. Park, J.K. et al. ICAM-3 enhances the migratory and invasive potential of human non-small cell lung cancer cells by inducing MMP-2 and MMP-9 via Akt and CREB. *International journal of oncology* **36**, 181-192 (2010).
105. Jhala, U.S. et al. cAMP promotes pancreatic beta-cell survival via CREB-mediated induction of IRS2. *Genes & development* **17**, 1575-1580 (2003).
106. Xu, X. et al. c-Met and CREB1 are involved in miR-433-mediated inhibition of the epithelial-mesenchymal transition in bladder cancer by regulating Akt/GSK-3beta/Snail signaling. *Cell death & disease* **7**, e2088 (2016).
107. Downward, J. PI 3-kinase, Akt and cell survival. *Seminars in Cell & Developmental Biology* **15**, 177-182 (2004).

108. Vivanco, I. & Sawyers, C.L. The phosphatidylinositol 3-Kinase–AKT pathway in human cancer. *Nature Reviews Cancer* **2**, 489 (2002).
109. Bousquet, E. et al. Loss of RhoB expression promotes migration and invasion of human bronchial cells via activation of AKT1. *Cancer research* **69**, 6092-6099 (2009).
110. Xiong, J. et al. Deregulated expression of miR-107 inhibits metastasis of PDAC through inhibition PI3K/Akt signaling via caveolin-1 and PTEN. *Experimental cell research* **361**, 316-323 (2017).
111. Li, S., Ma, Y.M., Zheng, P.S. & Zhang, P. GDF15 promotes the proliferation of cervical cancer cells by phosphorylating AKT1 and Erk1/2 through the receptor ErbB2. *Journal of experimental & clinical cancer research : CR* **37**, 80 (2018).
112. Zheng, Y. et al. Novel phosphatidylinositol 3-kinase inhibitor NVP-BKM120 induces apoptosis in myeloma cells and shows synergistic anti-myeloma activity with dexamethasone. *Journal of molecular medicine* **90**, 695-706 (2012).
113. Hu, Y. et al. Effects of PI3K inhibitor NVP-BKM120 on overcoming drug resistance and eliminating cancer stem cells in human breast cancer cells. *Cell death & disease* **6**, e2020 (2015).
114. Bedard, P.L. et al. A phase Ib dose-escalation study of the oral pan-PI3K inhibitor buparlisib (BKM120) in combination with the oral MEK1/2 inhibitor trametinib (GSK1120212) in patients with selected advanced solid tumors. *Clinical cancer research : an official journal of the American Association for Cancer Research* **21**, 730-738 (2015).
115. Li, Z. et al. Synergistic Antitumor Effect of BKM120 with Prima-1^{Met} Via Inhibiting PI3K/AKT/mTOR and CPSF4/hTERT Signaling and Reactivating Mutant P53. *Cellular Physiology and Biochemistry* **45**, 1772-1786 (2018).
116. Yang, S. et al. NVP-BKM120 inhibits colon cancer growth via FoxO3a-dependent PUMA induction. *Oncotarget* **8**, 83052-83062 (2017).
117. Cartharius, K. et al. MatInspector and beyond: promoter analysis based on transcription factor binding sites. *Bioinformatics* **21**, 2933-2942 (2005).
118. Griner, S.E., Joshi, J.P. & Nahta, R. Growth differentiation factor 15 stimulates rapamycin-sensitive ovarian cancer cell growth and invasion. *Biochemical Pharmacology* **85**, 46-58 (2013).
119. Urakawa, N. et al. GDF15 derived from both tumor-associated macrophages and esophageal squamous cell carcinomas contributes to tumor progression via Akt and Erk pathways. *Laboratory Investigation* **95**, 491 (2015).
120. Schwartzbaum, J.A., Fisher, J.L., Aldape, K.D. & Wrensch, M. Epidemiology and molecular pathology of glioma. *Nature clinical practice. Neurology* **2**, 494-503; quiz 491 p following 516 (2006).
121. Ostrom, Q.T. et al. The epidemiology of glioma in adults: a "state of the science" review. *Neuro-oncology* **16**, 896-913 (2014).
122. Seano, G. et al. Solid stress in brain tumours causes neuronal loss and neurological dysfunction and can be reversed by lithium. *Nature Biomedical Engineering* (2019).
123. Gamburg, E.S. et al. The prognostic significance of midline shift at presentation on survival in patients with glioblastoma multiforme. *International journal of radiation oncology, biology, physics* **48**, 1359-1362 (2000).
124. Kreth, F.W. et al. The role of tumor resection in the treatment of glioblastoma multiforme in adults. *Cancer* **86**, 2117-2123 (1999).

125. Piek, J., Plewe, P. & Bock, W.J. Intrahemispheric gradients of brain tissue pressure in patients with brain tumours. *Acta neurochirurgica* **93**, 129-132 (1988).
126. Ludwig, K. & Kornblum, H.I. Molecular markers in glioma. *Journal of neuro-oncology* **134**, 505-512 (2017).
127. Tomiyama, A. & Ichimura, K. Signal transduction pathways and resistance to targeted therapies in glioma. *Seminars in cancer biology* (2019).
128. Adamson, C. et al. Glioblastoma multiforme: a review of where we have been and where we are going. *Expert opinion on investigational drugs* **18**, 1061-1083 (2009).
129. Kalli, M. et al. Solid stress-induced migration is mediated by GDF15 through Akt pathway activation in pancreatic cancer cells. *Scientific reports* **9**, 978 (2019).
130. An, Z., Aksoy, O., Zheng, T., Fan, Q.-W. & Weiss, W.A. Epidermal growth factor receptor and EGFRvIII in glioblastoma: signaling pathways and targeted therapies. *Oncogene* **37**, 1561-1575 (2018).
131. Del Duca, D., Werbowetski, T. & Del Maestro, R.F. Spheroid preparation from hanging drops: characterization of a model of brain tumor invasion. *Journal of neuro-oncology* **67**, 295-303 (2004).
132. Kelm, J.M., Timmins, N.E., Brown, C.J., Fussenegger, M. & Nielsen, L.K. Method for generation of homogeneous multicellular tumor spheroids applicable to a wide variety of cell types. *Biotechnology and bioengineering* **83**, 173-180 (2003).
133. Foty, R. A simple hanging drop cell culture protocol for generation of 3D spheroids. *Journal of visualized experiments : JoVE* (2011).
134. Rodriguez, E.K., Hoger, A. & McCulloch, A.D. Stress-dependent finite growth in soft elastic tissues. *J Biomech* **27**, 455-467 (1994).
135. Stylianopoulos, T. et al. Coevolution of solid stress and interstitial fluid pressure in tumors during progression: Implications for vascular collapse. *Cancer research* **73**, 3833-3841 (2013).
136. Ambrosi, D. & Mollica, F. On the mechanics of a growing tumor. *Int J Eng Sci* **40**, 1297-1316 (2002).
137. Ciarletta, P. Buckling instability in growing tumor spheroids. *Phys Rev Lett* **110**, 158102 (2013).
138. Ambrosi, D. & Preziosi, L. Cell adhesion mechanisms and stress relaxation in the mechanics of tumours. *Biomechanics and modeling in mechanobiology* **8**, 397-413 (2009).
139. Kim, Y., Stolarska, M.A. & Othmer, H.G. The role of the microenvironment in tumor growth and invasion. *Progress in biophysics and molecular biology* **106**, 353-379 (2011).
140. MacLaurin, J., Chapman, J., Jones, G.W. & Roose, T. The buckling of capillaries in solid tumours. *Proc. R. Soc. A* **468**, 4123-4145 (2012).
141. Omens, J.H., Vaplon, S.M., Fazeli, B. & McCulloch, A.D. Left ventricular geometric remodeling and residual stress in the rat heart. *Journal of biomechanical engineering* **120**, 715-719 (1998).
142. Xu, G., Bayly, P.V. & Taber, L.A. Residual stress in the adult mouse brain. *Biomech Model Mechanobiol* **8**, 253-262 (2009).
143. Taber, L.A. Theoretical study of Beloussov's hyper-restoration hypothesis for mechanical regulation of morphogenesis. *Biomech Model Mechanobiol* **7**, 427-441 (2008).
144. Kalli, M. et al. Solid stress-induced migration is mediated by GDF15 through Akt pathway activation in pancreatic cancer cells. *Scientific Reports* **9**, 978 (2019).

145. Kalli, M., Papageorgis, P., Gkretsi, V. & Stylianopoulos, T. Solid Stress Facilitates Fibroblasts Activation to Promote Pancreatic Cancer Cell Migration. *Annals of biomedical engineering* **46**, 657-669 (2018).
146. Ridley, A.J. RhoA, RhoB and RhoC have different roles in cancer cell migration. *Journal of microscopy* **251**, 242-249 (2013).
147. Kao, C. et al. Critical functions of RhoB in support of glioblastoma tumorigenesis. *Neuro-oncology* **17**, 516-525 (2014).
148. Ader, I. et al. Inhibition of Rho pathways induces radiosensitization and oxygenation in human glioblastoma xenografts. *Oncogene* **22**, 8861 (2003).
149. Cohen-Jonathan Moyal, E. et al. Phase I Trial of Tipifarnib (R115777) Concurrent With Radiotherapy in Patients with Glioblastoma Multiforme. *International Journal of Radiation Oncology • Biology • Physics* **68**, 1396-1401 (2007).
150. Doshi, B.M., Hightower, L.E. & Lee, J. The role of Hsp27 and actin in the regulation of movement in human cancer cells responding to heat shock. *Cell stress & chaperones* **14**, 445-457 (2009).
151. Wettstein, G., Bellaye, P.S., Micheau, O. & Bonniaud, P. Small heat shock proteins and the cytoskeleton: an essential interplay for cell integrity? *The international journal of biochemistry & cell biology* **44**, 1680-1686 (2012).
152. Melle, C. et al. Protein profiling of microdissected pancreas carcinoma and identification of HSP27 as a potential serum marker. *Clinical chemistry* **53**, 629-635 (2007).
153. Bunger, S., Laubert, T., Roblick, U.J. & Habermann, J.K. Serum biomarkers for improved diagnostic of pancreatic cancer: a current overview. *Journal of cancer research and clinical oncology* **137**, 375-389 (2011).
154. Baylot, V. et al. OGX-427 inhibits tumor progression and enhances gemcitabine chemotherapy in pancreatic cancer. *Cell death & disease* **2**, e221 (2011).
155. Xia, Y., Rocchi, P., Iovanna, J.L. & Peng, L. Targeting heat shock response pathways to treat pancreatic cancer. *Drug discovery today* **17**, 35-43 (2012).
156. Kuramitsu, Y. et al. Heat-shock protein 27 plays the key role in gemcitabine-resistance of pancreatic cancer cells. *Anticancer research* **32**, 2295-2299 (2012).
157. Garrido-Laguna, I. & Hidalgo, M. Pancreatic cancer: from state-of-the-art treatments to promising novel therapies. *Nature reviews. Clinical oncology* **12**, 319-334 (2015).
158. Konishi, H. et al. Activation of protein kinase B (Akt/RAC-protein kinase) by cellular stress and its association with heat shock protein Hsp27. *FEBS Letters* **410**, 493-498 (1997).
159. Wu, R. et al. Hsp27 regulates Akt activation and polymorphonuclear leukocyte apoptosis by scaffolding MK2 to Akt signal complex. *The Journal of biological chemistry* **282**, 21598-21608 (2007).
160. O'Shaughnessy, R.F. et al. AKT-dependent HspB1 (Hsp27) activity in epidermal differentiation. *The Journal of biological chemistry* **282**, 17297-17305 (2007).
161. Havasi, A. et al. Hsp27 inhibits Bax activation and apoptosis via a phosphatidylinositol 3-kinase-dependent mechanism. *The Journal of biological chemistry* **283**, 12305-12313 (2008).
162. Kanagasabai, R. et al. Hsp27 Protects Adenocarcinoma Cells from UV-Induced Apoptosis by Akt and p21-Dependent Pathways of Survival. *Molecular Cancer Research* **8**, 1399-1412 (2010).

163. Ghosh, A. et al. HSP27 expression in primary colorectal cancers is dependent on mutation of KRAS and PI3K/AKT activation status and is independent of TP53. *Experimental and Molecular Pathology* **94**, 103-108 (2013).
164. Shin, K.D. et al. Blocking tumor cell migration and invasion with biphenyl isoxazole derivative KRIBB3, a synthetic molecule that inhibits Hsp27 phosphorylation. *The Journal of biological chemistry* **280**, 41439-41448 (2005).
165. Xu, L., Chen, S. & Bergan, R.C. MAPKAPK2 and HSP27 are downstream effectors of p38 MAP kinase-mediated matrix metalloproteinase type 2 activation and cell invasion in human prostate cancer. *Oncogene* **25**, 2987 (2006).
166. Golembieski, W.A. et al. HSP27 mediates SPARC-induced changes in glioma morphology, migration, and invasion. *Glia* **56**, 1061-1075 (2008).
167. Lee, J.-W. et al. HSP27 regulates cell adhesion and invasion via modulation of focal adhesion kinase and MMP-2 expression. *European Journal of Cell Biology* **87**, 377-387 (2008).
168. Papageorgis, P. et al. Tranilast-induced stress alleviation in solid tumors improves the efficacy of chemo- and nanotherapeutics in a size-independent manner. *Scientific reports* **7**, 46140 (2017).
169. Polydorou, C., Mpekris, F., Papageorgis, P., Voutouri, C. & Stylianopoulos, T. Pirfenidone normalizes the tumor microenvironment to improve chemotherapy. *Oncotarget* **8**, 24506-24517 (2017).

Table 1. Primers used for qPCR

Primer Name	Primer sequence
β-actin	Forward: 5'-CGAGCACAGAGCCTCGCCTTTGCC-3'
	Reverse: 5'-TGTCGACGACGAGCGCGGCGATAT-3'
Collagen I	Forward: 5'- GTGCTAAAGGTGCCAATGGT-3'
	Reverse: 5'- ACCAGGTTCACCGCTGTTAC-3'
TGFβ	Forward: 5'- GTACCTGAACCCGTGTTGCT-3'
	Reverse: 5'- CACGTGCTGCTCCACTTTTA-3'
Fibronectin I	Forward: 5'- CCCAGTGATTTCAGCAAAGG-3'
	Reverse: 5'- CCCAGTGATTTCAGCAAAGG-3'
Periostin	Forward: 5'- AGTTTGTTCGTGGCAGCAC-3'
	Reverse: 5'- GAAGTCGGGATCACCTTCAA-3'
a-SMA	Forward: 5'- CGGGACTAAGACGGGAATC -3'
	Reverse: 5'- CAGAGCCATTGTCACACACC -3'
GDF15	Forward: 5'-TCAAGGTCGTGGGACGTGACA-3'
	Reverse: 5'- GCCGTGCGGACGAAGATTCT-3'
RhoA	Forward: 5'-CGGGAGCTAGCCAAGATGAAG-3'
	Reverse: 5'-CCTTGCAGAGCAGCTCTCGTA-3'
RhoB	Forward: 5'-TGCTGATCGTGTTCAGTAAG-3'
	Reverse: 5'-AGCACATGAGAATGACGTCG-3'
RhoC	Forward: 5'-TCCTCATCGTCTTCAGCAAG-3'
	Reverse: 5'-GAGGATGACATCAGTGTCCG-3'
Rac-1	Forward: 5'-AACCAATGCATTTCCTGGAG-3'
	Reverse: 5'-CAGATTCACCGGTTTTCCAT-3
ROCK1	Forward: 5'-ACCTGTAACCCAAGGAGATGT-3'
	Reverse: 5'-CACAATTGGCAGGAAAGTGG-3'
cdc42	Forward: 5'-GCCCGTGACCTGAAGGCTGTCA-3'
	Reverse: 5'-TGCTTTTAGTATGATGCCGACACCA-3
Vimentin	Forward: 5'-CGAAAACACCCTGCAATCTT-3'
	Reverse: 5'-ATTCCACTTTGCGTTCAAGG-3'
E-Cadherin	Forward: 5'-TCCATTTCTTGGTCTACGCC-3'
	Reverse: 5'-CACCTTCAGCCAACCTGTTT-3'
β-catenin	Forward: 5'-ACAAACTGTTTTGAAAATCCA-3'
	Reverse: 5'-CGAGTCATTGCATACTGTCC-3'